Dipole-Dipole Interaction in Quasi One-Dimensional Harmonic Traps

Johannes Bjerlin

June 11, 2012

Supervisor: Prof. Stephanie M. Reimann

Abstract

Low-dimensional systems of dipoles show many interesting features in terms of both spectra and density distributions. Many external parameters of such a system can in fact be controlled in experiments, so simulations are invaluable in order to investigate how properties depend on such parameters. In particular the ideal dipole-dipole interaction in a quasi one-dimensional system of particles is dependent on the angle of the dipolar-moments relative to the alignment. In fact the inter-particle interaction can be tuned to become both attractive and repulsive by changing this "dipole angle" via an external field, so it is especially interesting to investigate how systems depend on this parameter.

In this project I perform simulations with a quasi one-dimensional harmonic system of a few ideal dipoles. Calculations using exact diagonalization are performed in order to find the energy-eigenvectors of systems with various numbers of dipolar fermions or bosons. The parameters for both the inter-particle dipole-dipole interaction and the transverse confinement are then altered in order to investigate the systems.

Some analytical work is also done investigating the features of the dipole-dipole interaction, which has been seen to give rise to ambiguities even for the ideal-dipole model.

This project mainly deals with a few specific features of one-dimensional systems of ideal dipoles. Among these features are separation, localization and fermionization of bosons. Fermionization of bosons essentially means that the repelling force between particles is so strong that they never overlap. Therefore the Pauli principle becomes unimportant and bosons and fermions show similar properties in a fermionized system. It will be investigated how these features depend on the parameters of the interaction, and how the they can be applied in order to improve models and predict new results in related areas of research.

Contents

Part I
Outline and Introduction

1 Introduction

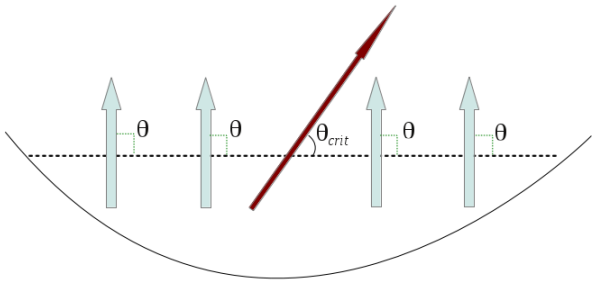

Figure 1: Pictorial view of four dipoles, denoted by blue arrows, at dipole angle $\theta = 90°$ in a one-dimensional harmonic trap. The critical angle $\theta_{crit} \approx 54.7°$ is also shown.

In recent years the prospect of ultracold atoms and molecules with dipole moments has lead to many studies. Quantum-gases with pure dipole-dipole interaction have been realized experimentally using Feshbach resonances [40], and many interesting effects of these systems have already been predicted [21] [41]. Exploiting the anisotropic nature of the dipole-dipole interaction a variety of prospects are currently investigated for systems of cold atoms.

A system of a few dipoles in a quasi one-dimensional trap is depicted in figure (1), where the dipole moments are denoted by the blue arrows. A specific feature of the effective one-dimensional dipole-dipole interaction is the *dipole angle* θ, which denotes the angle of the dipole moments relative to the spatial alignment of the one-dimensional trap. Tuning this dipole angle it is possible to change the interaction between particles so that for $\theta < \theta_{crit}$ the interaction becomes attractive, and that for $\theta > \theta_{crit}$ the interaction become repulsive. At the *critical angle* $\theta_{crit} \approx 54.7°$ the dipole-dipole interaction becomes zero.

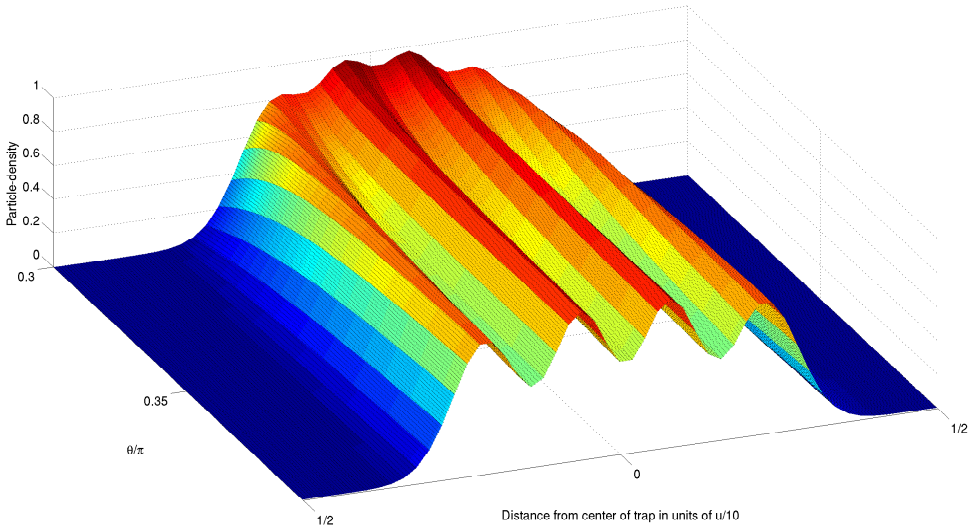

Figure 2: density distribution of the ground state for four fermions in a quasi one-dimensional harmonic trap with $l_p = 0.06$ (Electric dipole interaction coefficient $d^2 = 1$)

The anisotropy of the dipole-dipole interaction can give rise to interesting effects in cold quantum-gases.

In figure (2) one can for example see how the dipole angle $\theta > \theta_{crit} \approx 0.304\pi \approx 54.7^\circ$ is successively tuned towards larger values, i.e. to larger repulsive interaction, and causes particles in the four-fermion ground state to separate.

The purpose of this project is to investigate the dipole-dipole interaction, both from analytical results and from numerical studies of quasi one-dimensional systems. The project should serve to highlight a few important features of the dipole-dipole interaction. I will show some specific examples of how these features give interesting results in the physical simulations.
Due to the increasing interest in dipolar systems I have in particular also investigated some of the difficult areas of mathematics which are associated with ideal dipoles. This should be important since simulations often employ the ideal-dipole model, and it will be seen that the details of this model in many cases affect the results of the calculations. I shall both investigate the ideal-dipole model in itself, but also discuss how it can be used to in order to model systems of real dipoles. Contrary to ideal dipoles, which are point-like particles with dipole moments, the real dipoles can be, for example, finite-sized atoms or molecules which have charge-distributions that induce dipole moments.

In the case of low-dimensional systems an effective interaction expression is often used in simulations, and I will therefore also discuss how a concept such

as uniform convergence can complicate the setup of these models.

2 Outline

Theoretical background

The first sections in this report will be used to give some theoretical background on topics relating to the project. I will briefly discuss some concepts in many-particle theory, and also the configuration-interaction method.

In the later sections of part (3) I will in particular discuss the dipole-dipole force. The systems which I investigate are modeled so that the only inter-particle forces come from the dipole-dipole interaction, and it will therefore turn out to be especially important to investigate the subtle details of this interaction. The expressions for the dipole-dipole interaction will be derived and discussed, and in particular the **ideal-dipole model** will be evaluated.

Results

In part (III) I will in particular discuss two different types of results.

General effects of the dipole-dipole interaction seen from different observables

These results will be used to show how effects in the quasi one-dimensional system of dipoles can be analyzed by studying different observables. I will show that observables such as eigen energies and occupation-numbers can be used to investigate how the dipole-dipole interaction affects a system of ideal dipoles, and in particular how these observables can be used to evaluate the model itself. I will discuss concepts such as separation, fermionization and localization and show how these effects can be seen from different observables.

This part of the results is strongly connected to the theoretical discussion on the dipole-dipole force, since many of these concepts and methods are essential when evaluating the model for the interaction.

Details of the quasi one-dimensional system and suggested applications

Some details of the quasi one-dimensional system of dipoles will be discussed among the general effects. These details will be highlighted since they might be especially interesting or could be used for some possible application. Sections which contain such discussions are section6.3,10 and12.3.

Appendix

Some of the derivations will be put in the appendix of this report. In particular some discussion on the generalized function will be found in this part.

Part II
Theoretical background

3 Many-particle theory

This part will deal with some essential tools for describing many-particle systems. The main point will be a short summary on the theory of second quantization. The formalism of second-quantization is often used to simplify the treatment of systems with many particles, since the basic description of the system can be used for any number of particles. This section is mainly based on the proceedings in [10].

3.1 The many-particle wavefunction

The ket $\left|\Psi_{(v_1,..,v_N)}\right\rangle$ describes an N-particle quantum-state labeled $\Psi_{(v_1,...,v_N)}$, where the labels v_i denote single-particle states.

The many-particle state lies in a Hilbert-space defined as a tensor-product of one-particle Hilbert-spaces $H_1, ..., H_N$;

$$H(N) = H_1 \otimes H_2 \otimes ...H_N \tag{1}$$

The state $\left|\Psi_{(v_1,..,v_N)}\right\rangle \in H^{\otimes N}$ has a wavefunction representation which can be described in terms of products of single-particle wavefunctions $\varphi_n(x_i)$. It is implicit that these products represent tensor-products as in (1), but for simplicity they are denoted as regular products between functions.

The wavefunction of a one-particle state is usually defined by the scalar product of an eigen-bra $\langle x'|$ of the position-operator, and the ket $|\varphi_n\rangle$ which represents the state in question.

$$\varphi_n(x') = \langle x'|\, \varphi_n\rangle$$

The representation of an individual one-particle wavefunction $\varphi_n(x_i)$ includes two labels;

- The *orbital label* n points to a specific state in the one-particle Hilbert-space.
- The *particle label* x_i denotes a specific particle with index $0 < i \leq N$.

3.2 The anti-symmetric wavefunction

Fermions are a categorization of spin-$\frac{1}{2}$ particles among which we find electrons and positrons. One distinguishing property of fermions is the fact that their quantum-mechanical wavefunctions are anti-symmetric with respect to interchange of two identical particles.[10]

This can be written formally as

$$P_{ij}\Psi_{(v_1,..,v_N)}(x_1,..,x_i,..,x_j,..,x_N) = -\Psi_{(v_1,..,v_N)}(x_1,..,x_j,..,x_i,..,x_N)$$

where P_{ij} denotes an operator which interchanges two identical particles denoted by i and j.

Because of the anti-symmetry requirement a simple product of one-particle wavefunctions cannot represent a fermionic wavefunction.

An anti-symmetric wavefunction can instead be described in terms of one-particle functions using a Slater-determinant;

$$\frac{1}{\sqrt{N!}}\begin{vmatrix} \varphi_1(x_1) & \varphi_2(x_1) & . & . & \varphi_N(x_1) \\ \varphi_1(x_2) & \varphi_2(x_2) & . & . & \varphi_N(x_2) \\ . & . & . & . & . \\ . & . & . & . & . \\ \varphi_1(x_N) & . & . & . & \varphi_N(x_N) \end{vmatrix} = \Psi^k_{(v_1,...,v_N)}(x_1,...,x_N) \qquad (2)$$

Note that exchanging two indices in the total wavefunction equals the interchange of two columns in the Slater-determinant. By the general properties of determinants this will give a factor -1 in front of the wavefunction. Any many-fermion state could be described as a linear combination of different Slater-determinants, since they can be shown to form a basis in the N-fermion Hilbert-space.[10]

Each different Slater-determinant is built from a different set of one-particle orbitals. Such a set is know as a configuration, a word which is common in the nomenclature of atomic physics.

One should mention that labeling a Slater-determinant in terms of the one-particle states $(v_1,...,v_N)$ is somewhat insufficient. This is due to the fact that a Slater-determinant only is defined to within a sign for a specified set of states.

In the following sections this unambiguity will however be treated in a black-box manner, so that Slater-determinants are labeled by the included states $(v_1,...,v_N)$. It is then assumed that the Slater-determinant labeled by $(v_1,...,v_N)$ has a positive sign and that interchanging two particles gives a minus sign.

3.3 Second-quantization

As noted in the beginning, second quantization is a formalism which allows a handy description of many-particle systems.

The name second-quantization comes from the fact that a "second quantization" is performed on the classical dynamical variables like p_i and q_i. This essentially means that these variables are reinterpreted as operators which obey specific commutation-relations, which in turn quantize other operators, as for example the Hamiltonian, in such a description. [11]

Ladder-operators

Annihilation and creation-operators are central concepts in the second-quantization formalism. They can be described as operators which map between Hilbert-spaces of different particle numbers N so that;[10]

$$\begin{array}{l} a_k : \mathcal{H}(N) \rightarrow \mathcal{H}(N-1) \\ a_k^\dagger : \mathcal{H}(N) \rightarrow \mathcal{H}(N+1) \end{array} \tag{3}$$

For a specific function-basis $\Phi_{(v_1,..,v_N)}(x_1,...,x_N) = \left\{ \Psi^k_{(v_1,..,v_N)}(x_1,...,x_N) \right\}$ in an N-fermion Hilbert-space one could define the action of the annihilator operator a_k in (3) on this basis as[10];

$$\begin{array}{ll} a_k \Phi_{(v_1,..,v_N)}(x_1,...,x_N) \equiv 0, & if\ k \notin \{v_{1,..,}v_N\} \\ a_k^\dagger \Phi_{(v_1,..,v_N)}(x_1,...,x_N) \equiv 0, & if\ k \in \{v_{1,..,}v_N\} \\ a_k \Phi_{(v_1,..,v_N)}(x_1,...,x_N) \equiv (-1)^{j-1} \Phi_{(v_1,..,v_{j-1},v_{j+1},..,v_N)}(x_1,...,x_{N-1})\ if\ k = v_j & \\ a_k^\dagger \Phi_{(v_1,..,v_{j-1},v_{j+1},..,v_N)}(x_1,...,x_{N-1}) \equiv (-1)^{j-1} \Phi_{(c_1,..,c_N)}(x_1,...,x_N)\ if\ k = v_j & \end{array} \tag{4}$$

It is important to note that it is the definition of the basis Φ that determines the action of the ladder-operators (3).

The effect of operator a_k is interpreted as "annihilating" a particle in state v_k, while $a_k^\dagger$ "creates" a particle in state c_k.

The Fock space

The description of a general N-fermion system was discussed in earlier sections. While this procedure might be fruitful for a system with a fixed number of particles, it is somewhat less efficient for a description of a system with an arbitrary number of particles. For such a system one might know the Hamiltonian for any number of particles and it would therefore be tempting to use a formalism where one operator easily could be used for any number of particles. This is where the concept of second-quantization proves to become handy.

I shall begin the discussion by defining a new space called the Fock-space[17]

$$F_v(H) = \bigoplus_{n=0}^{\infty} S_v H^{\otimes n} = C \otimes H \oplus (S_v(H \otimes H)) \oplus (S_v(H \otimes H \otimes H)) \oplus ... \tag{5}$$

where C denotes a state of no particles.

The operator S_v has an important role in this expression, since it represents symmetrization or anti-symmetrization of the space. This essentially means that the elements in the Fock-space can either be symmetric or anti-symmetric with respect to interchange of two particle-labels.

The appearance of ladder operators $a_k^\dagger$ and a_k in the Fock-space (5) is especially interesting. Since the Fock-space is a space which describes any number of particles the ladder operators are now mappings within the space, instead of operators mapping between different spaces.

A general state in the anti-symmetric Fock-space can be labeled with a set of indicies $\{c\}$, denoting the one-particle states which are used in expansion of the state, for example; $\{c\} = \nu_1, \nu_3, \nu_4, \nu_{10}$

The complete position-spin wavefunction is then given according to;

$$\Psi^F_{\{c\}}(x_1, x_2..., x_N) = \langle x_1, x_2, ...x_N \,|\{c\}\rangle$$

The set of indicies $\{c\}$ are associated with the states of individual particles and one can formulate a representation of the Fock-state $|\{c\}\rangle$ in terms of *occupation numbers* n_{ν_1}, n_{ν_2},.. These numbers represent the numbers of particles in each one-particle basis-state denoted by ν_k. The supscriptions ν_1,ν_2,... are generally reduced to 1, 2, ... so that a general state $|\{c\}\rangle = |\nu_1, \nu_2, \nu_4\rangle$ is written in the occupation-number formalism according to, for example:

$$|\{c\}\rangle = |\nu_1, \nu_2, \nu_4\rangle \equiv |1_1, 1_2, 0_3, 1_4, ...\rangle \tag{6}$$

The formalism in (6) can be summarized as according to the simple rules

$$n_i = 0 \; if \; i \notin \{c\}$$
$$n_i = 1 \; if \; i \in \{c\}$$

where the index i in the set $\{c\}$ denotes the state ν_i so that for example:

$$\{c\} \equiv \{1, 2, 4\}$$

Note that size of the set of occupation numbers n_1, $n_2...n_S$ in theory is determined by the size, S, of the one-particle basis.

It is clear that this procedure always needs a specified one-particle basis, so that the states in the occupation-number representation always are well-defined.

Going back to the discussion on the ladder-operators $a^\dagger_k$ and a_k it is clear that the occupation-number representation of states is especially convenient when using ladder operators.

The action of these operators in the anti-symmetric Fock-space is defined by[10];

$$\begin{aligned}
a_k\,|n_1, ..., 1_k, ...\rangle &= (-1)^{\left[\sum_{j<k} n_j\right]}\,|n_1, ..., 0_k, ...\rangle \\
a_k\,|n_1, ..., 0_k, ...\rangle &= 0 \\
a^\dagger_k\,|n_1, ..., 0_k, ...\rangle &= (-1)^{\left[\sum_{j<k} n_j\right]}\,|n_1, ..., 1_k, ...\rangle \\
a^\dagger_k\,|n_1, ..., 1_k, ...\rangle &= 0
\end{aligned} \tag{7}$$

The last of these relations is a direct testament of the Pauli principle, stating that two identical fermions can not occupy the same quantum state at one time.

The commutation and anti-commutation relations of ladder operators in the Fock-space

An important state in the Fock-space is the vacuum state $|0_1, 0_2, ..., 0_S\rangle$, which describes a state with no particles given in terms of a one-particle basis of size S.

All possible N-fermion states can be obtained by applying ladder operators to this state according to

$$|\{c\}\rangle = a^\dagger_{c_1} a^\dagger_{c_2} .. a^\dagger_{c_N} |0_1, 0_2, ..., 0_S\rangle$$

The features of the fermionic ladder operators $a^\dagger_k$ and a_k can be summarized in the so-called anti-commutation relations [11];

$$\begin{array}{l} \{a_l, a_k\} = 0 \\ \left\{a^\dagger_l, a^\dagger_k\right\} = 0 \\ \left\{a^\dagger_l, a_k\right\} = \delta_{lk} \end{array} \tag{8}$$

These relations can be said to define the symmetry of the wavefunctions and the discussion on bosons can now proceed from the relations (8).

Just as for fermions the Fock space is ideal in order to describe a many-particle state of bosons, which is also clear from the fact that the expression (5) for the Fock-space also includes the possibility of a totally symmetric space.

The symmetrization of a many-boson wavefunction can be performed by summing over all permutations of the particle-indicies in a simple product-function.

$$\Psi^{sym}_{(v_1,...,v_N)}(x_1, ..., x_N) \propto \varphi_1(x_1)\varphi_2(x_2)\varphi_3(x_3).....\varphi_N(x_N) + \\ \varphi_1(x_2)\varphi_2(x_1)\varphi_3(x_3).....\varphi_N(x_N) + \varphi_1(x_1)\varphi_2(x_3)\varphi_3(x_2).....\varphi_N(x_N) + ...$$

This bosonic wavefunction is know as a "permanent" and fulfills the symmetric requirement for the boson wavefunctions.

Having discussed the second quantization formalism in terms of fermions, I will now only state the counterpart of the anti-commutation relations (8) as they appear for bosons[11];

$$\begin{array}{l} [b_l, b_k] = 0 \\ \left[b^\dagger_l, b^\dagger_k\right] = 0 \\ \left[b_l, b^\dagger_k\right] = \delta_{lk} \end{array} \tag{9}$$

These commutation-relations are a summary of the features of bosons in second quantization and they describe the properties which we associate with bosons, for example the fact the a single-particle state can hold any number of identical particles.

Operators in second quantization

The second quantization representation of single-particle and local two-particle operators are given by [10] as;

$$H_{single} = \sum_{i,j=1}^{\infty} \langle i| h |j\rangle a_i^\dagger a_j$$
$$V_{two} = \tfrac{1}{2} \sum_{ijkl=1}^{\infty} \langle ij| v |kl\rangle a_i^\dagger a_j^\dagger a_l a_k$$

with;

$$\begin{aligned} \langle i| h |j\rangle &= \int \phi_i^* (x) h (x) \phi_j (x) dx \\ \langle ij| v |kl\rangle &= \int\int \phi_i^* (x) \phi_j^* (x') v (x, x') \phi_k (x) \phi_l (x') dx dx' \end{aligned} \tag{10}$$

These operators are defined for the symmetric or anti-symmetric Fock-states in the occupation number representation (6), but their action on an arbitrary many-particle state gives the same results as the first quantization operators.

When the integrals (10) are performed for a given one-particle basis the operators are completely defined, and can be used in the same form independent on the number of particles in the quantum-mechanical system.

3.4 The configuration interaction method

The configuration-interaction method is commonly used in quantum-mechanic simulations in for example atomic or other many-body systems. The main idea is to extend the description of a system by introducing a basis of different configurations in terms of the one-particle wavefunctions, so that eigenstates can be described as linear combinations of these configuration-states.

A system of two interacting particles is of course different from a system of two non-interacting particles in the sense that the interaction perturbs the system where the one-particle states are eigenstates. In the configuration interaction method (CI-method), the one-particle states are used as a starting point for the description.

The basic task is to find eigenvalues b and eigenstates of some operator $\hat{B}$:

$$\hat{B} |b\rangle = b |b\rangle \tag{11}$$

The equation (11) can be rewritten using the completeness relation which states that for any complete set of eigenstates $|a\rangle$, the unit operator $\hat{1}$ can be given in the bracket notation as[12];

$$\hat{1} = \sum_a |a\rangle \langle a| \tag{12}$$

One could then put equation (11) on the form:

$$\sum_{a'}\sum_{a} |a'\rangle \langle a'| \hat{B} |a\rangle \langle a| b\rangle = b \sum_{a'} |a'\rangle \langle a'| b\rangle \tag{13}$$

Since $\{a'\}$ and $\{a\}$ are chosen as sets of eigenstates for the same operator, one defines $|a'_i\rangle = |a_i\rangle$ so that the scalars $\langle a'_i|\, b\rangle$ and $\langle a_i|\, b\rangle$ become equal and relation (13) turns into a matrix-equation:

$$\begin{pmatrix} \langle a'_1|\,\hat{B}\,|a_1\rangle & \langle a'_1|\,\hat{B}\,|a_2\rangle & . & . \\ \langle a'_2|\,\hat{B}\,|a_1\rangle & . & & \\ . & & . & \\ . & & & . \end{pmatrix} \begin{pmatrix} \langle a_1|\, b\rangle \\ \langle a_2|\, b\rangle \\ . \\ . \end{pmatrix} = b \begin{pmatrix} \langle a_1|\, b\rangle \\ \langle a_2|\, b\rangle \\ . \\ . \end{pmatrix} \leftrightarrow Bv_b = bv_b \tag{14}$$

Finding the eigenstates of $\hat{B}$ in terms of the a-basis now reduces to diagonalizing the matrix in (14).

This matrix is in principle infinitely large since the complete basis $\{a\}$ generally has infinitely many orthogonal states Truncation of the description is therefore required.

A limited set of basis states will generally not describe the proper eigenstates but depending on the chosen set it may be a good or a bad approximation.

In many cases the truncated basis set is chosen by applying the variational method. The variational method rests upon the theorem

$$\frac{\langle\tilde{0}|\, H\,|\tilde{0}\rangle}{\langle\tilde{0}|\,\tilde{0}\rangle} \geq E_0 \tag{15}$$

which states that for any arbitrary state $|\tilde{0}\rangle$, the normalized expectation value of the Hamiltonian is always larger than the proper ground state $|0\rangle$[14].

Using the Hylleraas-Undheim theorem [18] the relation (15) can be generalized to excited states, so the variational method also can be applied for other states than the ground state.

Expanding the state $|\tilde{0}\rangle$ in terms of basis states $|a\rangle$, one will get a lower expectation value by including a larger basis set. Depending on the physical quantities one wishes to asses, the convergence of eigen energies is often used to determine the sufficient set of basis functions $|a\rangle$.

There are different ways of performing the truncation for a basis of many-particle states, and one of the more common methods is the energy-cutoff. In this approach the non-interacting many-body Fock-states are cut from the basis depending on their energy, so that the high-energy Fock-states are not included in the description of the low-energy perturbed states.

Another possibility is to truncate the basis depending on the energies of the one-particle states, so that one cuts out all one-particle energy-states over some specific energy. From the specified set of one-particle states all possible many-body Fock-states are then retrieved and used as a basis. [14]

4 Model-Hamiltonian for the quasi one-dimensional harmonic system

In this project I will look at systems modeled by a three-dimensional harmonic trap according to

$$V_{trap}(\overline{r}) = \frac{m}{2}\left[\omega^2 z^2 + \omega_\perp^2\left(y^2 + x^2\right)\right] \tag{16}$$

where ω and $\omega_\perp$ are the trap frequencies in the "axial" z-direction and in the "transeverse" xy-plane, respectively.

The basic Hamiltonian for kinetic and potential energy is then:

$$H = \frac{p_z^2}{2m} + \frac{p_\perp^2}{2m} + \frac{m}{2}\left[\omega^2 z^2 + \omega_\perp^2\left(y^2 + x^2\right)\right] \tag{17}$$

The Schrödinger-equation for such a Hamiltonian is separable, so the energy-eigenfunctions can be written a products of functions $\Psi_z(x)$ and $\Psi_\perp(x,y)$. The energy is then given as $E = E_z + E_\perp$, and for the standard harmonic-oscillator energy-eigenvalues this becomes:

$$E = \hbar\omega\left(\frac{1}{2} + n_z\right) + \hbar\omega_\perp\left(1 + n_\perp\right) \tag{18}$$

Choosing the trap-frequencies so that $\omega << \omega_\perp$, the perpendicular directions will have a much stronger confinement than the axial direction and the trap become "cigar-shaped".[21]

Transitions between "axial states" now happen on a different energy-scale than transitions for the "perpendicular states", and the system can therefore be said to be quasi one-dimensional.

Assuming that the particle-energies are small one can assume that the perpendicular system always is in the ground state, so that small perturbations in the system only cause mixing between axial states.

The low-energy wavefunctions of the total quasi one-dimensional system are then written according to

$$\Psi^{low-E} = \sum_{n_z} c_{n_z} \Psi_z^{n_z}(x)\Psi_\perp^{gs}(y,x) \tag{19}$$

where it is assumed that the excitations between the axial energy-eigenfunctions $\Psi_z^{n_z}(z)$ involve much smaller energies than excitations from the perpendicular ground state. [23]

The quasi-one-dimensional system can now be described by an effective one-dimensional potential given according to

$$V^{1d}(z_1 - z_2) = \int V^{3d}(\overline{r}_1 - \overline{r}_2)\,\left(\Psi_\perp^{gs}(y_1,x_1)\right)^2\left(\Psi_\perp^{gs}(y_2,x_2)\right)^2 dy_1 dy_2 dx_1 dx_2 \tag{20}$$

where implementation of the ground state of the two-dimensional harmonic-oscillator $\Psi_\perp^{gs}(y,x) = \frac{1}{l_\perp\sqrt{\pi}} e^{-(y^2+x^2)/(2l_\perp^2)}$ gives the formula:

$$V(z)^{1d} = \frac{1}{2l_\perp^2\,\pi}\int V^{3d}(\overline{r})e^{-(y^2+x^2)/(2l_\perp^2)}dydx \tag{21}$$

with $l_\perp = \sqrt{\hbar m/\omega_\perp}$.

Here the coordinates were transformed according to $\overline{r}_1 = \overline{R} - \overline{r}/2$ and $\overline{r}_2 = \overline{R} + \overline{r}/2$ so that the integration first is performed over the centre-of-mass coordinates Y and X.[21]

The interaction expression (21) is now given in relative coordinates, something that is especially suitable for interaction-potentials since the relative distance between particles determines the strength of the force.

5 The electric dipole field

In this project I will in particular investigate quasi one-dimensional systems of dipole-dipole interacting particles, and some discussion on this interaction is needed.

The derivation of the classical electric-dipole field can be found in many textbooks on fundamental electromagnetism and it is an important concept for both applications and theoretical understanding of electrostatics. In this derivation of the classical dipole field I have chosen to follow the route of [16], and the figures which I use for explanations are similar to the ones found in this book.

In this derivation I will not deal with the concept of the delta term which in [1] appears as a "balancing" term in the dipole-field, added in order to get a consistent answer from relations such as volume integrals over spheres without internal dipoles. The delta term is said not to contribute to the field away from the site of the dipole, and in this derivation I will therefore omit this discussion. I will however return to the subject of the delta term at a later point in order to discuss the topic in a more mathematical fashion.

The dipole field generally appears as an approximation of more complex fields and it is often defined as the second term in the multipole expansion of a field[1]. In most physical situations the dipole-field is indeed an approximation, since the origin of a physical dipole-field generally is a set of point-particles. In the case of an **ideal dipole** the point-particles can however, as will be described in later sections, be thought of as infinitely close to each other, which intuitively seems to make the approximation of the dipole-field valid at any finite distance from the source.

The starting point of the dipole-field expression is depicted in figure (3) where a system with two point-charges $+q$ and $-q$ is shown. The potential at a point $\overline{r}$ is given as a superposition of the individual Coulomb-potentials from the two point-charges:

$$\Phi\left(\overline{r}\right) = \frac{q}{4\pi\epsilon_0\left|\overline{r}_1\right|} - \frac{q}{4\pi\epsilon_0\left|\overline{r}_2\right|} \tag{22}$$

$\overline{r}_1$ and $\overline{r}_2$ can also be given in terms of $\overline{r}$ and $\overline{d}$ according to:

$$\left|\overline{r}_1\right| = \left|\overline{r} - \tfrac{1}{2}\overline{d}\right| = \sqrt{\left(\overline{r}^2 + \frac{\overline{d}^2}{4} - \overline{d}\cdot\overline{r}\right)} = \left|\overline{r}\right|\sqrt{\left(1 + \frac{\overline{d}^2}{4\overline{r}^2} - \frac{\left|\overline{d}\right|}{\left|\overline{r}\right|}cos\beta\right)}$$
$$\left|\overline{r}_2\right| = \left|\overline{r} + \tfrac{1}{2}\overline{d}\right| = \sqrt{\left(\overline{r}^2 + \frac{\overline{d}^2}{4} + \overline{d}\cdot\overline{r}\right)} = \left|\overline{r}\right|\sqrt{\left(1 + \frac{\overline{d}^2}{4\overline{r}^2} + \frac{\left|\overline{d}\right|}{\left|\overline{r}\right|}cos\beta\right)}$$

For distances $\left|\overline{r}\right| >> \left|\overline{d}\right|$ the expression for the dipole (22) can be approximated using Maclaurin-expansions for the fractions $\frac{1}{\overline{r}_1}$ and $\frac{1}{\overline{r}_2}$[16].

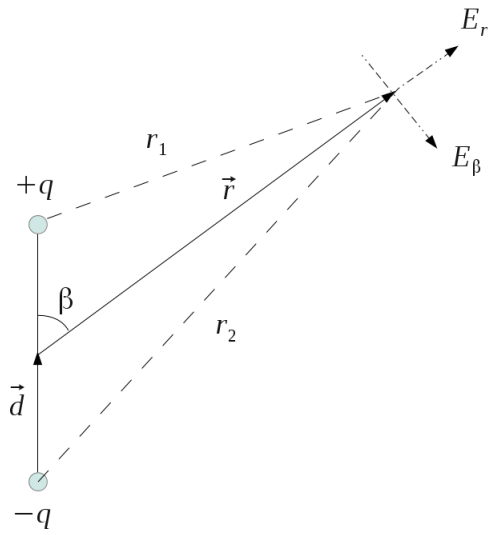

Figure 3: Sketch of a classical dipole as seen in [16]

$$\left(1+\frac{\overline{d}^2}{4\overline{r}^2}-\frac{|\overline{d}|}{|\overline{r}|}cos\beta\right)^{-1/2}\approx 1-\frac{\overline{d}^2}{8\overline{r}^2}+\frac{|\overline{d}|}{2|\overline{r}|}cos\beta$$
$$\left(1+\frac{\overline{d}^2}{4\overline{r}^2}+\frac{|\overline{d}|}{|\overline{r}|}cos\beta\right)^{-1/2}\approx 1-\frac{\overline{d}^2}{8\overline{r}^2}-\frac{|\overline{d}|}{2|\overline{r}|}cos\beta$$

When inserting these approximations into the expression (22) the formula reduces to:

$$\Phi\left(\overline{r}\right)=\frac{q}{4\pi\epsilon_0\left|\overline{r}_1\right|}-\frac{q}{4\pi\epsilon_0\left|\overline{r}_2\right|}\approx\frac{q}{4\pi\epsilon_0\left|\overline{r}\right|}\left(\frac{|\overline{d}|}{|\overline{r}|}cos\beta\right)=\frac{q\overline{d}\cdot\hat{r}}{4\pi\epsilon_0\left|\overline{r}\right|^2}$$

A common definition is also the **dipole moment** $\overline{p}=q\overline{d}$. For a charge-distribution $\rho(\overline{x})$ instead of two point-particles, a more general definition of the dipole moment is given as:

$$\overline{p}=\int\overline{x}'\rho(\overline{x}')d^3x' \tag{23}$$

In [1] this quantity appears as a coefficient in the expansion of a potential $\Phi(\overline{x})$ in terms of spherical harmonics, where (p_x-ip_y) and p_z are coefficients of the spherical harmonics $Y_{1\,0}(\beta,\phi)$ and $Y_{1\,1}(\beta,\phi)$, respectively. In the same way

the coefficient for $Y_{0\,0}(\beta,\phi)$ is given as $\int \rho(\overline{x})d^{\mathbf{3}}x$, which can be interpreted as the total charge q.

Using the dipole moment $\overline{p}$, the potential of the dipole is then given as:

$$\Phi\left(\overline{r}\right) = \frac{\overline{p}\cdot\hat{r}}{4\pi\epsilon_0\left|\overline{r}\right|^2} \tag{24}$$

The dipole-field is now derived from the potential using the relation; $\overline{E} = -\nabla\Phi$. This is most easily done by applying the spherical form of ∇

$$\nabla\Phi = \left(\frac{\partial\Phi}{\partial r}, \frac{1}{r}\frac{\partial\Phi}{\partial\beta}, \frac{1}{rsin\beta}\frac{\partial\Phi}{\partial\phi}\right) \tag{25}$$

and the components of the dipole-field are then given as:

$$\begin{array}{l} E_r = \frac{2|\overline{p}|cos\beta}{4\pi\epsilon_o r^{\mathbf{3}}} \\ E_\beta = \frac{|\overline{p}|sin\beta}{4\pi\epsilon_0 r^3} \\ E_\phi = 0 \end{array} \tag{26}$$

This can be generalized for a dipole at any point of origin $\overline{r}_0$ and rewritten using the vectors $\overline{p}$ and $\hat{r}$, where $\hat{r}$ is a unit vector in the direction from the dipole at $\overline{x}_0$ to the point $\overline{x}$. [1]

$$\overline{E}(\overline{x}-\overline{x}_0) = \frac{3\hat{r}\left(\overline{p}\cdot\hat{r}\right)-\overline{p}}{4\pi\epsilon_0\left|\overline{x}-\overline{x}_0\right|^3} \tag{27}$$

5.1 Energy of a dipole in an external field

In order to evaluate the force acting on a dipole in an external field one can follow the path taken in [1], where one first calculates the electrostatic energy W of a localized charge distribution $\rho(\overline{x})$ in a potential $\Phi(\overline{x})$.

$$W = \int \rho(\overline{x})\Phi(\overline{x})d^{\mathbf{3}}x \tag{28}$$

Providing the charge distribution $\rho(\overline{x})$ extends over a small enough region, so that the potential $\Phi(\overline{x})$ only varies slowly over it, one could expand the potential around a point x_0 according to

$$\begin{array}{l} \Phi(\overline{x}) = \Phi(x_0) + \overline{x}\cdot\nabla\Phi(x_0) + ... \Longleftrightarrow \\ \Phi(\overline{x}) = \Phi(x_0) - \overline{x}\cdot\overline{E}(x_0) + ... \end{array} \tag{29}$$

(Here the relation $\overline{E} = \nabla\Phi$ was used.)

Inserting this into the energy expression (28) one gets:

$$\begin{array}{l} W = \int \rho(\overline{x})\left(\Phi(x_0) - \overline{x}\cdot\overline{E}(x_0) + ...\right)d^{\mathbf{3}}x \\ = \Phi(x_0)\int\rho(\overline{x})d^{\mathbf{3}}x - \overline{E}(x_0)\cdot\int\overline{x}\,\rho(\overline{x})d^{\mathbf{3}}x + ... \end{array} \tag{30}$$

Using the definition of the dipole moment (23) and the expression for total charge q, one can rewrite (30) as:

$$W = q\Phi(x_0) - \overline{p} \cdot \overline{E}(x_0) + ... \tag{31}$$

One could now imagine a system where the external potential $\Phi(\overline{x})$ can be approximated by the first two terms of the expansion (29), and where the local charge distribution $\rho(\overline{x})$ gives zero net charge.

The electrostatic energy of such a system could then be given solely in terms of the dipole energy according to:

$$W = -\overline{p} \cdot \overline{E}(x_0)$$

In the case of a quantum-mechanical system where the dipole moment is represented by a quantum-mechanical object in a state Ψ, one naturally has to find the expectation values of the energy by integrating over possible points of origin x_0 for the dipole;

$$W_{exp} = \int \Psi^*(x_0) \left(-\overline{p} \cdot \overline{E}(x_0)\right) \Psi(x_0) d^3 x_0 \tag{32}$$

It is important to note that the handling of the entire dipole as a particle with a wavefunction Ψ is an approximation which assumes that the binding forces within the dipole acts on a higher energy scale than the interaction between the entire dipole and the external field. If this approximation was not valid the charge distribution $\rho(\overline{x})$ would need to be resolved into its constituent parts, so that the quantum-mechanical system could describe the internal properties of the "dipole" as well.

5.2 The ideal dipole

The followings sections contain discussions on dipole-dipole forces between **ideal dipoles** and I firstly give some different reasons why this situation is especially important.

- The features of ideal dipole-fields can in some cases be confusing, so a summary on the mathematical theory might highlight the relevance of certain properties of point-dipoles.
- It might be possible to create rewarding approximations for systems of non-ideal dipoles by starting from expressions derived for ideal dipoles.
- The program used in all my results was set up for ideal dipoles, so the calculations themselves are in all cases valid for particles which actually are ideal dipoles. In such calculations the details of the dipole-dipole force becomes very important in order to properly describe the physical system, so an investigation of the interaction is necessary.

It should be noted that when simulating molecules and atoms the ideal dipole model fails as an approximation for certain parameters of these simulations, and it will be seen that the details of the dipole-dipole force therefore become redundant in the actual simulations of such particles.

Definitions of an ideal dipole tend to differ slightly between sources. One will often find it described as a limit of two opposite point-charges moving infinitely close to each other[16]. This is a fairly intuitive definition, but for our purposes it is better to define the ideal dipole as the derivative of a point charge density ρ_{point}.

This process is well-described in [5]. Using certain "generalized derivatives" on limiting functions for the delta distribution $\delta^3(\bar{r})$ it is possible to show that the intuitive definition of a dipole in [16] can indeed be represented by a derivative. An ideal dipole taken in the z-direction can be properly described as in (33), where p denotes the constant dipole moment and $\frac{\partial}{\partial z}$ is a generalized derivative.

$$\bar{p}_{dip}(\bar{r}) = -p\frac{\partial \delta^3(\bar{r})}{\partial z} \tag{33}$$

In [5] T.B. Boykin also shows that this distribution, when properly applied to Maxwell's equations, gives back the field of a dipole as described in [1].

5.3 Discussion on the ideal model

When discussing charge distributions as in the previous sections, it is clear that a system of two interacting dipoles has to be handled very carefully. The approximations for both the dipole-potential and the energy of a dipole in an electric field are heavily dependent on the assumption that the dipoles are "very far" apart. The electric-field from a dipole is, as noted before, generally an approximation which is valid at large distances. Also, the energy of a dipole in an external field needs to be derived assuming that the field-strength varies very slowly over the dipole.

Clearly the relevant length scales in these kinds of expressions are dependent on the size of the dipoles themselves, and it is therefore important to investigate how things look if the dipoles are expressed as points in space.

Assuming an infinitely small dipole as the source of an electric field, it is clear that the ideal-dipole field can be used to describe the field-strength at all distances $0 < |\overline{x}|$ from the source.

One should however keep in mind that the infinitely small dipole is expressed in terms of a limit, and that a field-strength evaluated infinitely close to the source must also involve a limit for the distance. *It should be remembered that the limit for the size of the dipole always must be performed before the limit for the distance* $|\overline{x}|$.

The ideal dipole model may be useful in approximation of physical situations, but it also brings forward some mathematical ambiguities which have to be investigated. One should take special care when discussing physical situations in terms of the ideal-dipole model, since the ambiguities for the ideal dipole field will not necessarily be relevant for physical situations. In later sections I will however look at one example where the special features of the ideal dipole gives a clear contribution to the physical quantities.

5.4 Problems when handling point sources

Since the distribution of an ideal dipole is a delta distribution, the source of a dipole field will be a single point in space, and one could therefore expect spherical coordinates to be a good choice when describing the field.

Although spherical coordinates simplify the field expressions it is necessary be careful when handling Maxwell's equations for point sources in this manner [4].

As an example one can look at the Laplace operator, ∇^2, applied to the function $\frac{1}{r}$, where r is a spherical coordinate. One can evaluate this by integrating the expression over a sphere of radius R over the origin,

$$\begin{aligned} &\int \nabla^2 \left(\tfrac{1}{\bar{r}}\right) d^3\bar{r} = \int \nabla \cdot \left(-\tfrac{\bar{r}}{r^3}\right) d^3\bar{r} \\ &= \oint_S \left(-\tfrac{\bar{r}}{r^3}\right) \cdot d\bar{S} = \tfrac{-4\pi R^2}{R^2} = -4\pi \end{aligned} \tag{34}$$

where the divergence theorem has been used in the beginning of the second line.

By the integral representation of the three-dimensional delta function $\delta^3(\bar{r})$ we therefore have;

$$\nabla^2 \left(\frac{1}{r}\right) = -4\pi\delta^3(\bar{r}) \tag{35}$$

One might raise the question if this result can be achieved by some other procedure, not making use of the divergence theorem. In order to find an electric field from Gauss' law of electricity it is tempting to rewrite the nabla operator ∇ in spherical coordinates, so that one can use the spherical form of the Laplacian. This is done in [4] where S.Blinder shows that the use of this type of Laplacian in (35) does not give the expected delta function at the origin.

Since the spherical form of the Laplacian does not seem to give the proper result in the Poisson equation (35), one might ask if electric and magnetic fields derived in this manner are incorrect.

The answer to this question is generally yes, unless special care is taken in order to obtain the behavior of the fields *at* the point of the source.

In the literature this problem is handled in many different ways; In [4] S.Blinder modifies the radial potential by a sign function, giving an infinite derivative at the origin so that the delta source is obtained from Poisson's equation. In sources [7] and [8] Colombeau generalized functions are used to catch the behavior of fields at the source-points, but for my discussion on ideal dipole fields I have chosen to follow the procedure used in [6] where R. Skinner and J. A.Weil use the concept of generalized functions. The concept of generalized functions is discussed in the appendix (14).

5.5 Derivation of the ideal-dipole field

A common expression for the potential for an ideal electric dipole is:

$$\Phi_{dipole}(\bar{r}) = \frac{1}{4\pi\epsilon_0} \cdot \frac{\bar{p}_{dipole} \cdot \bar{r}}{r^3} \tag{36}$$

This potential is a classical function of position, so it is not suitable for describing an ideal dipole potential.

A generalized potential is instead suggested by [6], defining the generalized function ${}^g\Phi_{dipole}$ from $<^g\ \Phi_{dipole} \mid \tau >$ for all smooth test functions τ. The assignment of values for $<^g\ \Phi_{dipole} \mid \tau >$ is in this case defined as below, with the dipole moment $\bar{\mu}$ chosen in the z-direction. The integrals in the definition are volume integrals over the sphere S, where the test functions τ always disappear outside S.

$$< {}^g\Phi_{dipole} \mid \tau > \equiv \int_S \frac{\bar{p}_{dipole} \cdot \hat{r}}{4\pi\epsilon_0}\, \tau\, dr\, d\Omega = \frac{\mid \bar{p}_{dipole} \mid}{4\pi\epsilon_0} \int_S cos\beta\, \tau\, dr\, d\Omega \tag{37}$$

This is a solution to the generalized Maxwell's equations for a point-dipole source, and it can now be used to find the electric field.

The generalized electric field for the dipole is found from the equation:

$$<^g\ E_{dipole} \mid \tau > = - < \nabla\, [{}^g\Phi_{dipole}] \mid \tau > \tag{38}$$

Using (67) this becomes;

$$<^g\ E_{dipole} \mid \tau > = <^g\ \Phi_{dipole} \mid \nabla[\tau] > \tag{39}$$

The assigned values for $<^g\ \Phi_{dipole} \mid \tau >$ where defined through (37), and since $\nabla[\tau]$ is still a smooth test function one can find the assigned values for $<^g\ E_{dipole} \mid \tau >$;

$$<^g\ E_{dipole} \mid \tau > = \frac{\mid \bar{p}_{dipole} \mid}{4\pi\epsilon_0} \int_S cos\theta\, \nabla[\tau]\, dr\, d\Omega \tag{40}$$

One can extend the concept of the test function by defining components τ_i, and allowing a tensor-field $({}^gE_{dipole})_i$. The scalar-product is then defined in the usual way; ${}^g\bar{E}_{dipole} \cdot \bar{\tau} = ({}^gE_{dipole})_i \tau_i$, where Einstein's summation method is implicit. This extension allows a discussion in more than one dimension, where until now the ∇-operator has been defined in one dimension as; $\nabla \cdot F = \frac{d}{dx}F$.

Now (40) can be extended to

$$\left\langle {}^g\bar{E}_{dipole} \mid \cdot \bar{\tau} \right\rangle = \frac{\mid \bar{p}_{dipole} \mid}{4\pi\epsilon_0} \int_S cos\beta\, \bar{\nabla} \cdot \bar{\tau}\, dr\, d\Omega \tag{41}$$

where the dot inside the braket indicates a scalar product between the vector-field and the generalized vector-function $\bar{\tau}$.

Switching to spherical coordinates one obtains; (see [6] for details)

$$\begin{array}{l}\left\langle {}^{g}\bar{E}_{dipole}\ |\cdot\bar{\tau}\right\rangle = \\ \frac{|\bar{p}_{dipole}|}{4\pi\epsilon_0}\int\limits_{S}\left(\frac{\partial(\tau_r\, cos\beta\, sin\beta)}{\partial r}+2\frac{\tau_r}{r}\, cos\beta\, sin\beta+\frac{sin^2\beta}{r}\tau_\beta\right)\, dr\, d\beta\, d\phi\end{array} \tag{42}$$

In this expression I have removed terms that amounts to zero after integration over all angles.

Now, the first of the three terms in (42) is the only one which could actually be evaluated in the limit $r \to 0$, and for this term we perform the integral in r and *then* integrate over all angles. This is allowed since we know that $\bar{\nabla}\cdot\bar{\tau}$ is continuous through the origin.

$$\begin{array}{l}\int\limits_{S}\frac{\partial(\tau_r\, cos\beta\, sin\beta)}{\partial r}dr\, d\beta\, d\phi=\int\limits_{\Omega}\int\limits_{0}^{\infty}\frac{\partial(\tau_r\, cos\beta\, sin\beta)}{\partial r}dr\, d\Omega \\ =\int\limits_{\Omega}cos\beta\, sin\beta\left[\tau_r\right]_0^{\infty}d\Omega=\int\limits_{\Omega}cos\beta\, sin\beta\left(\lim_{r\to 0}\tau_r\right)d\Omega\end{array} \tag{43}$$

Note that the value at $r \to \infty$ disappears since $\bar{\tau}$ is defined to vanish at this limit.

Since the test-function $\bar{\tau}$ is continuous at the origin, one could rewrite the limit in (43) as;

$$\lim_{r\to 0}\tau_r=\tau_x\mid_{r=0}\, sin\beta\, cos\phi+\tau_y\mid_{r=0}\, sin\beta\, sin\phi+\tau_z\mid_{r=0}\, cos\beta$$

This limit is used since the component τ_r cannot be defined in the origin, even though the value $\tau\mid_{r=0}$ is well-defined.

Inserting this into (43) and integrating over the sphere Ω gives;

$$\begin{array}{l}\int\limits_{-\pi/2}^{\pi/2}\int\limits_{0}^{2\pi}cos\beta\, sin\beta\,(\tau_x\mid_{r=0}\, sin\beta\, cos\phi+\tau_y\mid_{r=0}\, sin\beta\, sin\phi+\tau_z\mid_{r=0}\, cos\beta)\, d\phi\, d\beta \\ =2\pi\int\limits_{-1}^{1}-\tau_z\mid_{r=0}\, cos^2\beta\, d(cos\beta)=\frac{-4\pi}{3}\tau_z\mid_{r=0}\end{array} \tag{44}$$

The dipole moment $\bar{p}_e$ was defined to lie along z, so one could simply rewrite $\frac{-4\pi}{3}\frac{|\bar{p}_{dipole}|}{4\pi\epsilon_0}\tau_z$ as;

$$\frac{\bar{p}_{dipole}\cdot\bar{\tau}}{-3\epsilon_0} \tag{45}$$

By symmetry this will hold for any initial direction of the dipole, as one always can define it to lie in the z-direction and choose to perform the integrals in the way it is done in the above.

Now, the remaining parts of the integral (42) are not evaluated, but kept inside the integral. This integral has to be evaluated using a limit for $r \to 0$, so this condition is now implemented as a "rule" for assigning values to $\left\langle {}^{g}\bar{E}_{dipole}\ |\cdot\bar{\tau}\right\rangle$.

This must be the case since the total integral used in the rule for (37) have been split into terms for $r = 0$ and $r > 0$.

The total expression for $\left\langle {}^{g}\bar{E}_{dipole} \mid \cdot \bar{\tau} \right\rangle$ can now be written down as

$$\begin{aligned}
\left\langle {}^{g}\bar{E}_{dipole} \mid \cdot \bar{\tau} \right\rangle &= \tfrac{|\bar{p}_{dipole}|}{4\pi\epsilon_0} \left[\int_S \tfrac{1}{r} sin\beta (2\,\tau_r\, cos\beta + \tau_\beta\, sin\beta)\, dr\, d\beta\, d\phi - \hat{p}_{dipole} \cdot \tfrac{4\pi}{3} \bar{\tau} \mid_{\bar{r}=0} \right] \\
&= \tfrac{1}{4\pi\epsilon_0} \left[\int_S \tfrac{1}{r^3} \left(2cos\beta \mid \bar{p}_{dipole} \mid \tau_r + sin\beta \mid \bar{p}_{dipole} \mid \tau_\beta \right) d^3x - \bar{p}_{dipole} \cdot \tfrac{4\pi}{3} \bar{\tau} \mid_{\bar{r}=0} \right] \\
&= \tfrac{1}{4\pi\epsilon_0} \left[\int_S \tfrac{1}{r^3} \left(2 \left(\bar{p}_{dipole} \cdot \hat{r} \right) \hat{r} + sin\beta \mid \bar{p}_{dipole} \mid \hat{\beta} \right) \cdot \bar{\tau}\, d^3x - \bar{p}_{dipole} \cdot \tfrac{4\pi}{3} \bar{\tau} \mid_{\bar{r}=0} \right] \\
&= \tfrac{1}{4\pi\epsilon_0} \left[\int_S \tfrac{1}{r^3} \left(2 \left(\bar{p}_{dipole} \cdot \hat{r} \right) \hat{r} - \left(\bar{p}_{dipole} - \left(\bar{p}_{dipole} \cdot \hat{r} \right) \hat{r} \right) \right) \cdot \bar{\tau}\, d^3x - \bar{p}_{dipole} \cdot \tfrac{4\pi}{3} \bar{\tau} \mid_{\bar{r}=0} \right] \\
&= \tfrac{\bar{p}_{dipole}}{4\pi\epsilon_0} \left[\int_S \tfrac{1}{r^3} \left(3\hat{r}\hat{r} - 1 \right) \cdot \bar{\tau}\, d^3x - \tfrac{4\pi}{3} \bar{\tau} \mid_{\bar{r}=0} \right]
\end{aligned} \tag{46}$$

where some indermediate steps are added to the basic calculation performed in [6].

Figure (4) can be used to explain the step between the third and fourth line of the equation, by noting that $\hat{\beta}$ is perpendicular to $\hat{r}$.

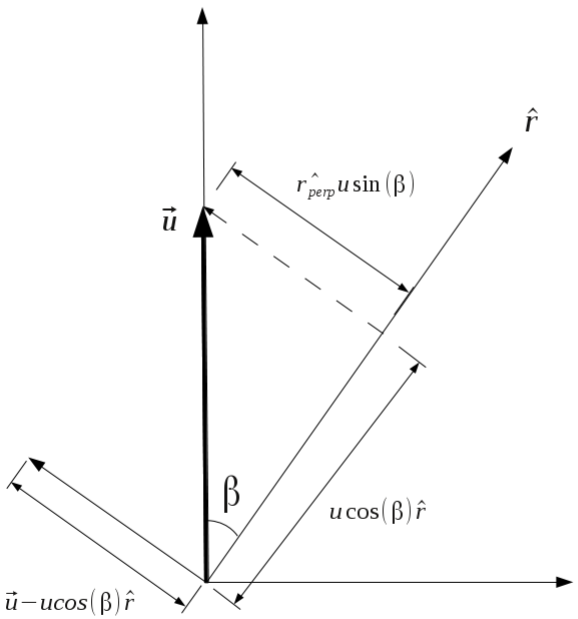

Figure 4: Relation between $\hat{r}_{perp}(u\, sin\beta)$ and $\overline{u} - \overline{u} \cdot \hat{r}$ (46)

The expression (47) is now a mathematically consistent expression for the electric field of an ideal dipole. It should be remembered that the rule for assigning values to $<^g \bar{E}_{dipole} \mid .\bar{\tau} >$ also includes the condition that the integral in the last line of (46) always has to be evaluated in the region $\epsilon < 0$ and that the limit $\epsilon \rightarrow 0$ is then taken.

$$\left\langle {}^{g}\bar{E}_{dipole} \,|\cdot\bar{\tau}\right\rangle = \frac{\bar{p}_{dipole}}{4\pi\epsilon_0}\left[\int_S \frac{1}{r^3}\left(3\hat{r}\hat{r}-1\right)\cdot\bar{\tau}\, d^3x - \frac{4\pi}{3}\bar{\tau}\,|_{\bar{r}=0}\right] \tag{47}$$

The classical expression for the field of an ideal-dipole

In many sources on electromagnetism, for example [1], a symbolic expression for the ideal dipole-field is used.

This symbolic expression can be obtained from the generalized field (47) by molding it into a classical expression;

$$\overline{E}_{dipole} = \frac{1}{4\pi\epsilon_0 r^3}\left[\left(3\hat{r}\left(\bar{p}_{dipole}\cdot\hat{r}\right)-\bar{p}_{dipole}\right) - \frac{4\pi}{3}\bar{p}_{dipole}\delta^3(\bar{r})\right] \tag{48}$$

The classical expression obscures the fact that the field is a generalized expression, and that there are requirements for the test-functions which are used. It is however often handy to use this expression since it give a more intuitive picture of the field, but also since it gives cleaner calculations when dealing with simple problems. When using the expression in the limits $r \to 0$, one should however always keep in mind that it is a generalized function, and that proper derivations of quantities related to the field must be calculated from the real expression.

5.6 interaction energy between two point-distributions

Having obtained a mathematically consistent expression for the field strength from an ideal dipole, one might wonder if it is possible to obtain an expression for the interaction energy between two ideal dipoles.

This would require products between generalized functions, since both distributions are point like. Such products are unfortunately not possible to define in a consistent manner [6], but the problem can still be dealt with by separating the calculations into two different scenarios;

- The distributions are point like and separated.
- The distributions are not separated, but one of them is not point like.

An example of this method is given in [6], where the hyperfine interaction between a point electron and a point nucleus is calculated.

The interaction energy for a system with a magnetic field $\overline{B}(\overline{x})$ interacting with a magnetization density $\overline{M}(\overline{x})$ is given by;

$$W_m = -\int \overline{B}(\overline{x})\cdot\overline{M}(\overline{x})\, d^3x$$

Assuming the field $\overline{B}(\overline{x})$ has a point-source it must be described in terms of a generalized function ${}^{g}\overline{B}$, so by using $\overline{M}(\overline{x})$ as a test function one can define the energy through the number:

$$W_m = -\left\langle {}^g\overline{B}\right| \cdot \overline{M}\rangle \tag{49}$$

Now the problem with two point sources becomes apparent; since a test-function has to be smooth one cannot choose $\overline{M}$ to be a point distribution when calculating values for W_m.

In [6] the problem is dealt with by letting an electron s-wave density distribution $|\Psi_s(\overline{x}-\overline{x}_e)|^2$ describe the the magnetization-density $\overline{M}$ so that;

$$\overline{M}(\overline{x}-\overline{x}_e) \propto |\Psi(\overline{x}-\overline{x}_e)|^2 = \frac{\alpha^3}{8\pi} e^{-\alpha(\overline{x}-\overline{x}_e)}$$

Using generalized functions for the magnetic field $\overline{B}$ it can be shown that the energy for the system has a mathematically consistent formulation, and the energy for the hyperfine interaction between a point nucleus and a magnetization density $\overline{M} \propto \frac{\alpha^3}{8\pi} e^{-\alpha(\overline{x}-x_e)}$ will be dependent on α.

$$W_m \propto \alpha^4 \int F(\overline{x},\overline{x}_e) e^{-\alpha \overline{r}_e} d^3x \tag{50}$$

Here $F(\overline{x},\overline{x}_e)$ is a function dependent on the integration variable $\overline{x}$ and the electron position $\overline{x}_e$, but also on the nuclear and electronic spin operators.

The main point of the relation (50) is however the dependence on α, since this factor determines how the distribution $\overline{M}(\overline{x}-\overline{x}_e)$ looks. The integral in (50) is now only part of the expression for the energy, and the limit $\alpha \to \infty$ can therefore be taken inside the integral. This would not be allowed for the quantity (49) since it would mean that $\overline{M}$ was not a valid test function, but having obtained the expression for the energy with the condition that $|r_e| > 0$ it is now just a matter of handling the integral itself. [6]

The choice for the magnetization $\overline{M}(\overline{x}-\overline{x}_e) \propto |\Psi(\overline{x}-\overline{x}_e)|^2 = \frac{\alpha^3}{8\pi} e^{-\alpha(\overline{x}-\overline{x}_e)}$ now seems very handy. The expression gives unity when integrating over all space and for $\alpha \to \infty$ the expression vanishes at all points expect the origin. These properties can be said to define a delta-function [7], so the integral is now easily evaluated.

Evaluating the integral with $\alpha \to \infty$ and$|r_e| > 0$ gives an energy expression which is not proportional to α.

$$W_{m,\,|r_e|>0} \propto \frac{1}{|r|^3} \tag{51}$$

This energy is in fact the common expression for the electric dipole interaction between an electron and a nucleus at different positions.

In the case where the distance $|\overline{r}_e|$ between the electron and nucleus is equal to zero the integral in (50) must be evaluated in a different manner. Having both $|\overline{r}_e| = 0$ and $\alpha \to \infty$ would give a divergent integral, so α must be kept finite.

The energy-expression for $|\overline{r}_e| = 0$ and finite α is now obtained by evaluating the integral, and it turns out that it depends on α.

$$W_{m,\,|\overline{r}_e|=0} \propto \alpha^{\mathbf{3}}$$

Now one is left with two expressions for the magnetic interaction energy of the electron and nucleus, and the derivation should be performed in a similar way for any situation involving the energy of two interacting point-like objects. The weakness of this formalism is naturally that the calculations always must be performed with a smooth test function, which will give a dependence on parameters like α for the energy expression at certain points. It is however satisfying that such derivations for the energy expression are mathematically correct, and that ambiguous features of point particles are handled correctly.

Looking at the expressions for the interaction energy one could argue that they behave like the symbolic expressions for the dipole field (48). Choosing $\alpha \to \infty$ for $W_{m,\,|\overline{r}_e|=0}$ will naturally result in an expression which gives infinity at just one point, but this is not enough to define a delta function. However, the behavior itself suggests that the delta function which often appears in "bad" derivations of interaction energies actually has some relevance. Therefore I will use the classical expression in this "bad" manner, and find a simple expression for the energy between two dipoles. It is however important to note that the excistance of the delta function in the classical expression is only made plausible by the derivations in the above, it is not actually proved!

Classical expression for the interaction energy between two ideal dipoles with aligned dipole moments

Remembering the final words of the last section I use the dipole-field given by [1], and apply it to the second term in the expression for the interaction energy (31) according to:

$$W(\overline{x}_0) = -\overline{p}_2 \cdot \overline{E}(x_0) = -\overline{p}_2 \cdot \left(\left[\frac{3\hat{r}\,(\overline{p}_1 \cdot \hat{r}) - \overline{p}_1}{4\pi\epsilon_0\,|\overline{x}_0|^3} \right]_{|\overline{x}_0|>0} - \frac{1}{3\epsilon_0}\overline{p}_1\delta^{(3)}(\overline{x}_0) \right) \quad (52)$$

Assuming that $\overline{p}_1 = \overline{p}_2 = \overline{p}$ (aligned dipole moments) the expression reduces to

$$W(\overline{x}_0) = -\left[\frac{d^{\mathbf{2}}\,(3cos^{\mathbf{2}}\beta_{rd} - 1)}{|\overline{x}_0|^3} \right]_{|\overline{x}_0|>0} + \frac{4\pi}{3} d^{\mathbf{2}}\delta^{(3)}(\overline{x}_0) \quad (53)$$

where β_{rd} denotes the angle between the vector $\hat{r}$ and the dipole moment $\overline{p}$, and the interaction coefficient d is defined through; $d^{\mathbf{2}} = \frac{|\overline{p}|^{\mathbf{2}}}{4\pi\epsilon_0}$.

This expression for the energy will now be used in the following, but the ambiguity of the delta term must always be remembered.

5.7 The quasi one-dimensional electric dipole-dipole interaction

Having highlighted the analytic problems the expression (48), it is still valuable to use it as a starting point when discussing dipole-dipole interaction in one dimension.

Section (5.6) ended with a somewhat sloppy expression for the interaction energy of two ideal dipoles with their dipole moments aligned, but I will use this as a starting point for the dipole interaction in one-dimensional systems. Such a system is pictured in figure (5) where it is understood that the z-axis is parallel to the axial direction of the trap.

$$V_{DDI}^{3D}(\bar{r}) = \left[\frac{d^2}{r^3}\left(1 - 3cos^2\beta_{rd}\right)\right]_{r>0} + \frac{4\pi}{3}d^2\delta^{(3)}(\bar{r}) \tag{54}$$

(As discussed before the function is in itself incorrect, but it can still be used in physical simulation.) The ambiguity of this expression lies in the second term, which only gives a contribution at $|\bar{r}| = 0$. For physical models involving spin-polarized fermions this term will therefore not have an effect due to the Pauli principle which states that two spin-polarized fermions with the same quantum numbers cannot be found at the same place. For bosons one can use both terms to perform calculations, but it is important to remember that the results which show strong influence by the second term will indeed be based on an ambigous expression for the dipole force.

The second term of the equation will be referenced as the dipole delta in this project, and its existence has been discussed in the previous sections. The first term is defined, in the relative coordinates, everywhere outside the origin and could in principle be used without any problems. Some ambiguity can however be found when using this expression in order to look at low-dimensional systems, and I will therefore go through the calculation of the quasi one-dimensional force obtained from (54).

The first term is defined for all $r \geq 0$ but it is important to note that it will **not** give uniform convergence for the limiting function $f(x,y) = \lim_{n\to\infty} f_n(x,y)$ with $f_n(x,y) = V_{DDI}^{3D}(x,y,z=\frac{1}{n})$. This fact is a clear weakness of the formula and will be seen to give rise to ambiguities when discussing one-dimensional systems.

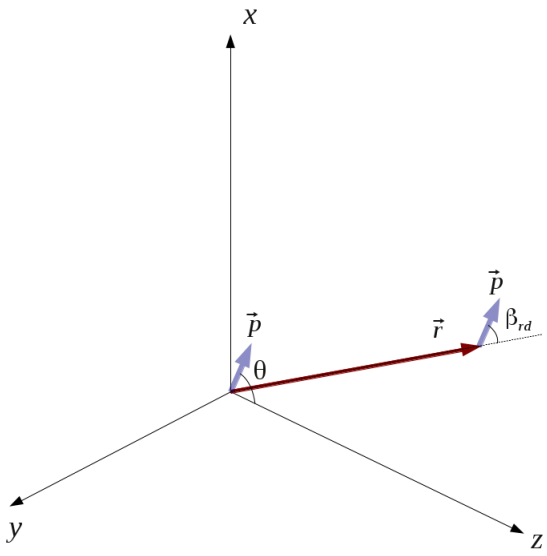

Figure 5: Sketch of two aligned dipoles in three-dimensional space

Parts of the following derivation was also performed in [21],[39] and [38].

As was shown in section (4), one could for circularly symmetric harmonic-trap use the Riemann-integral to obtain an effective one-dimensional potential for the transverse ground state.

Using cylindrical coordinates $\overline{r} = (\varrho cos\varphi, \varrho sin\varphi, z)$ the integral in (21) can be transformed into

$$V_{1D}(z) = \frac{1}{2\pi l_\perp^2} \int_0^{2\pi} d\varphi \int_0^{\infty} d\varrho\, \varrho\, V_{DDI}^{3D}(\varrho cos\varphi, \varrho sin\varphi, z)\, e^{-\varrho^2/(2l_\perp^2)} \tag{55}$$

where the **dipole angle** θ is the angle between the axial direction of the one-dimensional system, the z-axis, and the dipole moments of the particles.

Evaluating the first term, $V^{3D\,T1}$, of the expression $V_{DDI}^{3D}(\varrho cos\varphi, \varrho sin\varphi, z)$ one finds. (See appendix for details)

$$V_{1D}^{T1}(z) = \frac{d^2}{4l_\perp^3}\,(1 + 3cos2\theta) \int_0^{\infty} dw w \frac{w^2 - 2z^2}{(w^2 + z^2)^{5/2}} e^{-w^2/2} \tag{56}$$

Using *Matematica* the primitive of the integrand in (56) is found and the expression for $V_{1D}^{T1}(z)$ becomes;

$$V_{1D}^{T1}(z)/D(\theta) =$$
$$-2\left[\frac{e^{-\frac{w^2}{2}}}{2(z^2+w^2)^{3/2}}\left(\sqrt{2\pi}\left(-\left(z^2+1\right)\left(z^2+w^2\right)^{3/2}\right)e^{\frac{1}{2}(z^2+w^2)}erfc\left(\sqrt{\frac{z^2+w^2}{2}}\right)\right)\right.$$
$$\left.-2\frac{e^{-\frac{w^2}{2}}}{2(z^2+w^2)^{3/2}}\left(z^4+z^2w^2+w^2\right)\right]$$

where $D(\theta) = -\frac{d^2}{8l_\perp^3}(1+3cos2\theta)$. Taking the limits for the primitive function, P, one finds:

$$\frac{V_{1D}^{T1}(z)}{D(\theta)} = -2\left[\lim_{w\to\infty} P - \lim_{w\to 0} P\right] = -2\left(\frac{\sqrt{2\pi}\left(-\left(z^2+1\right)\right)e^{\frac{1}{2}z^2}}{2}erfc\left(\frac{z}{\sqrt{2}}\right) - 2z\right) + 0$$
$$\Longleftrightarrow \frac{V_{1D}^{T1}(z)}{D(\theta)} = \left(\sqrt{2\pi}\left(z^2+1\right)e^{\frac{1}{2}z^2}erfc\left(\frac{z}{\sqrt{2}}\right) - 2z\right) \tag{57}$$

Now, the dipole delta-term, $V^{3D\,T2}$, in (54) should also be integrated to find the total effective one-dimensional interaction. The calculation is performed in the appendix so only the result is given here.

$$V_{1D}^{T2}(z_1 - z_2) = \frac{2d^2}{3l_\perp^2}\delta(z_1 - z_2)$$

The total effective one-dimensional electric dipole-dipole interaction $V_{1D} = V_{1D}^{T1} + V_{1D}^{T2}$ can now be written according to;

$$V_{1D}(z) = D(\theta)\left(\sqrt{2\pi}\left(z^2+1\right)e^{\frac{1}{2}z^2}erfc\left(\frac{z}{\sqrt{2}}\right) - 2z\right) + \frac{2d^2}{3l_\perp^2}\delta(z) \tag{58}$$

with $z = z_1 - z_2$.

Possible pitfalls during the calculation

Having found an expression for $V_{1D}^{T1}(z)$ using *Matematica* it is now time to discuss how the integral (56) should be handled in general. In the beginning of section (5.7) I noted that the limiting function $f(x,y) = \lim_{n\to\infty} f_n(x,y)$ with $f_n(x,y) = V_{DDI}^{3D}(x,y,z=\frac{1}{n})$ was not uniformly convergent. This in an important fact when it comes to evaluating the integral (56), since one needs to think about in what order one is to take the limits. In order to solve the improper integral (56) one could for example define

$$f(w,z,\varepsilon) = \int_0^\infty dw w\frac{w^2-2z^2}{\left(w^2+z^2+\varepsilon^2\right)^{5/2}}e^{-w^2/2} \tag{59}$$

and argue that $\lim_{\varepsilon\to 0} f(w,z,\varepsilon) = \int_0^\infty dw w\frac{w^2-2z^2}{(w^2+z^2)^{5/2}}e^{-w^2/2}$. Now $\lim_{\varepsilon\to 0} f(w,z,\varepsilon)$ describes an integral which is only improper for the limit $w\to\infty$, and by rearranging one gets;

$$f(w,z,\varepsilon)=\int_0^\infty dww\frac{w^2-2\left(z^2+\varepsilon^2\right)}{\left(w^2+z^2+\varepsilon^2\right)^{5/2}}e^{-w^2/2}+2\varepsilon^2\int_0^\infty dww\frac{e^{-w^2/2}}{\left(w^2+z^2+\varepsilon^2\right)^{5/2}} \tag{60}$$

Now, evaluating the first term and taking the limit $\varepsilon\to 0$ gives the same answer as the integral (57). The primitive function of the second term, f^{T2}, is found using *Matematica* so the integral of this term becomes;

$$\begin{array}{l} I^{T2}(z,\varepsilon)= \\ \frac{e^{-\frac{w^2}{2}}}{6(z^2+w^2+\varepsilon^2)^{3/2}}\left(\sqrt{2\pi}\left(z^2+\varepsilon^2+w^2\right)^{3/2}e^{\frac{1}{2}(z^2+\varepsilon^2+w^2)}erfc\left(\sqrt{\frac{z^2+\varepsilon^2+w^2}{2}}\right)\right) \\ +2\left(w^2+z^2+\varepsilon^2-1\right)\Big]_0^\infty \end{array}$$

Now we want to look at the behavior of the second term in (60) when z becomes very small, so we naively choose $z^2=\varepsilon^2$ and let both variables go to zero. The upper limit of the primitive function will amount to zero, but for $w=0$ the second term gives;

$$I^{T2}(\varepsilon^2=z^2)=\frac{1}{12\varepsilon^3}\left(\sqrt{2\pi}2\varepsilon^3e^{\varepsilon^2}erfc\left(\varepsilon\right)+2(2\varepsilon^2-1)\right) \tag{61}$$

Taking the limit $\underset{\varepsilon\to 0}{lim}2\varepsilon^2I^{T2}$ we get;

$$\underset{\varepsilon\to 0}{lim}I^{T2}=\underset{\varepsilon\to 0}{lim}\frac{\varepsilon^2}{3\varepsilon^3}\left(\sqrt{2\pi}\varepsilon^3+(2\varepsilon^2-1)\right)=\underset{\varepsilon\to 0}{lim}-\frac{1}{3\varepsilon}=-\infty$$

so that;

$$\underset{\varepsilon\to 0}{lim}I=-\underset{\varepsilon\to 0}{lim}I^{T2}=\infty$$

Clearly this is a problem, since the first calculation gave a different result. This behavior can itself be understood by noting that when changing the condition $z^2=\varepsilon^2$ to $z=\sqrt{\varepsilon}$ the second term becomes zero:

$$\underset{\varepsilon\to 0}{lim}I^{T2}=\underset{\varepsilon\to 0}{lim}\frac{\varepsilon^{1/2}}{6}(2\varepsilon^2-1)=0$$

In this case it is clear that in the limit $\varepsilon\to 0$ the z-variable is chosen so that it goes to zero infinitely much slower than ε, since $\sqrt{\varepsilon}>>\varepsilon$ for small values of ε.

Due to the uniform-convergence issue discussed earlier, one gets different results depending on in what order one chooses the terms to go to zero. Letting the variable z go to zero before ε gives very different results than the reverse, and in this way it is possible to perform derivations which actually give a delta function for z, so that the result (57) is modified by a angular-dependent delta term.

Such a term can be shown to have large effects on the results of simulations with one-dimensional dipole-dipole interaction, so it is important to establish how one should deal with the problem.

There are a few basic reasons on why one should not expect an angular dependent delta term for the one-dimensional dipole-dipole interaction:

- The expression $V_{DDI}^{3DT1}(\bar{r}) = \left[\frac{d^2}{r^3}\left(1 - 3cos^2\beta_{rd}\right)\right]_{r>0}$ is not defined at zero, so it does not make sense that this expression contributes with a delta term *at* zero for the effective potential.
- When defining the effective potential one wants an expression which is dependent on the distance z, and before looking at any limits of this expression one should make sure that it indeed is the expression we want. If the expression itself is defined through a limit, one should of course perform this limit before using the expression. One has to decide whether to choose a value for z and then finding the energy of the system, or to find an expression depending on z which is evaluated at a later point. One should of course expect infinite energy when one is deciding that $z = 0$ and that the two dipoles lie in the harmonic ground state in the perpendicular directions, but this fact cannot be used in an expression for z. Taking the limits of the transverse integral inside the limit of z is therefore very bad practice, and finding an angular-dependent delta term is a consequence of this.

5.8 Asymptotic expansion of effective dipole-dipole interaction in one dimension

This last point in the discussion of the dipole-dipole interaction is the fact that the long-range behavior might give rise to numerical difficulties. The far-distance limit of the one-dimensional dipole-dipole interaction will therefore be approximated for the simulations in this project. In order to increase the speed of calculations the complementary error function in the expression 73 will be expanded in polynomials according to: (See appendix for details.)

$$V_{DDI}^{1DT1}(z)/D(\theta) \approx \frac{4}{z^3} - \frac{24}{z^5} + \frac{180}{z^7} - \frac{210}{z^9} \tag{62}$$

Part III
Results and discussion

Realization of systems with pure dipole interaction

It has been seen that the concept of Feshbach resonances can be used to significantly alter the scattering length of atoms in optical traps[24].

With tunable magnetic fields it is possible to create a system where the scattering length is increased by more than a factor of ten. This would allow for systems where the inter-particle interaction solely is governed by the comparatively weak dipole-dipole interaction. Using a static or induced dipole moment the properties of a system of electric or magnetic dipoles can be controlled by the alignment of the objects, but also by the size of the dipole moment itself [29].

In this project I have investigated systems of a few electric dipoles in one-dimensional harmonic confinement by tuning the parameters of the effective dipole-dipole interaction.

The quasi one-dimensional system of dipoles and the confinement parameter l_p

Before I present any results I will give a short summary on the essential units and expressions which are used in this part.

In the quasi one-dimensional system the particles are trapped in an anisotropic harmonic trap, giving an effective one-dimensional dipole-dipole interaction according to

$$V_{1D}(z) = D(\theta, d)\left(\sqrt{2\pi}\left(z^2+1\right)e^{\frac{1}{2}z^2}erfc\left(\frac{z}{\sqrt{2}}\right) - 2z\right) + \frac{2d^2}{3l_{\perp p}^2}\delta\left(z\right)$$

where $erfc(z/\sqrt{2})$ is the complementary error-function and $D(\theta, d) = -\frac{d^2}{8l_p^3}\left(1 + 3cos2\theta\right)$.

The dipole moments of the particles gives an electric coupling strength $d^2 = \left(\widetilde{D}\right)^2/(4\pi\epsilon_0)$ where $\widetilde{D}$ is given in units of Debye.

In the following, the energies from the calculations are given in terms of the trap-frequency ω of the one-dimensional trap.

The value of $\omega\hbar$ is set to unity, and the trap anisotropy is described in terms of the parameter λ[21].

$$\lambda = \frac{l_p}{l} = \frac{\sqrt{\hbar/(m\omega_p)}}{\sqrt{\hbar/(m\omega)}} \tag{63}$$

When going to stronger transverse confinement, which equals going to lower values of l_p, the system can be interpreted as elongated in the one-dimensional direction, since we discuss lengths in terms of $u =\mid z \mid /l_p$.

This elongation will be seen when comparing the energy spectra for different l_p, with the energies given in terms of $\hbar\omega$. Because of the elongation the particles have a larger separation in u for small l_p compared to larger l_p, so the effect of interaction between particles will be different for different l_p.

The quasi-potential approximation requires $\omega_\perp >> \omega$, so one must use small values $\lambda \lesssim 0.1$.

When using different values of l_p in the simulations, it is also important to note that the absolute energy of the total system will change, since the ground state energy of the transverse system scales with $\hbar\omega_p = \frac{\hbar^2}{ml_p^2}$.

The energies for the one-dimensional system will always be given in terms of $\omega\hbar$ relative to the ground state of the transverse system, so directly comparing energies for different values of l_p is meaningless. Excitation energies will however still be a useful measure when comparing internal properties of the one-dimensional systems at different l_p . Keeping the transverse confinement fixed one can also directly compare the absolute energies of different three-dimensional systems.

Other effects of the confinement can be discussed with an example:
Look at a harmonic system in one dimension with a Hamiltonian

$$H = -\frac{\hbar^2}{2m}\frac{d^2}{dx^2} + \frac{1}{2}m\lambda\omega_p^2 x^2 + C\frac{1}{\sqrt{x^2+c^2}}$$

where $\omega^2 = \lambda\omega_p^2$.
One could transform this system introducing the coordinate $x = \xi \cdot l_p$, with $l_p = \sqrt{\frac{\hbar}{m\omega_p}}$ so that;

$$\begin{aligned} H &= -\tfrac{\hbar^2}{2m}\tfrac{d^2}{d(\xi l_p)^2} + \tfrac{1}{2}m\lambda\left(\tfrac{\hbar}{ml_p^2}\right)^2(\xi l_p)^2 + C\tfrac{1}{\sqrt{(\xi l_p)^2+c^2}} \\ &= \tfrac{\hbar^2}{ml_p^2}\left[-\tfrac{1}{2}\tfrac{d^2}{d\xi^2} + \tfrac{\lambda}{2}\xi^2 + \tfrac{Cml_p}{\hbar^2}\tfrac{1}{\sqrt{(\xi)^2+(c/l_p)^2}}\right] \end{aligned}$$

From this transformation it is apparent that the elongation of the system, which is represented by $\lambda\omega_p^2$, determines the relative strength of the interaction term. The shape of the confining potential will determine the relative strength of the interaction, so when using different values of l_p for the three-dimensional harmonic oscillator, the systems "response" to the interaction will differ.

In this project the length scale $u = \frac{|z|}{l_p}$ is chosen for the one-dimensional potential, so the interaction is given according to;

$$V_{1D}(u) = D(\theta, d)\left(\sqrt{2\pi}\left(u^2+1\right)e^{\frac{1}{2}u^2}erfc\left(\frac{u}{\sqrt{2}}\right) - 2u\right) + \frac{2d^2}{3l_{\perp p}^2}\delta(u) \qquad (64)$$

The behavior of $V_{1D}(|z|/l_p)/D(\theta,d)$ can be seen in figure(6). For smaller values of l_p the expression decays faster with $|z|$, resulting in a more "local" force.

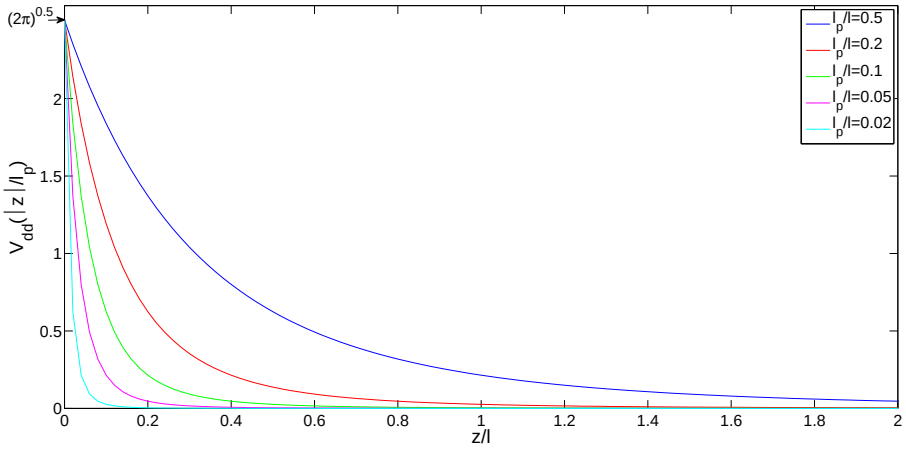

Figure 6: Dimensionless dipole-dipole potential $V_{1D}(|z|/l_p)$

As a starting point of the discussion on my results I will first show a figure published by F.Deuretzbacher et. al. in [21]. Here a general comparison between the energy contributions to the ground state in a system of four particles was shown, and the plot predicts some of the behavior of dipolar particles in a quasi one-dimensional trap. The idea of plotting system properties as functions of the dipole-dipole interaction strength will be widely used in this project, and figure (7) is an example of how such plots can give insight into the system.

The shaded region in this figure shows the so called Tonks-Giradeau regime, where the repulsive dipole-dipole interaction becomes so strong that the overlap

between the interacting bosons is lost. At even higher repulsive interaction this effect causes bosons to somewhat mimic the behavior of fermions, a process known as fermionization [35]. These are some of the effects which can be seen from figure (7), and I shall use this approach to investigate properties of other system.

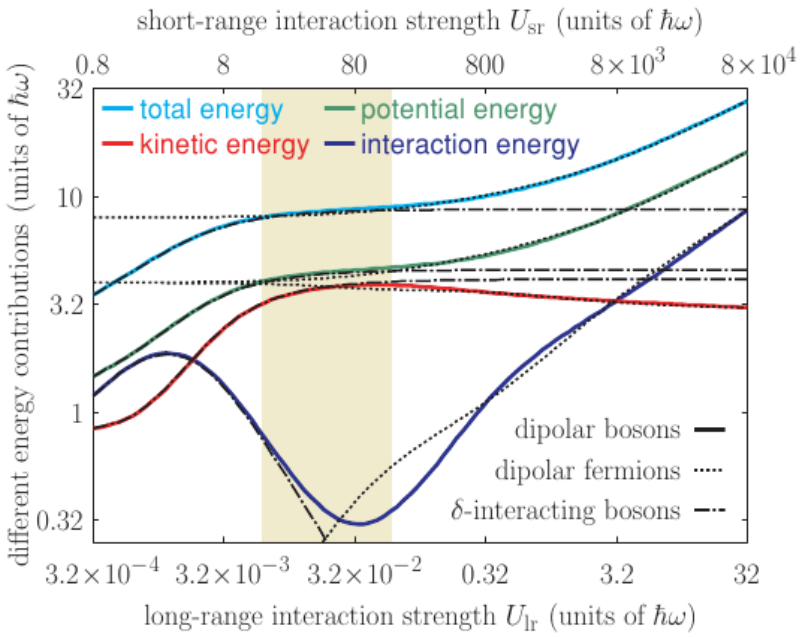

Figure 7: Contributions to the total energy of four particles as a function of the repulsive interactions U_{sr} and U_{lr} obtained for a trap anisotropy of $\lambda = 50$. (From Ref. (63)) [22]. Note that the lost overlap between bosons reduces the interaction energy for $8 \lesssim U_{sr} \lesssim 80$.

In the following sections of this chapter I will discuss some features of the spectra of fermions in a quasi-one-dimensional trap. For clarity some key notions are first stated.

- For the fermion results all calculations are performed with spin-polarized fermions, so that the overlap-dependent delta term of the dipole-dipole force is irrelevant. (See the theory part of the project for details.)
- The factor $D(\theta, d)$ in the dipole-dipole interaction expression (64) is factorized according to: $D(\theta, d) = d^2 \cdot Ang(\theta) \cdot \frac{1}{8l_p^3}$
- The **angular factor** $Ang(\theta) = -(1 + 3cos2\theta)$ in $D(\theta, d)$ only depends on the **dipole angle** θ.
- Due to the angular factor $Ang(\theta)$ in the dipole-dipole force, some dipole angles cause the total expression for the interaction (64) to become zero. The *critical angle* for which the expression amounts to zero is calculated from $Ang(\theta)$ according to:

$$\theta_{crit} = arccos(1/\sqrt{3}) \approx 0.304\pi \approx 54.7^\circ \tag{65}$$

- For dipole angles $\theta > \theta_{crit} \Rightarrow Ang(\theta) > 0$ the mutual interaction term $V_{1D}(x)$ becomes positive, so that the interaction between two dipoles becomes repulsive.
- For dipole angles $\theta < \theta_{crit} \Rightarrow Ang(\theta) < 0$ the mutual interaction term $V_{1D}(x)$ becomes negative, so that the interaction between two dipoles becomes attractive.

A sketch of a one-dimensional system of dipoles is seen in figure (8), where the critical angle θ_{crit} also is shown.

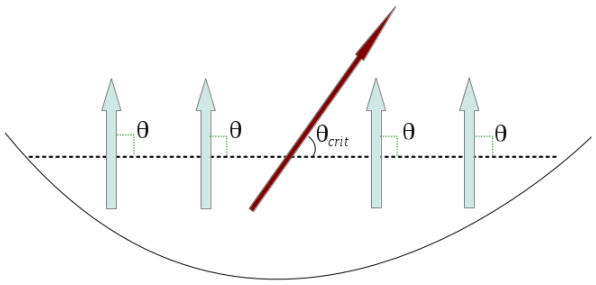

Figure 8: Pictorial view of four dipoles, denoted by blue arrows, at dipole angle $\theta = 90^\circ$ in a one-dimensional harmonic trap. The critical angle $\theta_{crit} \approx 54.7^\circ$ is also shown.

Spectra and density distributions shown in the following sections will be results from calculations performed for dipole angles $0° \leq \theta \leq 90°$. This set of angles is enough to give all possible values of the factor $Ang(\theta)$ where

- $Ang(\theta = 0°) = -4$ gives the *maximum attractive interaction* for a given **interaction coefficient** d^2.
- $Ang(\theta = 90°) = 2$ gives the *maximum repulsive interaction* for a given **interaction coefficient** d^2.

In figure (9) $Ang(\theta)$ is plotted for the dipole angle interval $0.2\pi \leq \theta \leq 0.5\pi$. Note that $Ang(\theta)$ can be approximated to depend linearly on θ for dipole angles $0.2\pi \lesssim \theta \lesssim 0.4\pi$. In the following sections some results will be plotted directly against the dipole angle, since it for $0.2\pi \lesssim \theta \lesssim 0.4\pi$ roughly represents a linear change in the interaction strength.

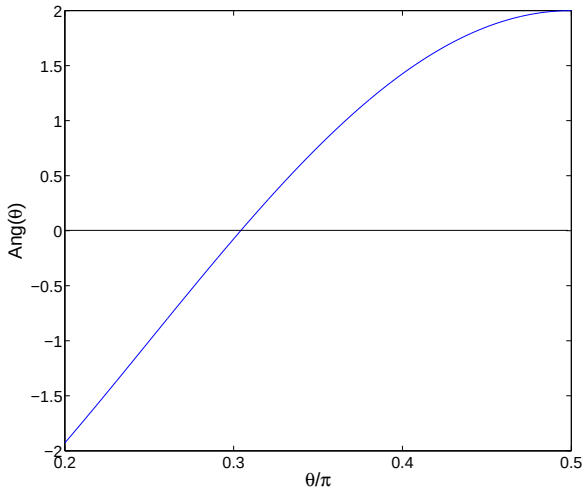

Figure 9: Plot of the angular factor $Ang(\theta)$ which appears in the interaction expression.

In general, a change in the strength of the interaction between two particles changes the energy spectra. The factor $D(\theta)$ in the expression for the one-dimensional dipole-dipole force (64) is dependent on both the **interaction coefficient** d^2 and the **dipole angle** θ. The parameters d and θ can therefore be used to alter the spectra of one-dimensional systems of dipoles.

As noted before, it is possible to do experiments where the interaction is controlled via dipole angle θ, and it should also be possible to tune the interaction via the interaction coefficient d^2 by changing the induced dipole moment [31]. It should therefore be beneficial to investigate properties of the spectra as functions of these parameters.

Work has already been done investigating the ground state properties for quasi-one-dimensional systems of dipoles [29],[21]. Investigating the ground state of such systems has led to a deeper understanding of the effects of dipole-dipole interaction in such systems. In the following I give a few reasons why also analyzing the low-lying energy spectra and the excited states would be beneficial.

- I believe that more insight into the interaction and the system itself can be gained by investigating the low-lying spectra at different values of the dipole interaction. In both atomic and nuclear physics the effects of introducing an interaction into a system are often discussed in terms of, for example, the splitting of degenerate levels, and also in terms of mixing between energy eigenstates. One example is the Zeeman splitting of spin-degenerate energy levels in atoms as a result of a magnetic field. The splitting can be interpreted in terms of the polarization states of the magnetic field[18], showing that specific features of the interaction between the magnetic field and the atom are highlighted when looking at degenerate states. Another example is the Stark effect which gives more insight into the atomic systems themselves, but is also used in techniques which exploit transitions in atoms [33]. I have seen that observables such as the eigen energies are especially useful in order to find different regimes of the dipole-dipole interaction strength, since it often is easier to find clear "signatures" of the different regimes in the spectra than in, for example, the density distributions.

- Some algorithms which are used to find eigenvalues of hermitian matrices can be made more efficient if the eigenvectors themselves are not computed. Algorithms which reduce hermitian matrices to Hessenberg (Tridiagonal) forms can be used in order to solve eigenvalue problems. Such algorithms can be made faster if only eigenvalues are computed, comparing this to calculations where the eigenvectors are also found[36]. It can therefore be beneficial to analyze systems only by looking at the energy spectra and not the eigenvectors.

- For future purposes it might be of interest to look at excited states of a quasi one-dimensional system of dipoles. This might be valuable in order

to investigate transitions between energy levels within the system. When simulating tunneling transport through quasi one-dimensional systems of dipoles the excited states of the systems become important for the descriptions [28], so it should be beneficial to investigate how the excited states dependend on the dipole-dipole interaction.

- It might be possible to create devices which directly exploit the properties of the excited states. The density distributions of particles are interesting for any state of the dipole-system since they can be directly changed by varying, for example, the dipole angle θ. For the numbers of particles I have investigated, $N < 5$, the density distribution for the ground state of a one-dimensional system changes smoothly as a function of increasing dipole-repulsion due to the separation of particles. The density distributions of the excited states can however change rapidly between two dipole angles due to the fact that two levels might cross. The fact that the dipole angle can be tuned in experiments could therefore give interesting results if it is possible to use excited states.

6 Two fermions in a quasi-one-dimensional harmonic trap with weak, $d^2 = 1$, dipole-dipole interaction

The first results in this section will show how some general effects of the dipole-dipole interaction can be discussed in terms of the spectra of the quasi-one-dimensional harmonic system. In particular I will look at the concept of **separation**, which will be described later in this chapter. Separation is one of the key topics in this project, especially since the validity of simulations for bosonic systems relies on this concept. I will investigate how separation can be implied from different results and for different systems of particles. I will begin by discussing separation for fermions, but in later section the techniques for detecting separation will be employed when performing simulations of bosonic systems.

The energy spectrum for two fermions at successively stronger repulsive interaction is shown in figure (10). Stronger interaction is achieved for a fixed d by increasing the dipole angle θ from $\theta = \theta_{crit} \approx 0.304\pi$ to the maximum repulsion angle $\theta = 0.5\pi = 90°$.

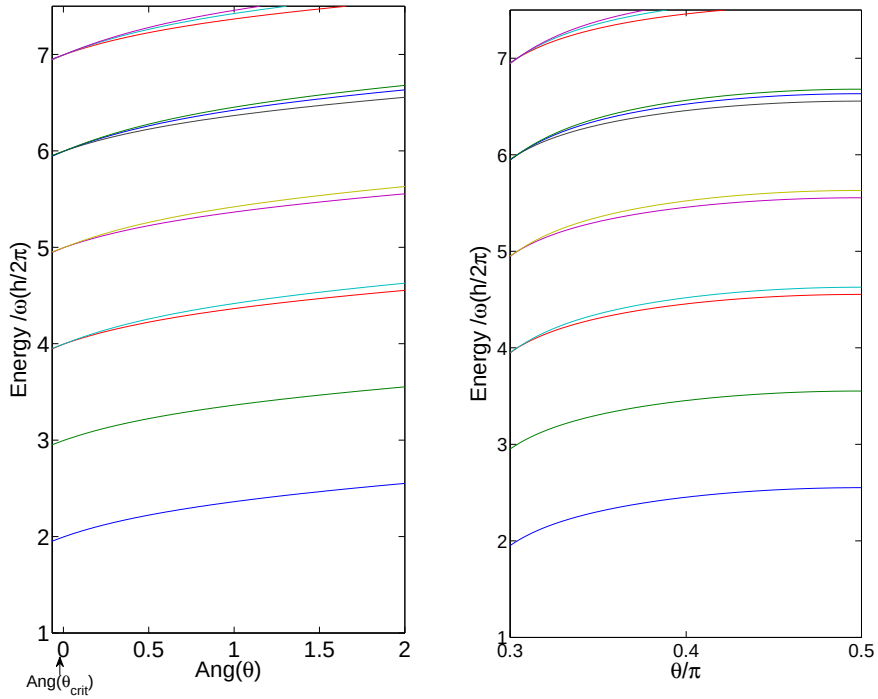

Figure 10: Left: Energy spectrum for two fermions in a pseudo one-dimensional harmonic trap with $l_p = 0.1$ as a function of the angular factor $Ang(\theta)$. (Electric dipole interaction coefficient $d^2 = 1$) Right: Energy spectrum for two fermions in a pseudo one-dimensional harmonic trap with $l_p = 0.1$ as a function of the electric dipole angle θ. (Electric dipole interaction coefficient $d^2 = 1$)

I will in the following discuss a few key results that can be seen from the figure (10):

1. The energies increase as a function of a linearly increasing interaction strength. The energies also grow more slowly, for linearly increasing interaction strength, for $Ang(\theta) \gtrsim 1.5$ than for $Ang(\theta) \lesssim 0.5$.

2. There are degeneracies in the one-dimensional harmonic spectrum which are lost when introducing the dipole interaction.

3. At the critical angle $\theta_{crit} \approx 0.304\pi \rightarrow Ang(\theta_{crit}) = 0$ the energies of the system are those of two non-interacting particles in one-dimensional harmonic oscillator. This is seen directly from the energies at $Ang(\theta) = 0$ in figure (10). At smaller angles $\theta < \theta_{crit}$ the degeneracies will be seen to split due to attractive interaction, and at larger angles $\theta > \theta_{crit}$ the degeneracies are also lost due to repulsive interaction.

6.1 Separation of two fermions seen from the energy spectrum at successively higher interaction

The increase in the energies as functions of the dipole angle in figure (10) shows a specific feature of the dipole interaction. In this figure all the plotted states show the same increase in energy as a function of the angular factor when $Ang(\theta) \gtrsim 1.5$.

One can draw the conclusion that for $Ang(\theta) \gtrsim 1.5$ the effect of the increasing dipole interaction is basically the same for all the plotted states. This feature is also seen when freezing the dipole angle at the maximum-repulsion angle $\theta = 0.5\pi$ and varying the interaction coefficient d^2 as in figure (11).

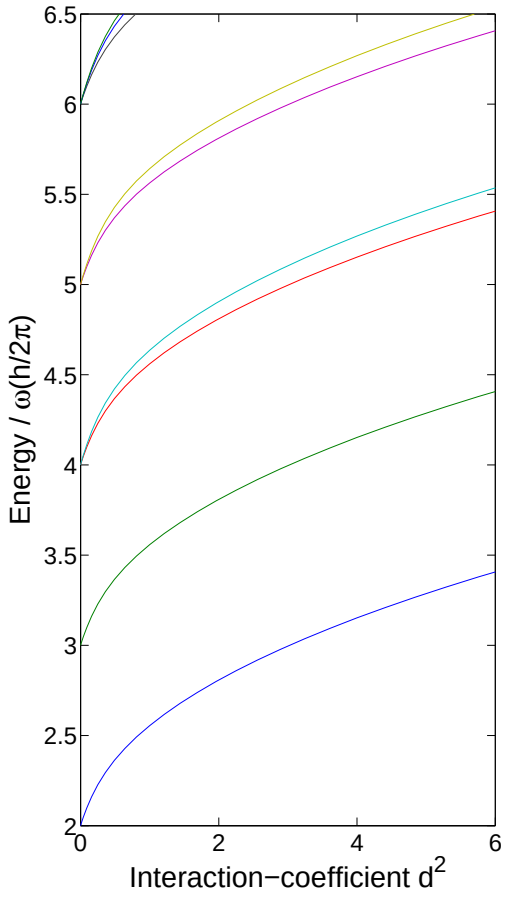

Figure 11: Energy levels 1 to 9 for two fermions in a quasi one-dimensional harmonic trap with $l_p = 0.1$ (Electric dipole angle $\theta = \frac{\pi}{2} \Rightarrow Ang(\theta) = 2$)

Figure (11) shows that for interaction coefficients $d^2 \gtrsim 1.5$ the plotted energy-states all have a similar change in energy for a linear increase in the interaction strength.

The fact that the energy levels all have the same general dependency on the interaction for $d^2 \gtrsim 1.5$ shows that the effect of dipole interaction in this way is similar to the effect of an external potential. For example, adding an external potential V to a Hamiltonian according to $H(x) = H_0(x) + V$ would in the same way raise the energy of all the excited states of H_0 with V.

This behavior is an indication of the **separation** of the states in the system.

Separation

It has been seen that the repulsive short range interaction part of the dipole-dipole force causes dipolar bosons in the ground state of a quasi-one-dimensional harmonic traps to separate[21]. A consequence of this separation is that an increase in interaction energy of the separated ground state, as a result of increasing interaction strength, mainly comes from the long-range dipole-dipole interaction. The separation happens when the short range dipole-dipole interaction becomes so large that the particles separate from each other and therefore feel less of the short range interaction. In figure (12) one can see that the interaction energy relative to the interaction strength of the two-fermion ground state rapidly decays with the interaction coefficient when $d^2 \lesssim 1$, and that it begins to saturate for $d^2 \gtrsim 1$. This is caused by the successive separation of the particles in the ground state at $d^2 \lesssim 1$. The saturation occurs since the long-range interaction in the separated state is much weaker than the short range interaction, so for a state with long-range interaction the quantity E_{int}/d^2 will be comparatively small. For few-fermion systems, $N < 5$, the separation of the ground states be seen directly from the ground state density distributions. The density distribution of an N-fermion ground state generally has N regions of high density which can be interpreted as particles. For increasing repulsive interaction the overlap between these regions is reduced and the repulsion successively causes the regions to separate from each other. For excited states it is not so straightforward to make such interpretations by looking at the density distributions. These states do not generally show N distinct regions of high density which could be interpreted as particles. It is however possible to look at other properties which indicate separation in these states, and I will discuss this in the following sections. I will also make a distinction between separation and other effects, such as localization and high-harmonic-mixing which will be seen in later sections. The separation occurs when there is a clear change in the low-harmonic expansion, $n < 10$, of the wavefunctions, so that the basic shape of the density distribution of particles is altered in order to reduce the short range interaction between particles.

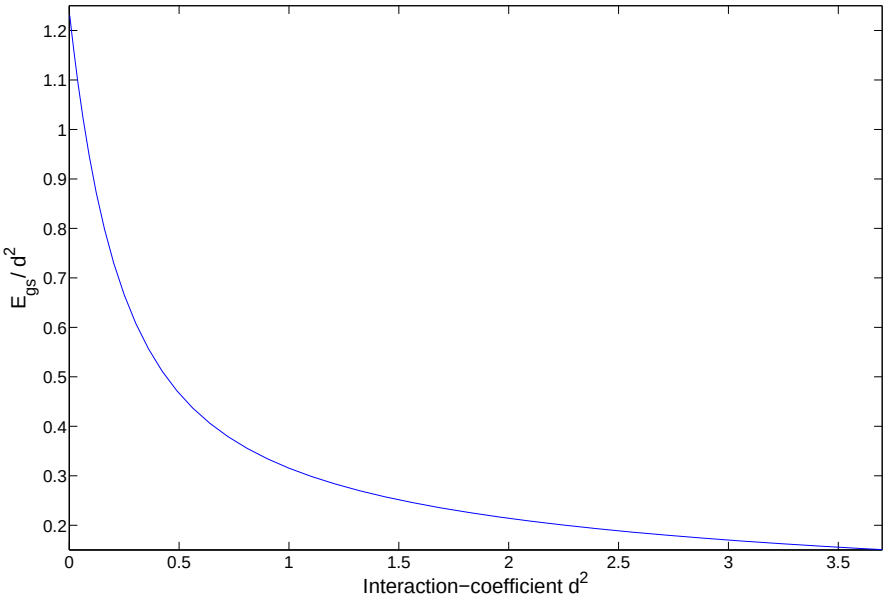

Figure 12: Ground state interaction energy scaled with the interaction coefficient d^2 for two fermions in a quasi one-dimensional harmonic trap with $l_p = 0.1$ (Electric dipole angle $\theta = \frac{\pi}{2} \rightarrow Ang(\theta) = 2$)

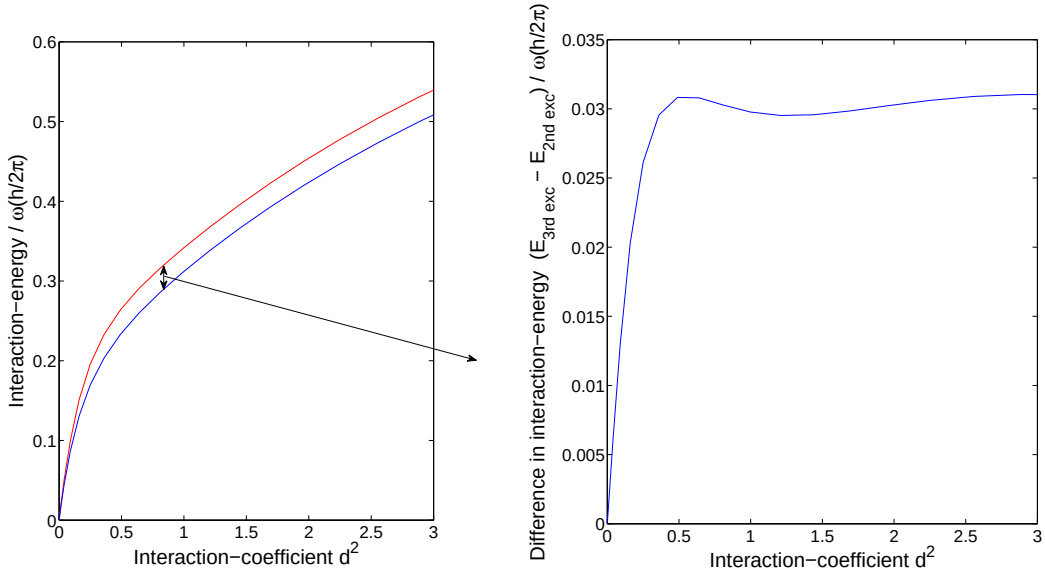

Figure 13: Interaction-energies of the second and third excited state of two fermions in a quasi one-dimensional harmonic trap with $l_p = 0.1$ (Electric dipole angle $\theta = \frac{\pi}{2} \rightarrow Ang(\theta) = 2$)

As noted before, all the states in figure (11) seem to increase linearly with the interaction coefficient d^2 for $d^2 \gtrsim 1$. For $d^2 \gtrsim 1$ all the plotted states also scale with roughly the same factor. So in this interaction regime this means that if the strength of the interaction is increased, all the plotted energy levels are equally affected by the change. This indicates that the increase in interaction energy for the plotted states mainly comes from the long-range dipole-dipole interaction. In figure (13) expectation-values, $\langle \Psi_{2nd\,exc} | H_{int} | \Psi_{2nd\,exc} \rangle$ and $\langle \Psi_{3rd\,exc} | H_{int} | \Psi_{3rd\,exc} \rangle$, of the interaction energy in the second and third excited state are shown. The results support the notion that particles in these states have become separated at $d^2 \approx 1.5$. The interaction energy increases more slowly as a function of the interaction strength for $d^2 \gtrsim 1$ than for $d^2 \lesssim 1$, which suggests that the increase in energy comes from the weaker long-range interaction. Comparing the two different states it is also evident that the difference in interaction energy saturates for $d^2 \approx 1$. This saturation indicates that both states have become separated. How can these statements be explained?

One explanation can be found when looking at the some pair-correlated densities of different excited states for a system with two weakly interacting fermions. A few pair-correlated densities are shown in figure (14) and one can see that the plots differ between the various excited states.

For example, when the reference particle is placed in the center of the trap there is a higher probability of finding two fermions within a "small distance" ($\frac{u}{4} \lesssim 0.5$) from each other for the second excited state than for the third excited state.

Looking at the dipole-dipole potential in figure (6) one can see that such differences should be important in terms of the energy from the short range interaction. The potential of the dipole-dipole interaction has large variations for small distances comparing to large distances. If the probability of finding two particles "close" to each other differs between the states the interaction energy should therefore not be the same when perturbing the system with dipole-dipole interaction.

For the long-range interaction the distance between particles is less important in terms of the interaction energy. This can again be seen from the dipole-dipole potential plotted in figure (6). In the region where the dipoles are "far apart", $\frac{|z|}{l} \gtrsim 1.5$, it is clear that a small difference in distance would only make a small difference in terms of the interaction energy.

Now, the states in figure (11) all depend on the interaction strength in the same way, so the different density distributions of these states do not seem to make much difference in terms of the interaction energy. This indicates that there is only a small probability of finding the two dipoles "close" to each other in any of the plotted states, and that the interaction energy mainly comes from the long-range interaction.

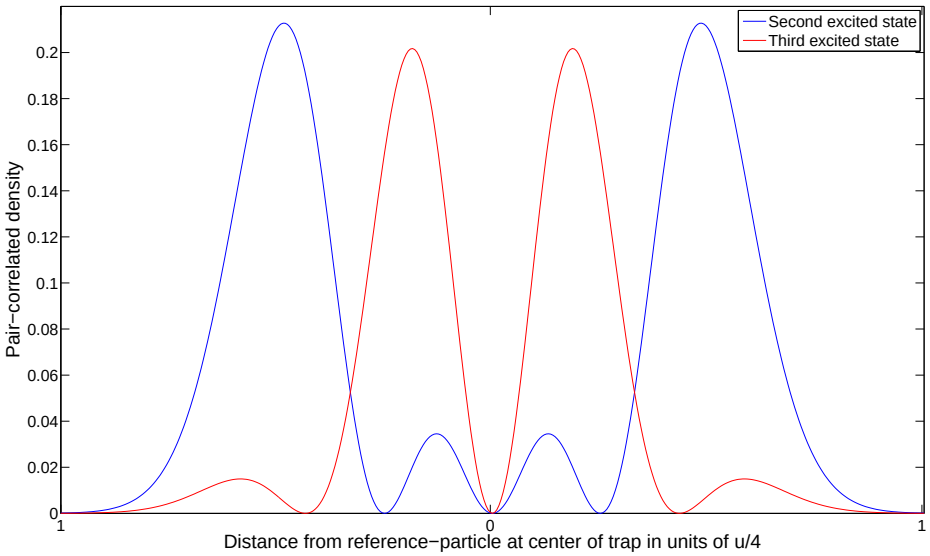

Figure 14: Pair-correlated density distributions for two fermions in a quasi one-dimensional harmonic trap with $l_p = 0.1$ (Dipole angle $\theta = \frac{\pi}{2} \rightarrow Ang(\theta) = 2$ and interaction coefficient $d^2 = 0.01$)

Separation in the two-fermion ground state is also indicated when looking directly at the density distribution in figure (15). One can see that the density distribution change when linearly increasing the repulsive interaction. In this figure the interaction is increased by successively changing the dipole angle θ from the critical-angle $\theta_{crit} \approx 0.304\pi$ to $\theta = 0.4\pi$ which, as discussed before, roughly represents a linear increase in the interaction strength.

From the density distribution of the ground state it is intuitive to interpret the redistribution of matter as separation between two particles; the two regions of high density are pushed apart for successively higher interaction.

The separation of the second and third excited states can also be seen from their pair-correlated particle densities at successively larger repulsion, which both are shown in figure (16). It is clear that for stronger repulsion it is less likely to find two particles close to each other in the center of the trap. The saturation of the energy splitting between these two levels can then be understood from the fact that they are separated and both depend similarly on the long-range interaction.

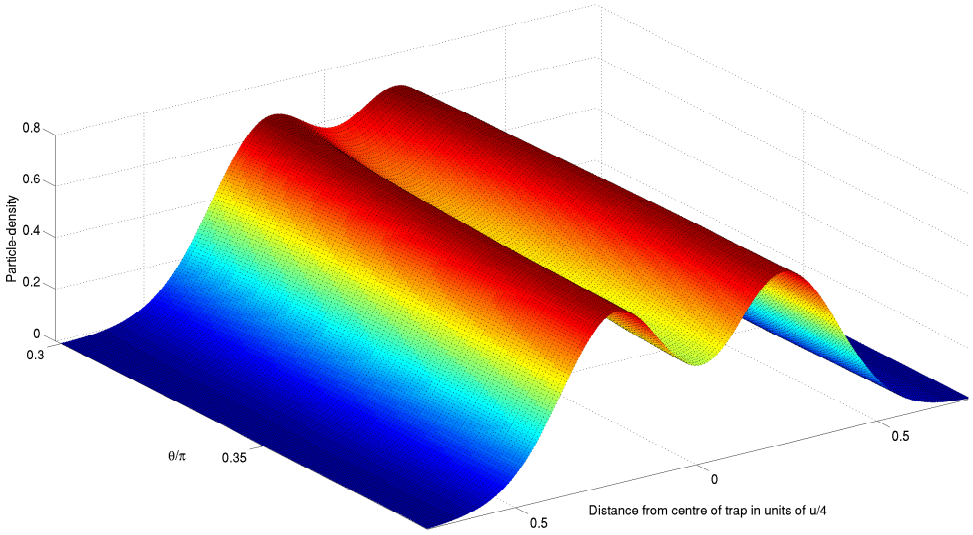

Figure 15: Density distribution for the ground state of two fermions in a quasi one-dimensional harmonic trap with $l_p = 0.1$ (Electric dipole interaction coefficient $d^2 = 1$)

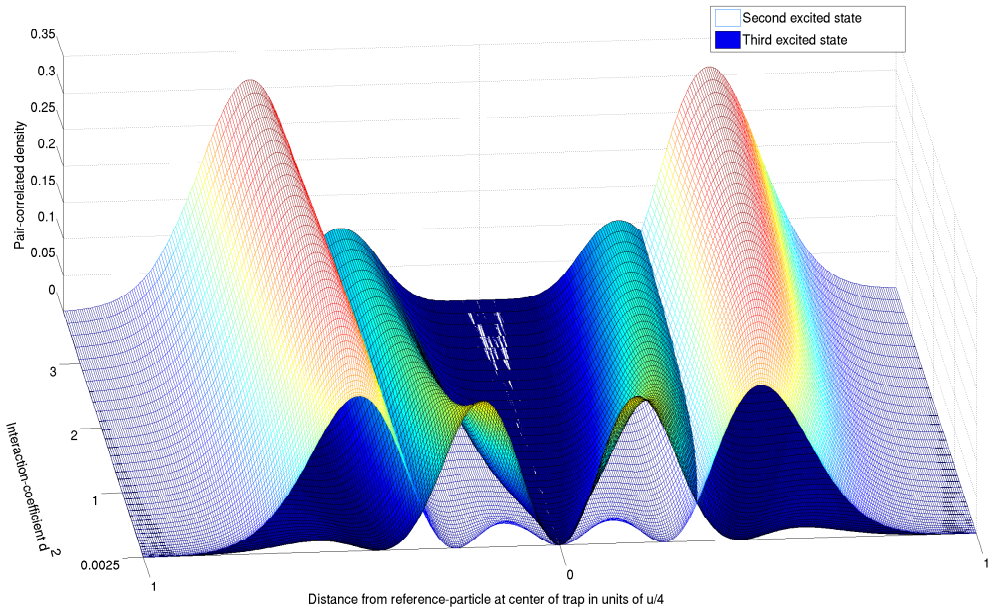

Figure 16: Pair-correlated density distributions for the second and third excited state of two fermions in a quasi one-dimensional harmonic trap with $l_p = 0.1$ (Electric dipole interaction coefficient $d^2 = 1$)

The separation in the excited states can also be seen when comparing results at different transverse confinements l_p, as is done in figure (17). As discussed in section (III) the total energy for states in the three-dimensional system is dependent on the transverse confinement l_p. The energies in figure (17) are therefore given relative to different transverse ground state energies, but can still be used to compare the intrinsic properties of different one-dimensional systems.

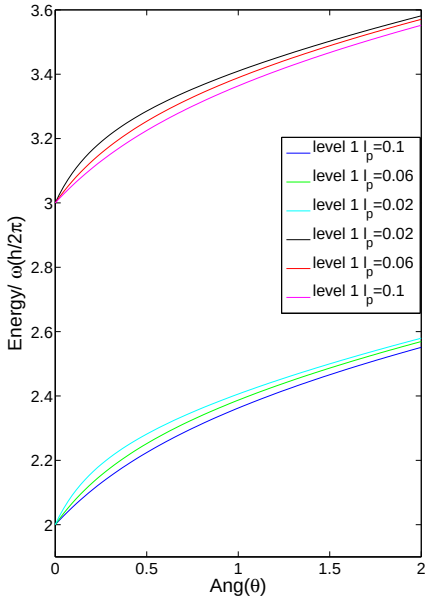

Figure 17: Energy levels 1 and 2 for two fermions in a quasi one-dimensional harmonic trap at different transversely confinements l_p (Electric dipole interaction coefficient $d^2 = 1$) Note that the energies for different transversal confinements are given relative different transverse ground state-energies.

Looking at the potential in figure (6) it is clear that the transversal confinement parameter l_p affects the interaction between two dipoles differently depending on the distance between the dipoles. At "small" distances ($\frac{|z|}{l} \lesssim 0.5$) the potential is more affected by a change in the transverse confinement than at "large" distances $\frac{|z|}{l} \gtrsim 1.5$. From this one might therefore expect the energy of a separated one-dimensional state to be less dependent on the transverse confinement than a state which depends on the short range dipole-dipole interaction. Figure (17) shows that this indeed is the case for a system with two fermions. In previous results it was seen that the ground state and first excited state of the two-fermion system became separated for $d^2 \approx 1$ and $Ang(\theta) \gtrsim 1.5$. Further indications of this separation can now also be seen from figure (17) by noting that the transversal confinement affects the energies, (relative to the transverse ground state), less for $Ang(\theta) \gtrsim 1.5$ than for $Ang(\theta) \lesssim 1.5$.

6.2 Separation and confinement-dependence seen from the splitting of degenerate energy levels

The energy spectrum of two non-interacting fermions in a one-dimensional harmonic trap have degeneracies for all levels above the first excited state. The introduction of the dipole-dipole interaction between particles will cause these degenerate energy-states to split. How could the system of dipolar fermions be analyzed in terms of this splitting?

In figure (18) the energy spectrum for two fermions in shown relative to the ground state energy. Again it is clear that all levels show a similar dependence on the interaction strength for $Ang(\theta) \gtrsim 1.5$. What can be seen from the splitting itself?

- The splitting again indicates **separation** for the excited states in the two-fermion system, which essentially was explained in relation to the previous results. Looking at the right part in figure (18) one can see that the energy levels 7, 8 and 9 are degenerate at the critical dipole angle. For larger angles levels 8 and 9 increase in energy relative to level 7, so the degenerate **"bundle"** of levels is split by the repulsive dipole-dipole interaction. One can also see that the splitting begins to saturate for $Ang(\theta) \gtrsim 1$. This saturation is an indication of the separation between particles as discussed in the previous section. Again the two different states now begin to depend similarly on the dipole-force for $Ang(\theta) \gtrsim 1.5$.

- The splitting between, for example, levels 7 and 9 in the one-dimensional system can be used to show the effect of the transverse confinement l_p. In figure (19) the splitting between these two levels is shown as a function of the angular factor $Ang(\theta)$. As seen in figure (18), the levels 7, 8 and 9 are degenerate at the critical dipole angle $\theta_{crit} = 0.305\pi \Rightarrow Ang(\theta) = 0$, but are split due to the dipole interaction for larger angles. In the following I will call these three levels a "**bundle**" since they lie close in to each other in terms of energy in all my simulations. Comparing the

splitting at different transverse confinements in figure (19) it is clear that lower values of l_p (stronger transverse confinement) causes the splitting to saturate at weaker repulsive interaction than for larger values of l_p. One can explain this by looking at the plot of the potential (6). For $l_p = 0.02$ the comparatively large potential of the short range interaction falls away when the dipoles are further apart than $\frac{|x|}{l} = u \gtrsim 0.1$. For $l_p = 0.1$ the short range interaction falls away at larger distances. For strong transversal confinement particles will therefore feel a strong short range interaction-potential which quickly falls off if the particles separate. This effect can be seen directly from the splitting of energy levels for two fermions in figure (19). The strong confinement causes the particles in the excited states to separate already for weak interaction, and the increase in energy of these states comes mainly from the long-range part of the dipole-force. When the states are separated the energies are therefore similarly dependent on the long-range interaction strength, and the energy splitting saturates. The splitting is in this way a clear indication of the effect of the transverse confinement of the system, and shows how properties in general can be expected to vary as functions of the confinement. For example it should be clear that a strong confinement causes separation to occur at smaller values of d^2 and θ then for weak confinement. This is not unexpected since the interaction factor $D(\theta, d) = -\frac{d^2}{8l_p^3}(1 + 3cos2\theta)$ scales with the inverse of l_p^3. It was however seen in section (III) that other observables of the system might also be dependent on l_p, so the simulations should be valuable in order to establish the effects of l_p. The most important result seen in figure 19 is the fact that stronger transverse confinement causes a "sharper" transition into the separated state. This is important since such sharp transitions makes it easier to categorize a state as separated or not separated. In order to simulate realistic systems of dipoles a separated state is generally required in order for the dipole approximations to be valid, as will be discussed further in later sections. This makes it important to be able to categorize states as separated or non-separated, so a sharp transition between the two might be beneficial.

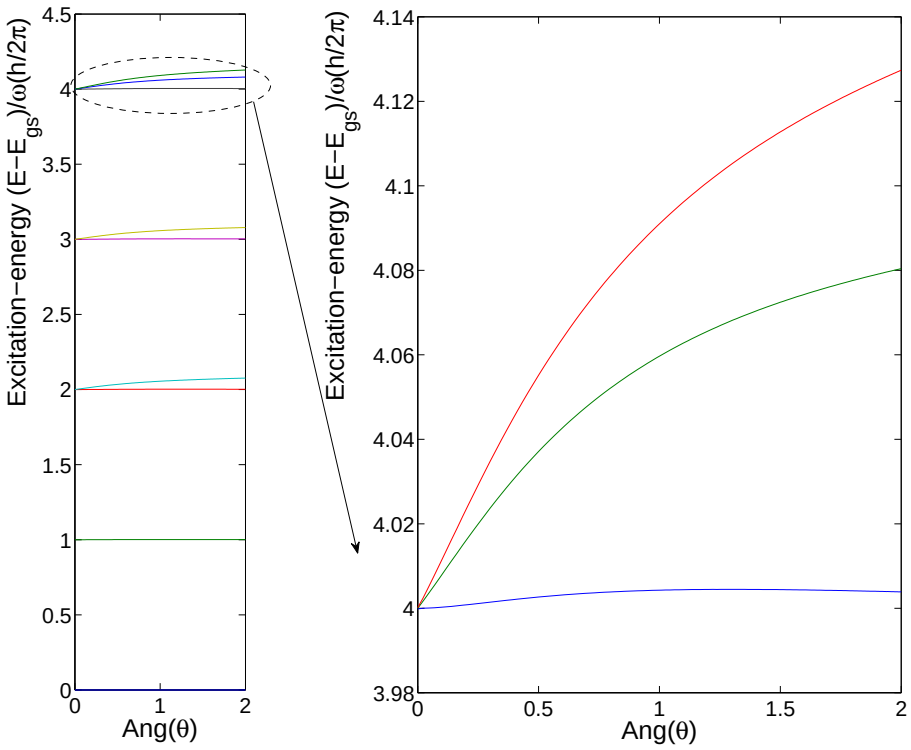

Figure 18: Excitation energies relative the ground state for two fermions in a pseudo one-dimensional harmonic trap with $l_p = 0.06$ (Electric dipole interaction coefficient $d^2 = 1$) Note that in each bundle of energy levels, one level depends on the increasing interaction strength similarly to the ground state. This feature might suggest that these states are collective excitations in terms of the center-of-mass motion [34]. If these states came from such excitations the inter-particle interaction would be similar for all such states, since the states would not differ in terms of the relative distances between particles. I have not seen any evidence that these states indeed come from collective excitations in terms of center-of-mass motion. Investigating these excited states is a possible continuation of this project.

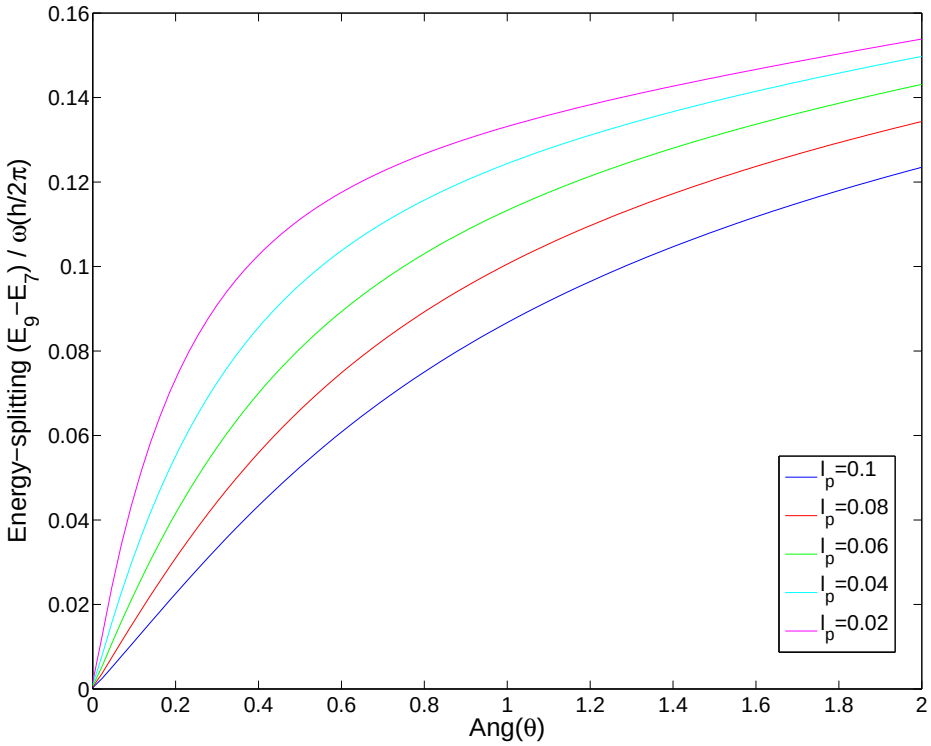

Figure 19: Energy difference between levels 7 and 9 for two fermions in a pseudo one-dimensional harmonic trap with different transversely confinements l_p (Electric dipole interaction coefficient $d^2 = 1$)

6.3 Special features of excited energy levels at the critical dipole angle θ_{crit}

The fact that some energy levels become degenerate at the critical angle θ_{crit} might be important for various reasons.

- The critical angle θ_{crit} can be directly observed from the energy spectra. If it was possible to see the excited states in experiments one could therefore expect that the degeneracy at $\theta = \theta_{crit}$ also can be seen. This fact could possibly be used in order to calibrate the dipole angle θ in experiments. This is however only a suggestion for a possible application of the critical angle, and at this point it is not possible to measure excited states. For this purpose it could also be interesting to see how the transverse confinement l_p affects the point where the energy levels cross. In particular it should be of interest to see if different confinements could make the crossings more pronounced and possibly easier to detect. In figure (19) of the previous section we saw that the successive splitting at $\theta > \theta_{crit}$ between some of the crossing energy levels was steeper for strong transverse confinement. For a steeper crossing between the levels, one could in theory except to make better measurements of the critical angle from the spectra.

- The degeneracy at θ_{crit} has in the case of two fermions been seen to give sharp transitions in *density distributions of energy levels* when passing the critical angle θ_{crit}. For example one can look at the second excited level for the two-fermion system. For dipole angles $\theta = \theta_{crit} - \epsilon$,where ϵ is small, this level has an energy of about $2\,\hbar\omega$. For dipole angles $\theta = \theta_{crit} + \epsilon$ the second excited level has roughly the same energy. The density distribution of the second excited level is however different for these two dipole angles. This can be seen from figure (20) where the density distributions of the second and third excited levels are plotted. The fact that some levels cross at θ_{crit} is interesting. For example, the transport properties of the quasi-one-dimensional system are dependent on the density distribution of the states [37], so one would need to be careful when looking at excited states in such simulations. Results for tunneling transport at a specific "energy windows" of an excited state should because of the crossing at θ_{crit} be very sensitive to values of θ. This can be explained by looking at figure (21). Depending on the value for dipole angles close to the critical angle the transport properties might be very different depending on the density distribution of the "accessed" state.

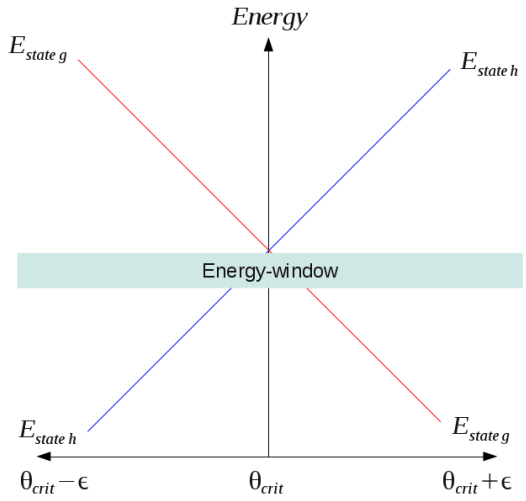

Figure 21: Sketch of two states crossing at the critical angle θ_{crit}. Depending on the value of the dipole angle θ the level in the "energy window" has different density distributions, as seen in figure (20). If the energy window represents a level which is "accessed" in a tunneling transport simulation, the value of θ should be important for the results since the different density distributions in principle would give different transport properties.

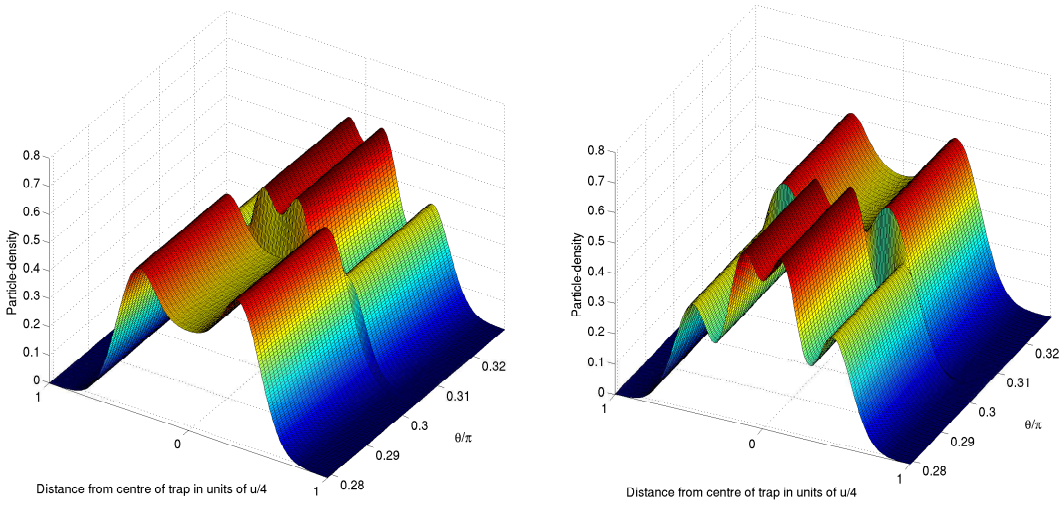

Figure 20: Density distribution of the second (left) and third (right) excited state of two fermions in a quasi one-dimensional harmonic trap with $l_p = 0.1$ (Electric dipole interaction coefficient $d^2 = 0.0625$)

- The way different density distributions are affected by the dipole-dipole interaction is by their behavior around the critical angle θ_{crit}. In figure (22) the energy levels 7, 8 and 9 are shown for a number of different dipole angles θ. For angles $\theta < \theta_{crit}$ the dipole-dipole interaction between the two fermions is attractive. The change from repulsive to attractive interaction can be seen directly from the crossing energy levels in figure (22). In this figure I define the **states** g,h and i. As noted before, these states could possibly be labeled in terms of some conserved quantum number, but for this discussion it is only necessary to distinguish between them in terms of their different density distributions. The density distributions do not change much for the weak interaction, $d^2 = 0.0625$, used to obtain the results shown in figures (22) and (23). I will therefore discuss these distributions in terms of states which become perturbed by weak dipole-dipole interaction. In figure (22) the states labeled h and i increase in energy relative state g for successively larger angles $\theta > \theta_{crit}$, i.e. for linearly increasing repulsion. The states h and i are therefore more affected by the short range repulsive interaction than the state g. These density distributions should therefore also be more affected by the attractive interaction, since the particles in general are found closer to each other in these states. The expression for the attractive potential is the same as for the repulsive potential, only with a different sign. For attractive interaction the states h and i will therefore have lower energies than the state g. The density distributions of **energy levels** 7 and 8 are compared in figure (23). Note that the crossing of states g and i can directly be seen in the density distribution of the sixth excited level. An important result seen from figure (22) is that the confinement parameter l_p affects states differently. It has already been seen that level g is less dependent on the strength of the interaction than levels i and h. This also causes level g to be less affected by a change in the confinement than levels h and i, which can be seen by the fact that the energies of states h and i change more relative to the ground state when changing the confinement l_p.

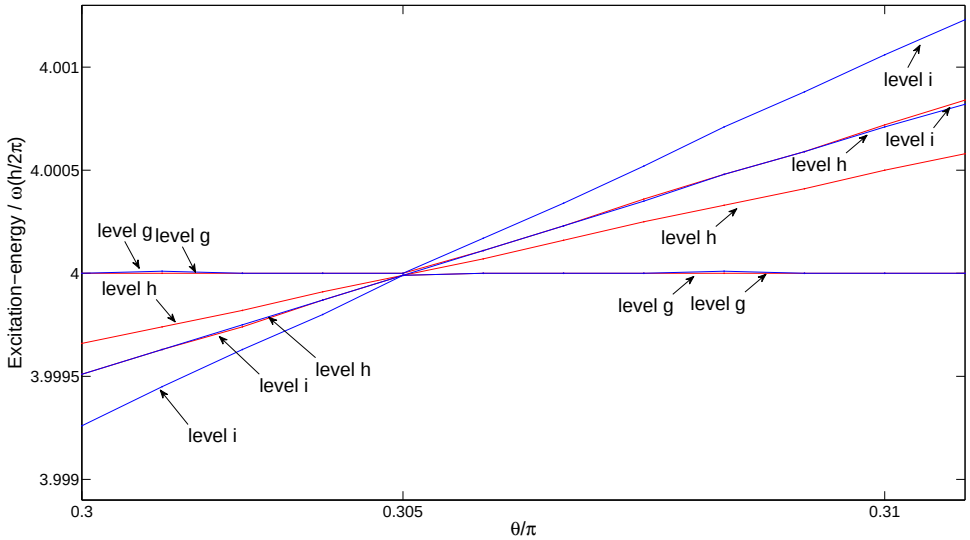

Figure 22: excitation energies for levels g,h and i, (levels 7,8,9 in the repulsive region) for two fermions in a quasi-one-dimensional harmonic trap with $l_p = 0.1$ (red) and $l_p = 0.08$ (blue), (Electric dipole interaction coefficient $d^2 = 0.0625$)

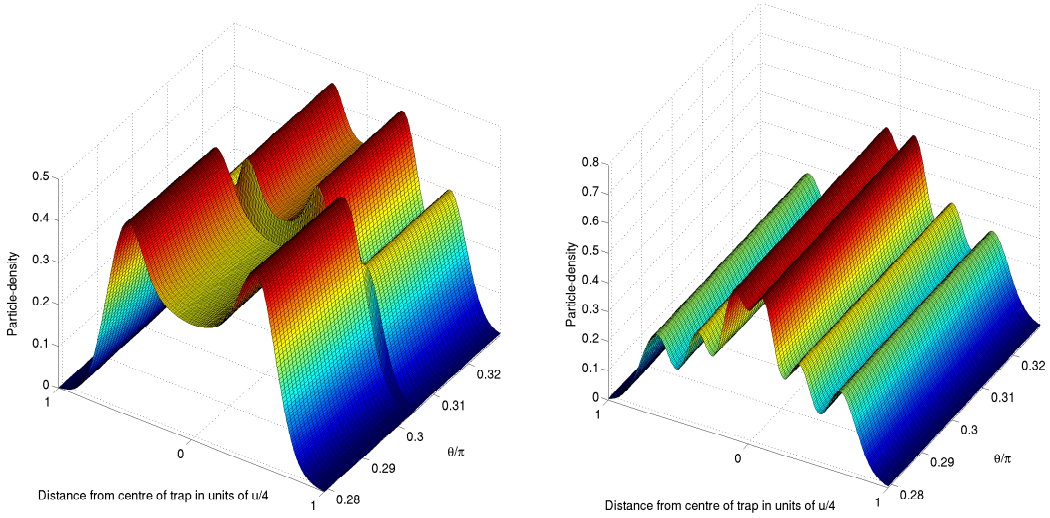

Figure 23: density distribution of the sixth (left) and seventh (right) excited state of two fermions in a quasi one-dimensional harmonic trap with $l_p = 0.1$ (Electric dipole interaction coefficient $d^2 = 0.0625$)

7 Three fermions in a quasi-one-dimensional harmonic trap with weak, $d^2 = 1$, dipole-dipole interaction

In the following some of the simulations which were performed for two fermions will be done for three fermions. In my simulations it has in general been harder to reach convergence for three particles than for two particles. Because of this issue I have not performed simulations with attractive interaction for more than two particles, so the discussion regarding crossing energy levels is in this project limited to two particles.

As in the beginning of section (6) I will first outline the key results seen from the three-fermion energy spectrum at different dipole angles in figure (24). These results are published in order to show that what was seen for two particles also can be seen for higher numbers of particles.

1. The plotted energies increase as a function of a successively larger interaction strength. The energy also grows more slowly for $Ang(\theta) \gtrsim 1.5$ than for $Ang(\theta) \lesssim 0.5$.

2. There are degeneracies in the one-dimensional harmonic spectrum which are lost when introducing the the dipole interaction.

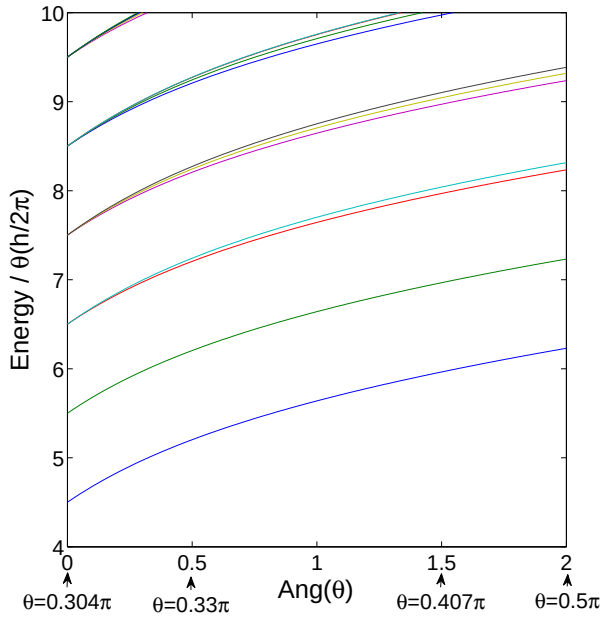

Figure 24: Energy spectrum for three fermions in a quasi one-dimensional harmonic trap with $l_p = 0.1$(Electric dipole interaction coefficient $d^2 = 1$)

7.1 Separation of three fermions seen from the energy spectrum at successively higher interaction

For two particles it was seen that repulsive dipole-dipole interaction caused the energy-eigenstates of the quasi-one-dimensional system to separate.

In figure (24) all the plotted states show the same increase in energy as functions of the linearly increasing interaction strength when $Ang(\theta) \gtrsim 1.5$.

In section (6.1) this behavior was related to the **separation** of the energy eigenstates. Using the same reasoning as in section (6.1) it seems like the states in the low-lying spectra of three fermions also become separated.

The separation can also be seen directly from the density distribution of the ground state in figure (25). For $d^2 = 1$ one can see that there is a change in the ground state density distribution when increasing the dipole angle from θ_{crit}, and that the three regions of high density become pushed apart for successively higher dipole-dipole repulsion. The density distributions of a few excited states are also shown in the same figure. As noted in section (6.1) the interpretation of these density distributions in terms of separation of particles is less intuitive than for the ground state. However, one can see that the density distributions change in the plots, and since the energy spectrum indicates separation also for these states one can draw the conclusion that the redistribution of matter serves to decrease the short range interaction between the particles.

7.2 Separation seen from the splitting of degenerate energy levels

In figure (26) the excitation energies relative to the ground state are plotted for a system with three dipolar fermions at different dipole angles $\theta > \theta_{crit}$. One can see that the splitting begins to saturate for $Ang(\theta) \gtrsim 1$. This behavior was also seen for a system with two fermions where it was related to the separation on the energy eigenstates of the quasi-one-dimensional system. The discussion in section (6) can also be used to interpret the results for three particles since the reasoning in section (6.1) is not limited to a system of two particles.

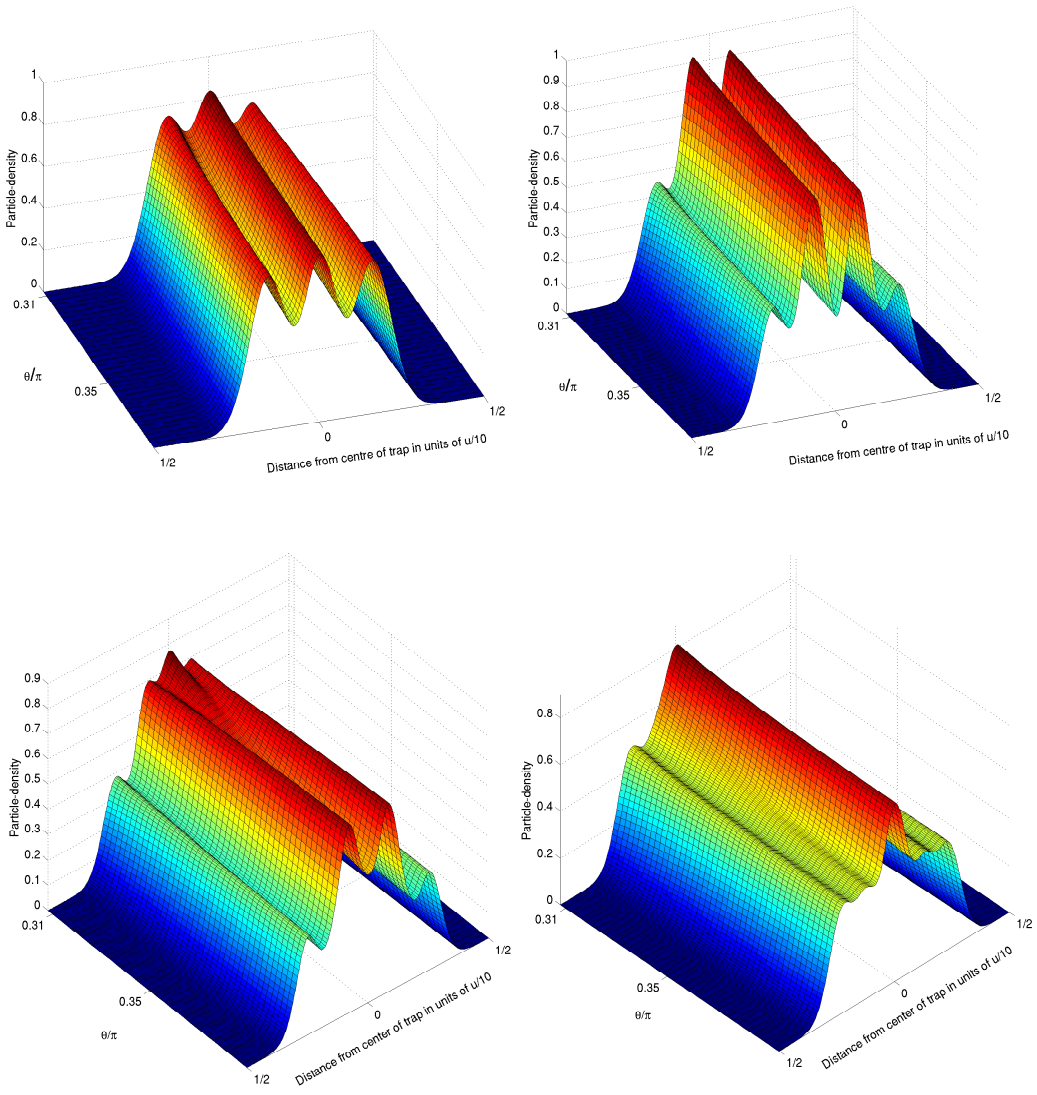

Figure 25: Upper: Density distribution of the ground state (left) and first excited state (right) for three fermions in a quasi one-dimensional harmonic trap with $l_p = 0.1$ (Electric dipole interaction coefficient $d^2 = 1$) Lower: Density distribution of the second excited state (left) and third excited state (right) for three fermions in a quasi one-dimensional harmonic trap with $l_p = 0.1$ (Electric dipole interaction coefficient $d^2 = 1$)

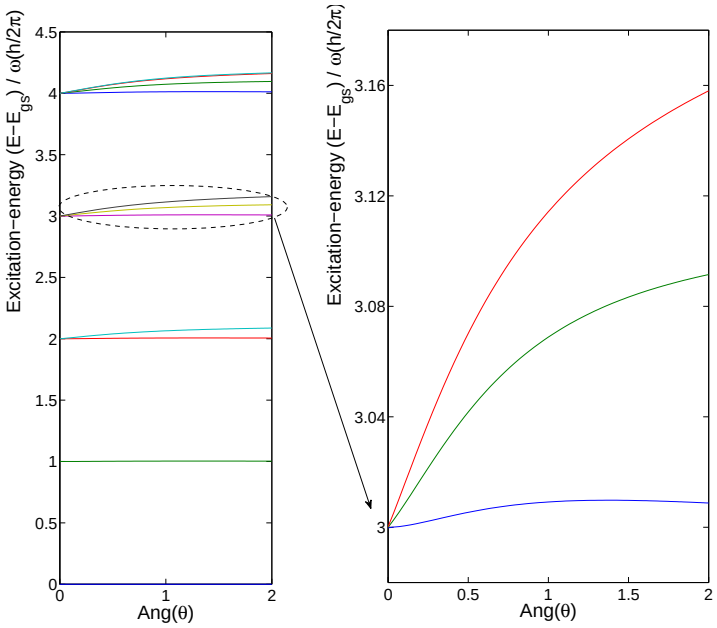

Figure 26: Excitation energies relative to the ground state for three fermions in a quasi one-dimensional harmonic-trap with $l_p = 0.1$. (Electric dipole interaction coefficient $d^2 = 1$) Again note that some states have similar short range interaction dependence as the ground state. This was also seen for two fermions and was briefly discussed in relation to figure (18).

8 Four fermions in a quasi-one-dimensional harmonic trap with weak, $d^2 \approx 1$, dipole-dipole interaction

8.1 Separation of four fermions seen from the energy spectrum at successively higher interaction.

The low-lying energy spectrum of four fermions for different angular factors $Ang(\theta) \geq 0$ is shown in figure (27). One can again see that that all the plotted states show the same general increase in energy as a function of the dipole angle when $Ang(\theta) \gtrsim 1.5$.

In figure (28) one can, for $d^2 = 1$, see how the density distribution of the ground state separates for successively larger dipole angles θ.

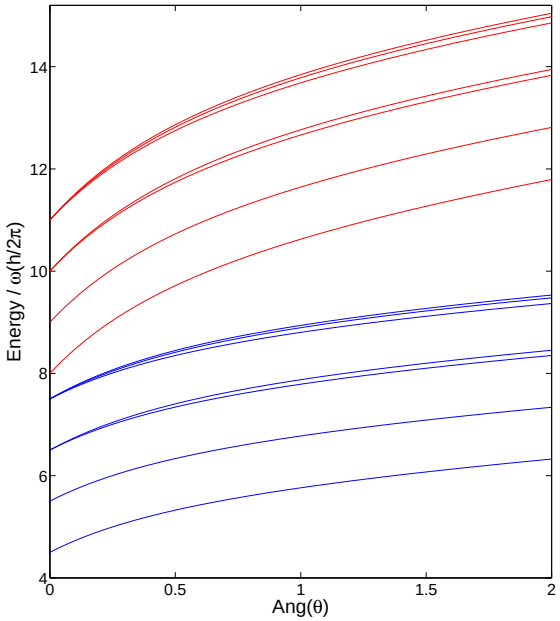

Figure 27: Energy levels 1 to 7 for three (blue lines) and four (red lines) particles in a quasi-one-dimensional harmonic trap with $l_P = 0.06$ (Electric dipole interaction coefficient $d^2 = 1$)

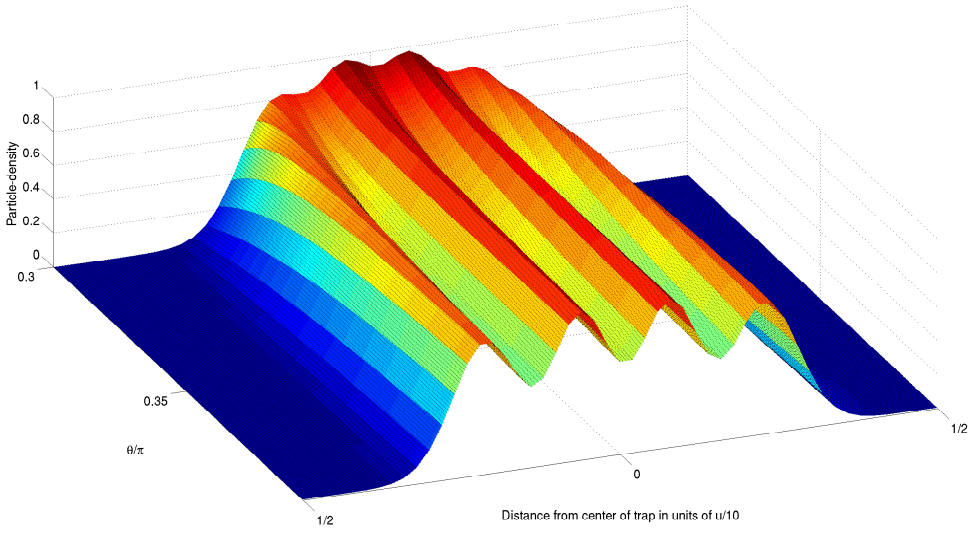

Figure 28: Density distribution of the ground state for four fermions in a quasi one-dimensional harmonic trap with $l_p = 0.06$ (Electric dipole interaction coefficient $d^2 = 1$)

8.2 Separation seen from the splitting of degenerate energy levels

Figure (29) shows that the splitting saturates for sufficiently large repulsive dipole-dipole interaction.

As was the case for two and three particles one can again argue that this is an effect of the separation in the states of the low-lying spectra.

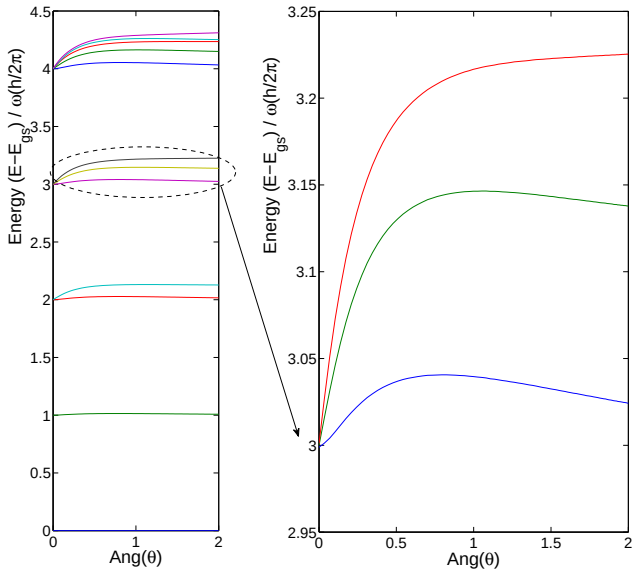

Figure 29: Excitation energies relative to the ground state for three fermions in a quasi one-dimensional harmonic-trap with $l_p = 0.02$. (Electric dipole interaction coefficient $d^2 = 1$)

9 Localization of fermions in a quasi-one-dimensional harmonic trap with strong, $d^2 \rightarrow 100$, dipole-dipole interaction

In the previous sections it has been seen that for weak, $d^2 \approx 1$, repulsive dipole-dipole interaction the the low-lying energy-eigenstates for $N < 5$ fermions become separated. The separation serves to reduce the short range interaction energy between particles in the states, which for two fermions was discussed in some detail in section (6.1). It was seen that for two, three and four fermions the splitting of degenerate energy-eigenstates can indicate separation of the particles also in the excited states. Figure (24) showed that the splitting of the degenerate energy levels for three fermions began to saturate at weak dipole-dipole repulsion. What happens at higher repulsive interaction?

The splitting of degenerate states at stronger repulsive interaction is shown in figure (30). According to this figure the splitting does not saturate entirely, but continues to grow for a successively larger interaction coefficient d^2. This behavior is caused by the long-range dipole-dipole interaction in the states of the quasi-one-dimensional system. The particles in these states were pushed apart already for weak interaction, so at these interaction strengths there is very little short range interaction between particles. There is however still long-range interaction between particles in the states. Compared to the short range interaction the long-range part of the dipole-dipole force affects the different states similarly, so the splitting grows more slowly in the long-range interaction regime.

Because of the long-range interaction the density distributions continue to change with the interaction after the particles have become separated, something that can be seen directly for three particles in figure (31). For the ground state and the third excited state one can see that the particles are separated into three regions which are pushed further and further apart for stronger interaction. In a system of four bosons it has been seen that for increasing long-range interaction these density-regions also become more and more "localized" at their respective positions. In this way the long-range interaction energy was reduced, since the particles were localized as far from each other as possible. The localization is a special feature of the long-range interaction, since the initial separation has greatly reduced the short range dipole-dipole force in this regime.

At interaction coefficients $d^2 \gtrsim 50$ the first excited state also begins to become separated into three regions of higher density, and for $d^2 \gtrsim 100$ this also seems to be the case for the second excited state. The figures indicate that for a sufficiently strong repulsive dipole-dipole interaction, the particles in these states will become separated into three regions which are pushed further and further apart for successively higher interaction.

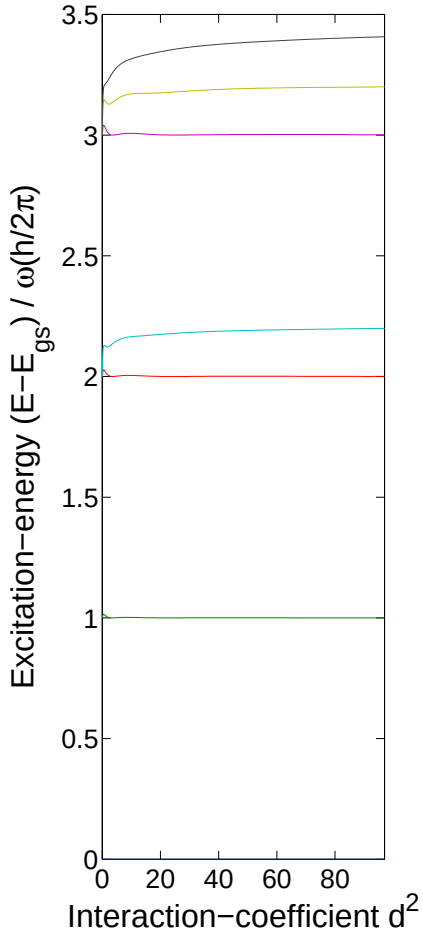

Figure 30: Excitation energies relative to the ground state for three fermions in a quasi one-dimensional harmonic trap with $l_p = 0.1$. (Dipole angle $\theta = 0.5\pi \ \rightarrow Ang(\theta) = 2$)

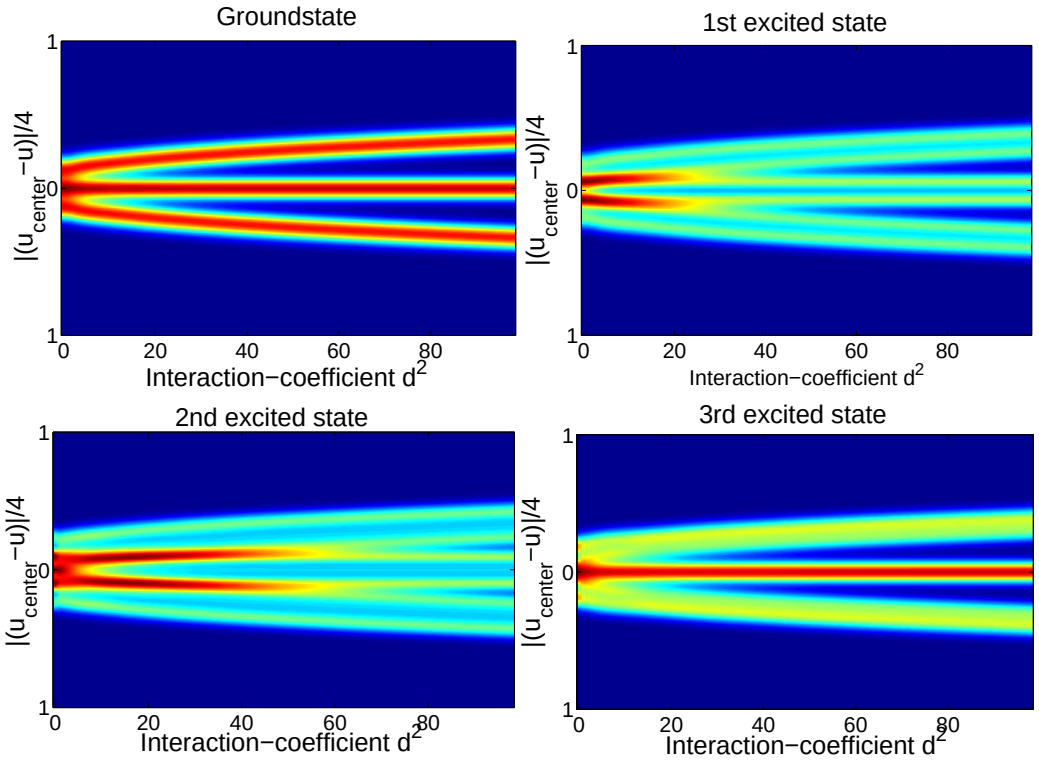

Figure 31: Images of the density distributions of three fermions in a quasi-one-dimensional harmonic oscillator with $l_p = 0.1$ (Dipole angle $\theta = 0.5\pi \rightarrow Ang(\theta) = 2$) Each color scale is normalized separately, so the absolute values for the particle densities cannot be compared in this figure.

10 Outlook for tunneling transport of fermions through quasi one-dimensional harmonic traps

In this last section on dipolar fermions in quasi one-dimensional traps I will investigate features in the spectra possibly could be used in order to find interesting results in terms of tunneling transport.

Choosing one value for l_p it is possible to directly compare the spectra of the different numbers of particles. When discussing transport in terms of tunneling through the system, this is an interesting aspect. The appearance of transport Coulomb diamonds is dependent on the spectra of different particle numbers of the transporting system [28], so one might expect that when altering the spectra, the transport properties will also be changed. The experimental realization

of systems with only dipole-dipole interaction rests heavily upon the concept of Feshbach resonances, which allows the experimentalist to cancel collision scattering of two particles. It is important to note that the parameters which allow such a system do not depend on the particle number, so it is not irrelevant to compare energies of pure dipole interaction systems with different numbers of particles. [24]

From figure (32) it can be seen that energy levels for different numbers of particles intersect at some dipole angles.

These intersections might be interesting when discussing tunneling transport through the system. In particular it should be investigated if these interactions mean that resonant tunneling channels are open for two different particle numbers.

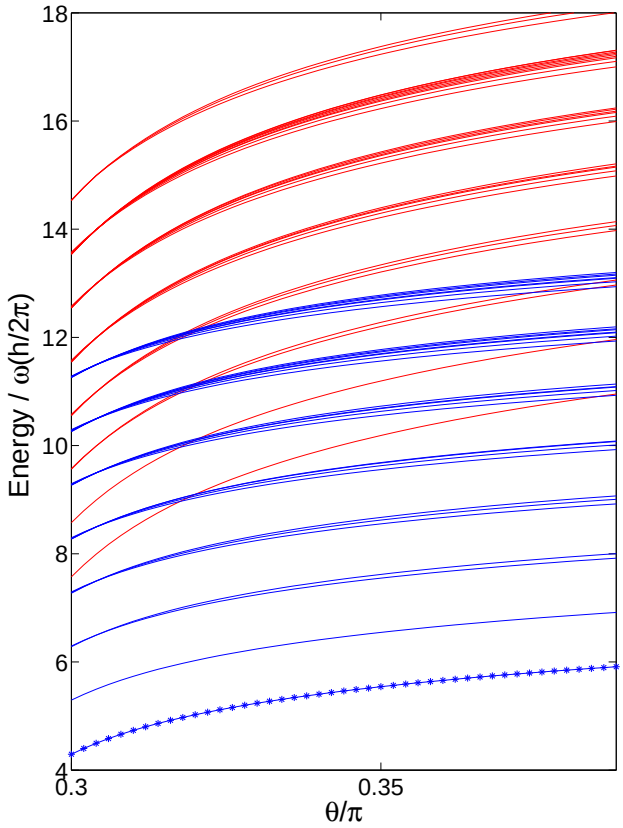

Figure 32: Energy levels 1 to 30 for three (blue lines) and four (red lines) fermions in a quasi one-dimensional harmonic trap with $l_p = 0.06$ (electric dipole interaction coefficient $d^2 = 1$)

Each specific intersection-point between two levels, from different particle numbers N, appear at different angles depending on the interaction coefficient d^2 and transverse confinement l_p. If the tunneling transport properties could be found to depend on these intersection this could allow a certain control over the transport properties of a harmonic quasi one-dimensional system of dipoles. Since the interaction strength between dipoles in actually can be tuned via the dipole angle θ or the interaction coefficient d^2, this could allow experimentalists to also tune the transport properties. This is one of the most interesting properties of the quasi one-dimensional system of dipoles, and it should be investigated if the possibility to tune the interaction could allow realization of new transport features.

For example it is in principle possible find specific angle in order to intersect two bundles of closely spaced energy levels. It might then be possible to open a large transport-channel for some "energy window" at specific angles for the aligned dipoles. More channels generally give higher transport, so these results may be beneficial when building tunneling transport devices which use one-dimensional structures.

These result could be even more interesting in the case of weak attractive dipole-dipole interaction. The attractive force is harder to deal with in the numerical sense, meaning that the calculations do not easily converge. However, when discussing the possibilities of transport by "modifying" the energy spectra the attractive interaction is particularly interesting, which will be discussed in the following.

The results in this project have indicated that the relative contribution from the interaction energy to the total energy of the ground state increases with the number of particles.

In the spectra of three and four dipoles in figure (27) one can see that the successively increasing repulsion causes all the plotted energy levels to increase in energy. It is clear that the energies of the four-particle states increase more due to the interaction than the energies of the three-particle states. This fact becomes interesting when one wants to intersect energy levels for different particle numbers.

In figure (34) the lowest few energy levels of one, two and three particles are plotted for both attractive, $\theta \lesssim 0.304\pi$, and repulsive, $\theta \gtrsim 0.304\pi$, dipole angles.

The results in figure (34) clearly demonstrate the fact that any one-particle level will intersect levels for two particles for a strong attractive potential. One should expect that for strong attraction, the binding energy of two particles in the ground state will be larger that the kinetic and potential energy contributions associated with introducing a second particle in the trap. In this case the ground state of the two-fermion system will have lower energy than the one-particle ground state. In the same way the three-particle ground state will end up lower than both the one- and two-particle ground states for a sufficiently strong attractive potential. In figure (32) one can see that the four-particle ground state is more affected by the repulsive-interaction than the three-particle

ground state, and this was also seen to be the case for the attractive interaction. Therefore ground state of four particles should have lower energy than the three-particle ground state at strong attraction, but higher energy for strong repulsive interaction. From this fact one can draw the conclusion that the two ground states must intersect at some interaction strength. This can be explained by figure (33).

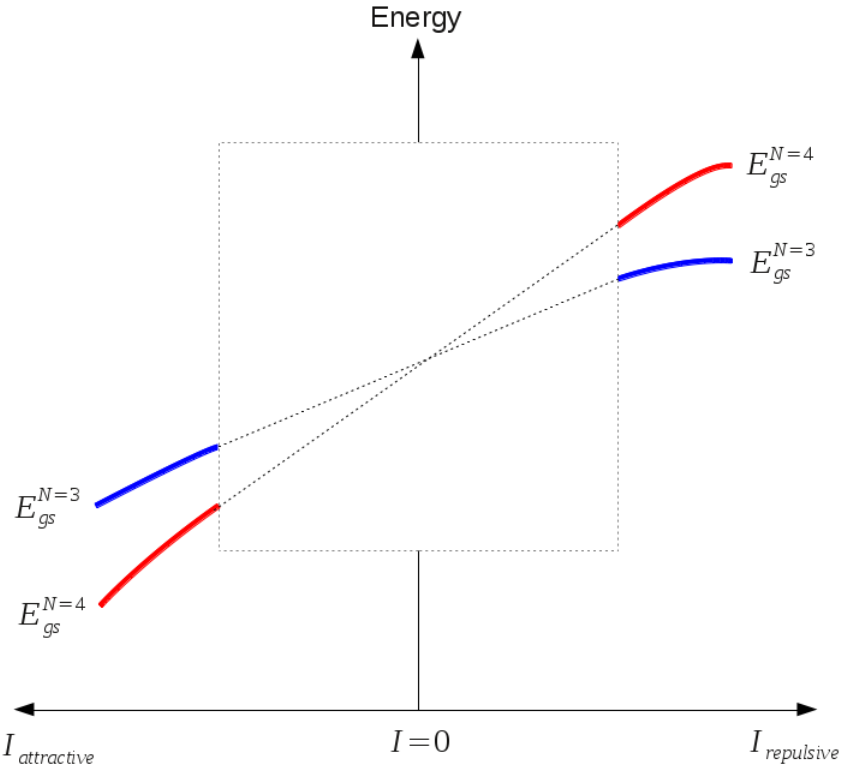

Figure 33: Sketch of ground states for three and four dipoles. The ground state of four dipoles has the lowest energy for strong attractive interaction, and highest for strong repulsive interaction. Somewhere between these two interaction regions the energy levels will intersect.

As seen in section (6), the dependence on the dipole angle θ and the interaction coefficient d^2 of two-fermion energy-states was dependent on the parameter l_p. (This was also seen for $N = 3$ and $N = 4$, but these results are not shown.) Depending on the number of particles, the energies depend differently on l_p.

Using this fact one might argue that it could be possible to control at *what* energies these crossings occur. In principle one could possibly find parameters so that the ground states for one, two and three particles cross at the same energy.

The great challenge of finding these parameters is the fact that convergence is very hard to reach for the strong attractive interaction in simulations. For strong attractive interaction the harmonic-oscillator basis seems to be a bad choice, since the energies of the ground states do not converge even for large numbers, $n \approx 45$, of oscillator-orbitals. One could however examine the properties of weakly attractive systems in order to show how the energy levels are affected by the choice of l_p and d. In this way one can show that it in principle should be possible to cross the ground states of many different numbers of particles.

In figure (35) one can see that the change in energy of the ground state for successively higher attraction is larger for three than two particles. One can also see that the ground state energy of three particles is more dependent on the transverse confinement l_p. This fact is encouraging since it could allow control over the crossing of energy levels from different numbers of particles.

As will be discussed later, the system may collapse at strong attractive interaction. In the case of a collapsed system the crossings of ground states would not realizable, and that the discussion therefore becomes somewhat esoteric. Luckily a total collapse is impossible for a system of spin-polarized fermions due to the Pauli principle, but for strong attraction I have not yet been able to reach convergence in the calculations.

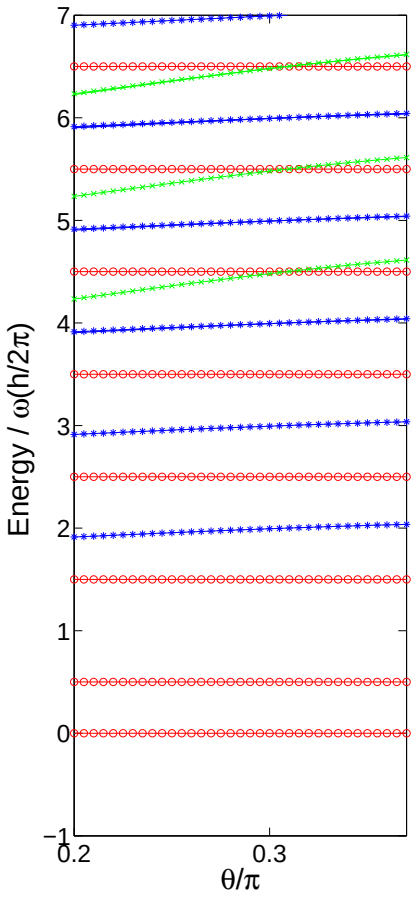

Figure 34: Energy levels of one (red lines), two (blue lines) and three (green lines) fermions in a quasi one-dimensional harmonic trap with $l_p = 0.08$. (electric dipole interaction coefficient $d^2 = 0.0625$)

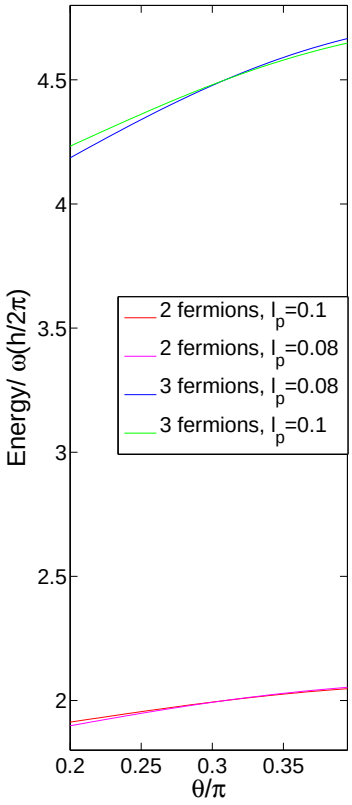

Figure 35: Ground state energies of two and three fermions in a quasi one-dimensional harmonic trap with different transverse confinements l_p (Electric dipole interaction coefficient $d^2 = 0.0625$)

10.1 Collapse of the system

The problem with convergence in the previous section appears to be related to the problem of dipolar collapse of the system. A collapse essentially means that the particle density collapses into a "lump" at the center due to attraction [25]. As noted before this collapse cannot happen for a system of spin-polarized fermions with the same quantum numbers since the Pauli principle prevents them from overlapping, but there are still problems for attraction. At $d^2 \approx 0.01$ and $Ang(\theta = 0) = -4$ the particles in the few-fermion ground states are tightly bound to each other and when successively expanding the harmonic basis the density distribution of the ground state becomes more and more peaked in the center of the trap. This behavior can be seen in figure (36). The basis-set needed for convergence in both energy and density distribution becomes very large, $n \gtrsim 40$, already for two fermions, so this situation is evidently difficult to handle also for fermionic systems.

A collapse for bosons can be counteracted in many ways, for example by introducing a repulsive contact-delta interaction between particles.

In the results of this project I have naturally only included converged results, so there will be no need to worry about a collapse. The main point of this section is however that harmonic systems with attractive inter-particle interaction are difficult to simulate, and that only weak attraction, $d^2 \approx 0.06$ and $Ang(\theta \approx 0.2\pi) \approx -2$, has been used in this project.

11 Failure of the dipole approximation

At this point one should mention another caveat to the results; The calculations for attractive potentials are dependent on the close-range behavior of the dipole-dipole interaction. In this limit there is some ambiguity in terms of the interaction, since the dipole approximation is invalid at very short distances. In the theory part of this project it was seen that, for real dipoles, the expression for the dipole-dipole interaction was built upon an approximation which is only valid at "large" distances between the interacting particles. It was noted that if particles came too close their mutual interaction should be "resolved", meaning that the interaction should be described in terms of Coulomb interacting charge-distributions and not by interacting dipoles. The approximation would fail if the particles came within "small" distances from each other. What these "small" distances might be, and for which limits the calculations can be performed, varies for different particle types. It is important to note that this ambiguity causes problems for both spin-polarized fermions and bosons, even though two spin-polarized fermions with identical quantum numbers are never found at the same position. As noted before, the separation of particles is important in order to find systems where this problem is reduced, so the results in the previous sections should be important when discussing these situations.

One could of course discuss the concept of interaction between actual ideal dipoles, but at this point it would not describe any physical situation of interest.

A possible continuation of this project would be to perform more elaborate simulations where the dipoles are resolved. In this project it has been seen that the eigen energies of different states can indicate features of the systems which are hard to see from, for example, the density distributions of the states, so the energy spectra should in particular be a good way of comparing these models.

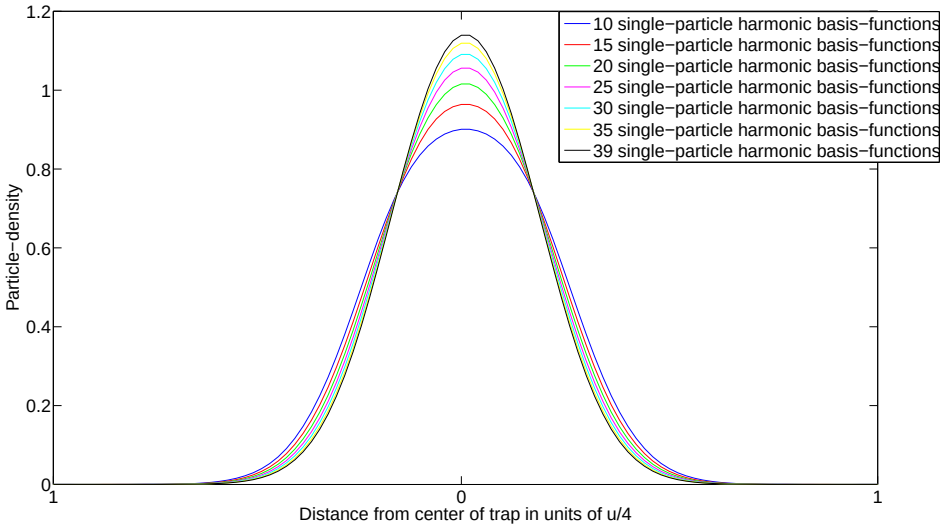

Figure 36: Density distribution of the ground state for two fermions in a quasi one-dimensional harmonic trap with $l_p = 0.06$ (electric dipole interaction coefficient $d^2 = 0.015$ and $\theta = 0 \Rightarrow Ang(\theta) = -4$)

12 Simulations of $N < 5$ bosons in quasi one-dimensional harmonic traps

Due to the ambiguity of the dipole-dipole interaction between two particles at the same position, special care has to be taken when performing calculations involving bosons. The Pauli principle forbids two spin-polarized fermions with the same quantum numbers to be at the same place. A delta interaction term will therefore have no effect on a system only populated by such particles. In the previous section I mentioned that it is generally best to stay away from systems which allow particles to come "too" close, but this is especially true for bosons. The Pauli principle does not apply for bosons so there is no rule which prevents two spin-polarized bosons with the same set of quantum numbers to be found at the same position in space.

This fact causes ambiguities in terms of the dipole interaction *even for a system of ideal dipoles*. For ideal dipoles the interaction expression derived in the theory part of this project is well-defined if the particles are separated by any finite distance. For two particles at the same position the expression is however ambiguous, which also was discussed in the theory part.

Depending on the parameters of the quasi one-dimensional system and the inter-particle interaction some calculations may be dependent on the existence, or non-existence, of a delta term in the interaction expression. For other parameters the delta term might however not make a difference for the results,

since particles can become separated in the states. *A separation of particles like what was seen in the states of the low-lying spectra of $N < 5$ fermions would in the case of bosons in fact be necessary for the calculations involving these states to be correct.* The separation will be seen to give states where the dipole delta interaction between dipoles is suppressed.

In order to examine which system parameters to avoid for bosons, one could simply perform the calculations for systems with a delta term and then compare them to calculations without the delta interaction. This investigation should be performed in each individual case so that one is certain that the ambiguous delta term has no effect on the relevant results.

In the case of $N < 5$ fermions, separation could be seen when analyzing the spectra. This might also be the case for bosons, and it could therefore be possible to find "safe" parameters by looking directly at the energy spectra of the boson systems.

It should also be mentioned that when discussing short range interaction for bosons, one can see a stronger interaction than for fermions. The bosons can come "very close" to each other compared to spin-polarized fermions and some interesting effects can be seen from this "very short range" interaction.

Many of the results presented in this section are continuations on the paper [21], where occupation-numbers and density distributions where shown for the ground state of a system with four bosons in an quasi one-dimensional harmonic trap. In my simulations I have investigated similar systems with repulsive long-range interaction up to $U_{lr} = \frac{d^2\lambda^3}{l_p^3} \sim 10\,\hbar\omega$, including also excited states of the system.

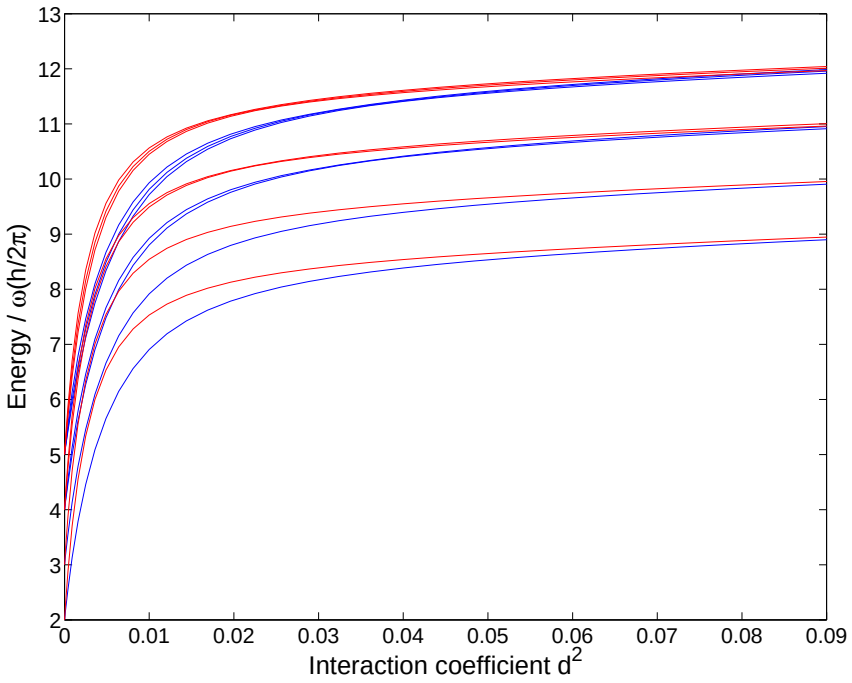

Figure 37: Energy levels 1-7 for four bosons with (red) and without (blue) dipole delta interaction in a quasi one-dimensional harmonic trap with $l_p = 0.1$. (Repulsive dipole angle $\theta = \frac{\pi}{2} \Rightarrow Ang(\theta) = 2$)

In figure (37) the energy spectrum of the four bosons is dependent on the delta term for interaction coefficients $d^2 \lesssim 0.1$.

Looking at the boson spectrum for different angular factors $Ang(\theta)$ in figure (38) one can see that the delta term has a clear stabilizing effect for $Ang(\theta) \lesssim 0.5$. Since the dipole delta-term is independent on the angular factor, $Ang(\theta)$, of the dipole-dipole interaction it will always act as a repulsive force between particles. The delta term scales with the interaction parameter d squared, just as the rest of the interaction, so performing simulations with a changing interaction parameter d is different from simulations where the dipole angle is changed. This can also be seen from figure (38), where it is clear that the energies obtained with and without a delta term differ. Changing the dipole angle in simulations is a fruitful approach when it comes to comparing simulations with experiments. In the following I will however perform most simulations for bosons by changing the interaction parameter d . This ensures that the dipole delta scales as the

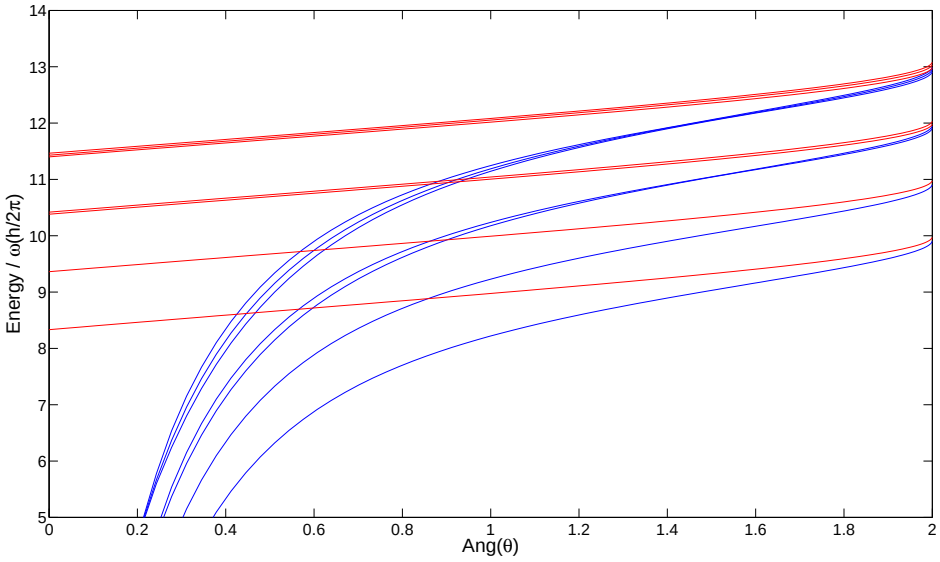

Figure 38: Energy levels 1-9 for four bosons in a quasi one-dimensional harmonic trap with $l_p = 0.1$ (Electric dipole interaction coefficient $d^2 = 1$). Results are shown for simulations with dipole delta (red) and without dipole delta (blue). Also note that the dipole delta-term is non-zero at the critical angle $\theta = \theta_{crit} \rightarrow Ang(\theta) = 0$ since it does not depend on the angular factor $Ang(\theta)$. The excited states are therefore split at $\theta = \theta_{crit}$ due to the delta interaction.

rest of the dipole-dipole interaction, and therefore makes it easier to find regions where results can be trusted, i.e where the delta term does make a difference for the results.

12.1 Separation and fermionization of four bosons in a quasi one-dimensional harmonic trap.

For repulsive dipole-dipole interaction it has been seen that the ground state of a quasi one-dimensional system of bosons tends to fermionize, resulting in the fact that the occupation-number distribution of this state becomes the same as for the corresponding fermion-system[21].

The fermionization happens as the mutual repulsion of the bosons pushes them so far apart that the overlap between the particles is lost. If particles do not overlap the exchange symmetry of identical particles makes less difference between bosonic and fermionic systems. Indications of this fermionization for the four-bosons ground state can be seen from figures (39) and (40) where the energies of four fermions and four bosons are shown relative the four-fermion

ground state. For successively larger repulsive interaction one can see that the eigen energies of the fermionic and bosonic systems converge onto the same values, so fermionization is indicated for all the states in the low-lying spectrum.

The largest difference between bosons and fermions lies, as expected, in the interaction region $d^2 \lesssim 1$ where the particles are not separated. As mentioned before one has to make sure that results in this region do not depend to much on the ambiguous delta term of the dipole-dipole interaction, so all results should include both dipole delta interacting bosons and bosons interacting without the dipole delta.

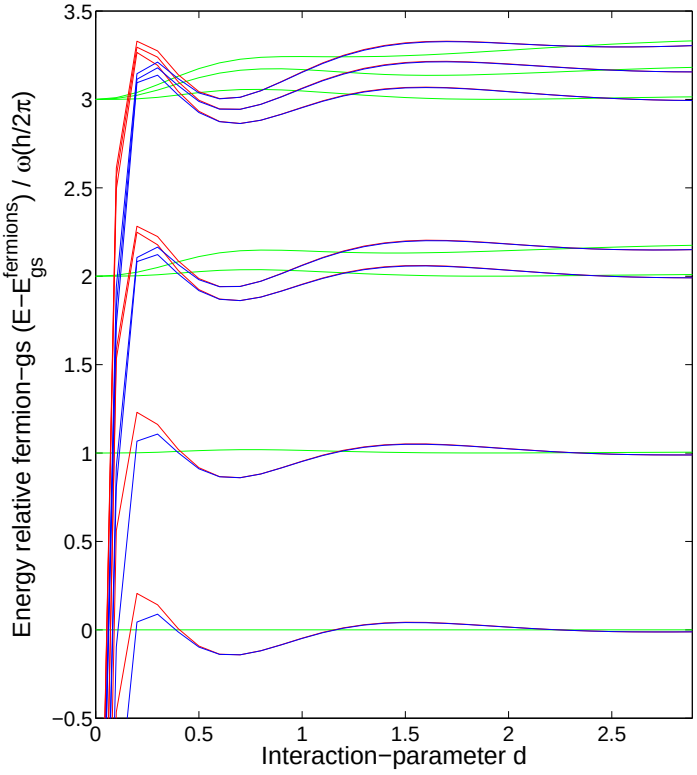

Figure 39: Eigen energies of four particles relative the four-fermion ground state in a quasi one-dimensional harmonic trap with $l_p = 0.04$ (dipole angle $\theta = \frac{\pi}{2}$). Results are shown for simulations with four fermions (green), four bosons with dipole delta (red), and four bosons without dipole delta (blue). The energies are plotted against the parameter d. Previous results have been plotted against the interaction coefficient d^2 which scales linearly with the interaction strength. In order to see the behavior in the very short range interaction regime it is however better to plot the results against d.

Comparing the simulations for fermions and bosons in figures (39) and (40)

one can see that in the interaction regime for which the energies differ there is no "conclusive" difference between the particle types. Depending on the strength of the interaction, fermions or bosons have the larger ground state energy. However, that difference is similar for all the states in the low-lying spectra, so this must be an effect which is only dependent on the particle type, and not the individual wavefunctions. It is interesting that the exchange symmetry of the wavefunctions in this way determines some collective property of all the states in the low-lying spectra, and that this can be seen directly from the energies. This has also been seen for different numbers of particles, $N < 5$, but these results are not shown here.

For the bosons, **separation** can be seen in terms of the splitting of the degenerate energy levels in figure (40). Comparing the differently scaled figures (39) and (40) one can see that the influence of the delta term is lost for $d \approx 0.7 \rightarrow d^2 \approx 0.5$ and that the splitting between boson energy levels begins to saturate at $d^2 \approx 2$. One can see that there is some initial separation of bosons which reduces the delta dependence, but that there is another "phase" of separation, seen from the saturation of the energy increase, which occurs at stronger repulsive interaction. These "phases" of separation for bosons will be discussed in more detail in the following sections.

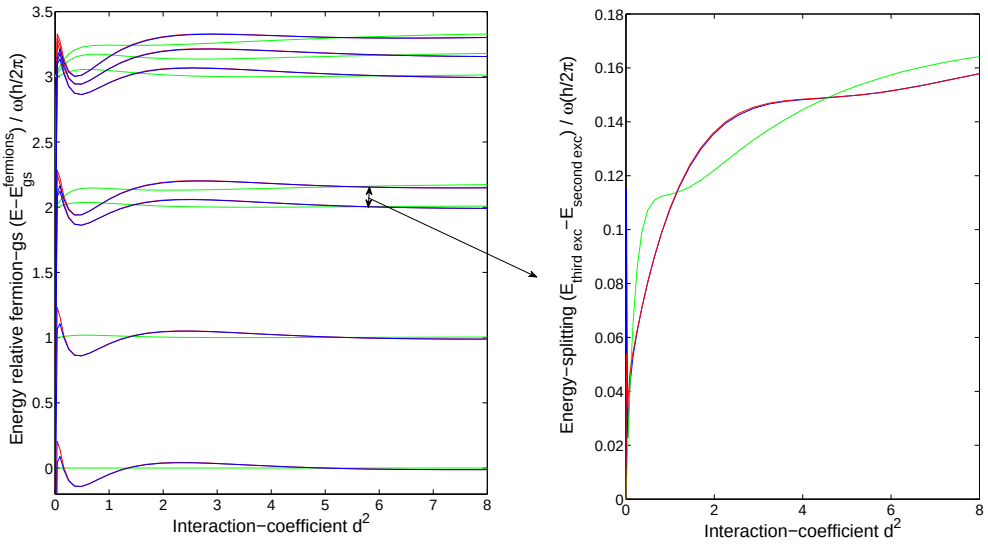

Figure 40: Eigen energies of four particles relative the four-fermion ground state in a quasi one-dimensional harmonic trap with $l_p = 0.04$. (dipole angle $\theta = \frac{\pi}{2}$) Results are shown for simulations with four fermions (green), four bosons with dipole delta (red), and four bosons without dipole delta (blue).

12.2 interaction regimes of the four-boson ground state

In order to investigate the different interaction regimes of the four-boson ground state I will look at the occupations of single-particle harmonic levels in the quasi one-dimensional system. Just as for all properties of bosons one needs to establish the effect of the ambiguous delta term in of the dipole-dipole force, so all results should as before include a comparison between calculations performed with and without a delta term in the dipole interaction.

In figure (50) the occupation numbers for the ground state of four dipolar bosons are shown.

Note that for parameters $d \lesssim 1.2$, the interaction causes the ground state to mix with higher configurations. The separation however reduces the mixing with these configurations to a minimum at $d \approx 1.2$.

In the interaction region $d \lesssim 1.2$ the description of the ground state include many high harmonic states due to the influence of the "very short range" dipole-dipole interaction, which will be explained later in this section. At higher repulsive interaction the bosons begin to become pushed apart by the interaction, which also can be seen in figure (41) by noting that the effect of the delta term vanishes for these higher interaction strengths.

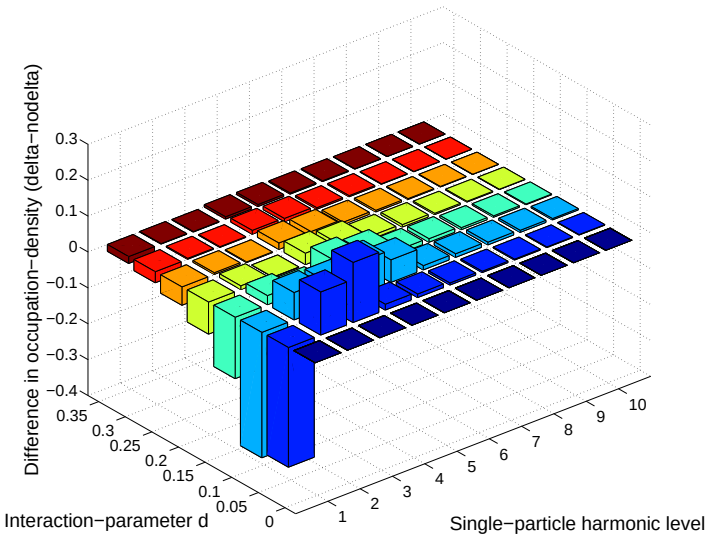

Figure 41: Difference in occupation between simulations performed with and without the dipole delta-term for a system of four bosons in a quasi one-dimensional harmonic trap with $l_p = 0.04$ (Dipole angle $\theta = \frac{\pi}{2} \rightarrow Ang(\theta) = 2$)

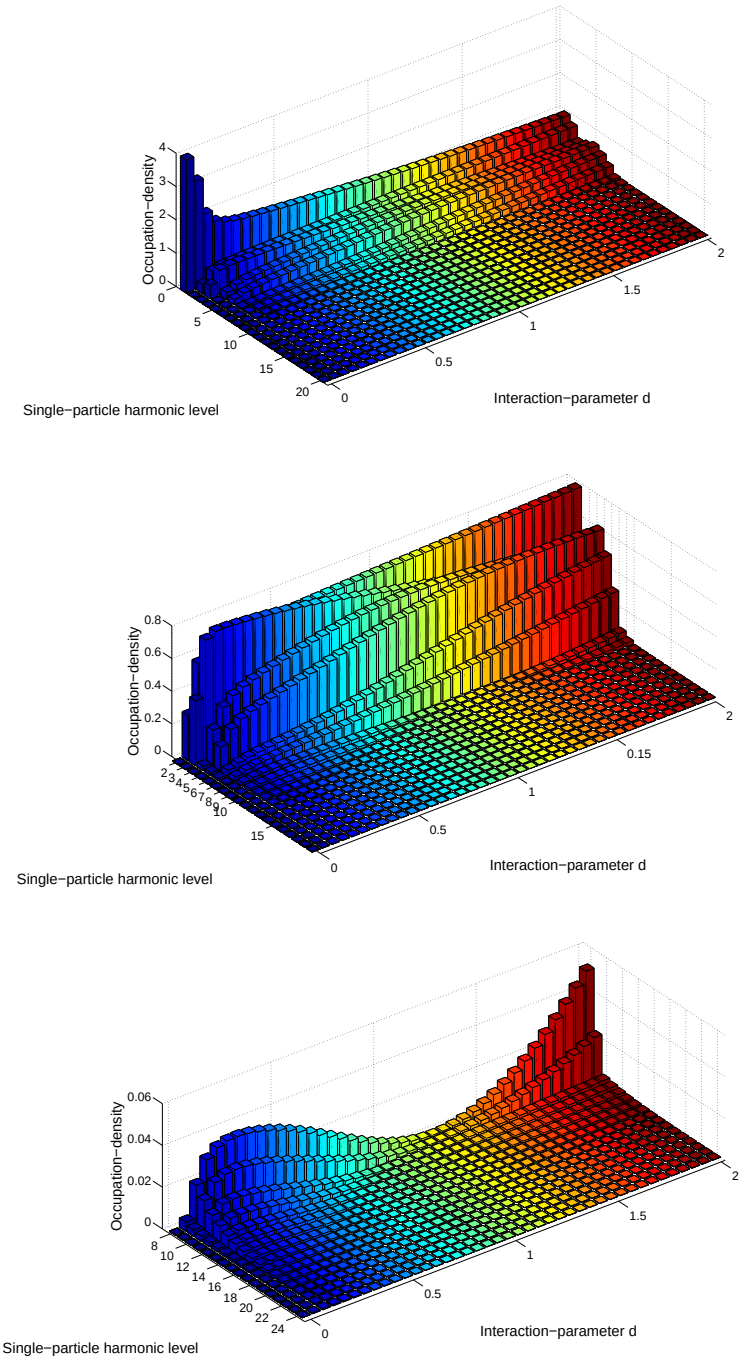

Figure 42: Occupation of single-particle states for the ground state of four dipolar bosons in a quasi one-dimensional harmonic trap with $l_p = 0.04$ (Dipole angle $\theta = \frac{\pi}{2} \rightarrow Ang(\theta) = 2$ and electric dipole delta-term)

Looking at the density distribution of the four-boson ground state in figure (44) one can directly see that the bosons become separated at larger interaction strengths, something which also was seen in [21].

The density distributions at $d = 0.4$ and $d = 1.3$ are directly compared in figure (45). One can clearly see the separation at $d = 1.3$ compared to the density distribution at $d = 0.4$.

In the regime $d \gtrsim 1.3$ the repulsive interaction is so strong that the particles begin to become influenced by the long-range dipole-dipole interaction. This is also indicated in figure (7) where the contribution from the interaction energy to the total energy of the ground state starts to increase with the long-range interaction at $d^2 \approx 1 \rightarrow U_{lr} \approx 1\,\hbar\omega$. This causes the ground state to mix with higher orbitals again, which is a sign of the localization of particles due to the long-range interaction.

In figure (46) the sum of the occupation densities for the lower harmonic levels are shown as a function of the interaction coefficient d for a system of four bosons.

This figure can be discussed in terms of different "regions" of repulsive interaction seen in the ground state:

1. **Large overlap between particles for** $d \lesssim 0.12$ and only little "high-harmonic" mixing. From figure (48) on can see that the interaction energy in this region is large compared to $d \gtrsim 0.12$, and figure (47) shows that the delta dependence is at its largest in this region. In the following I will call the region $d \lesssim 0.12$ the "very short range" interaction region.

2. **High-harmonic mixing strongly reduces the "very short range" interaction at** $d \approx 0.12$. This can be seen from figure (48) where the interaction energy reaches a minimum. Note that the high-harmonic mixing supresses the "very-short range" interaction but not the "short range" interaction, since the high-harmonic mixing only changes the inter-particle correlations on a very small length scale. Since the number of nodes in the harmonic oscillator states increase with the oscillator-number n (see figure (43)), it is clear that mixing with higher harmonic states can change the behavior of particles at smaller length scales compared to lower harmonic states.

3. **For stronger interaction** $0.12 \lesssim d \lesssim 1$ the short range interaction becomes so strong that the ground state begins to separate. In the following I will call the region $0.12 \lesssim d \lesssim 1$ the "short range" interaction region.

4. **High-harmonic mixing at minimum for** $d \approx 1.2$**.** At this repulsive interaction strength the ground state has become separated by mixing with "lower", $n \lesssim 10$, harmonic states and the interaction energy therefore show less contribution from the short range interaction. Since the particles become separated the mixing with high orbitals is successively lost when increasing the interaction for $d \gtrsim 0.1$. The separation have pushed particles apart so the "very-short range" interaction is also reduced, which

can be seen from the fact that the high-harmonic mixing, which supressed the "very-short range" interaction in the non-separated region, is reduced.

5. **High-harmonic mixing due to long-range interaction for** $d \gtrsim 1.3$. The ground state begins to localize through mixing with higher harmonic states. In the following I will call this the "long range" interaction region.

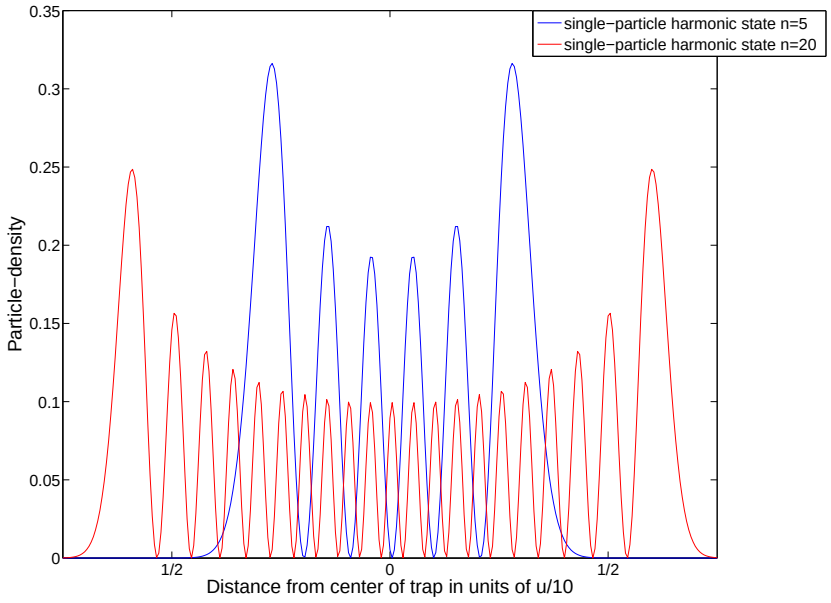

Figure 43: Density distributions of single-particle harmonic levels for a quasi one-dimensional harmonic trap with $l_p = 0.1$

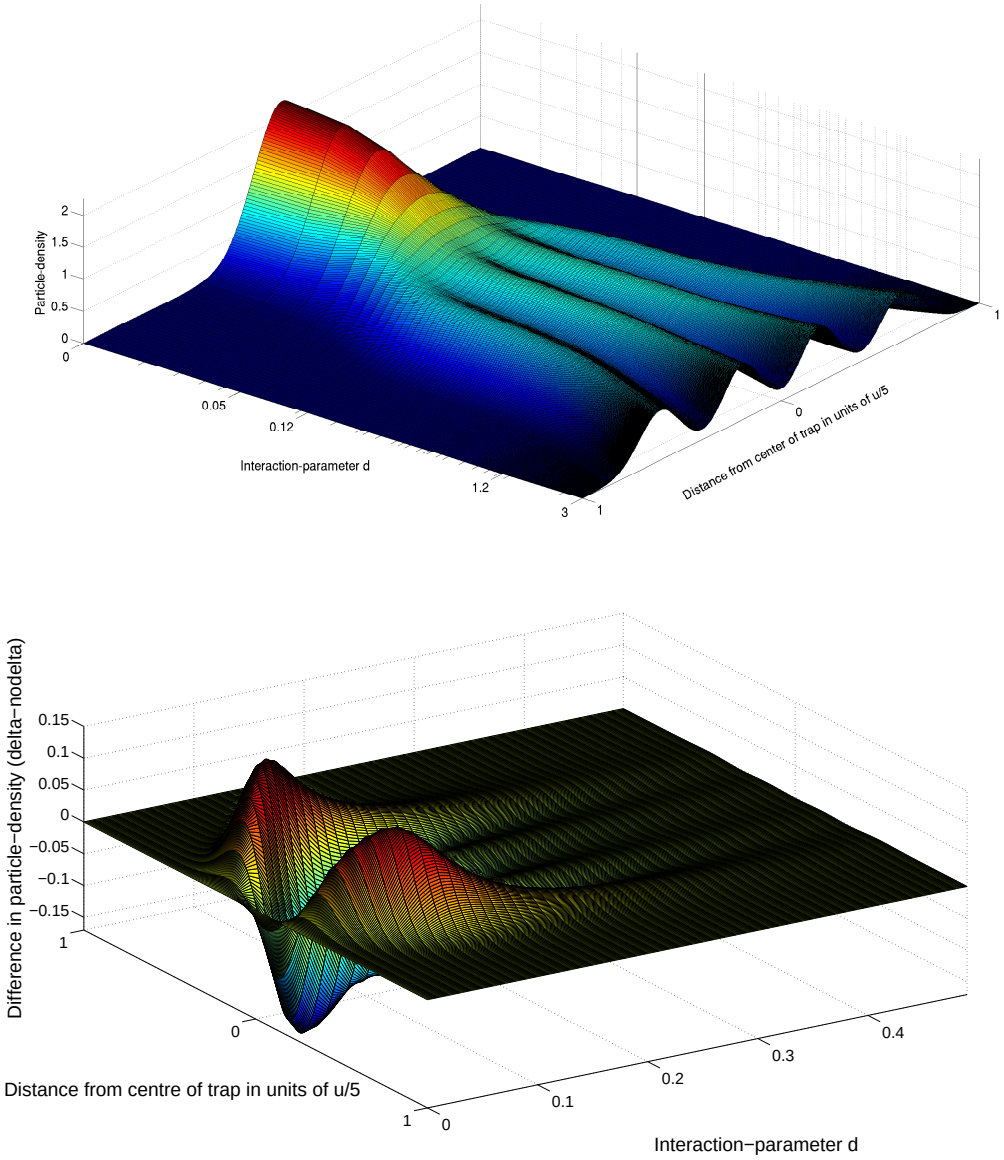

Figure 44: Upper: Density distribution for the ground state of four bosons in a quasi one-dimensional harmonic trap with $l_p = 0.04$ (Dipole angle $\theta = \frac{\pi}{2} \rightarrow Ang(\theta) = 2$ and electric dipole delta-term) Lower: Difference in density distribution between simulations performed with or without dipole delta-term.

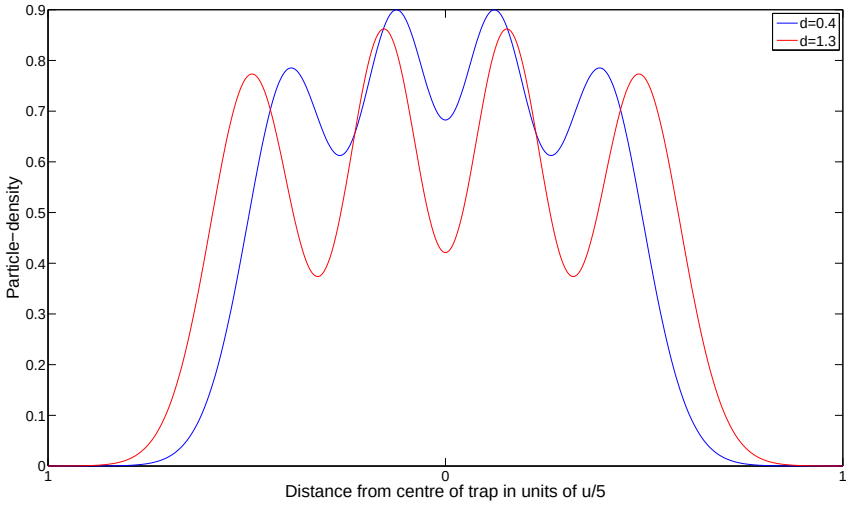

Figure 45: Density distribution for the ground state of four bosons in a quasi one-dimensional harmonic trap with $l_p = 0.04$ (Dipole angle $\theta = \frac{\pi}{2} \rightarrow Ang(\theta) = 2$ and electric dipole delta-term)

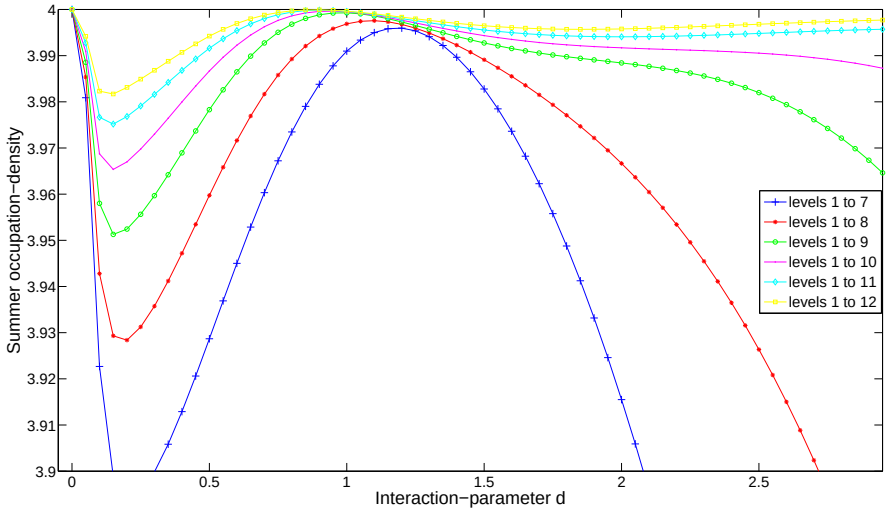

Figure 46: Summed occupation numbers for the ground state of four bosons in a quasi one-dimensional harmonic trap with $l_p = 0.04$. (Dipole angle $\theta = \frac{\pi}{2} \rightarrow Ang(\theta) = 2$ amd the lines are interpolations between data points indicated by the markings.) An indication of the rate of convergence for the results are shown in figure (61)

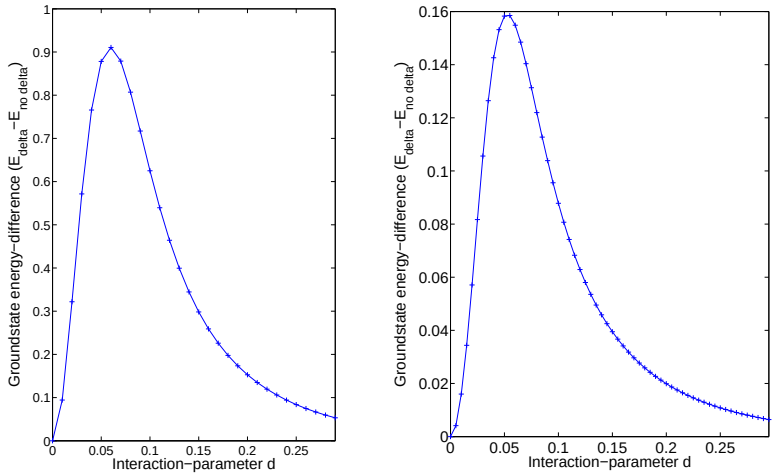

Figure 47: Difference in ground state energy between calculations with and without the dipole delta-term for a quasi one-dimensional harmonic oscillator with $l_p = 0.04$ (Dipole angle $\theta = \frac{\pi}{2} \rightarrow Ang(\theta) = 2$) (The lines are interpolations between data points indicated by the markings.) Left: Four bosons Right: Two bosons

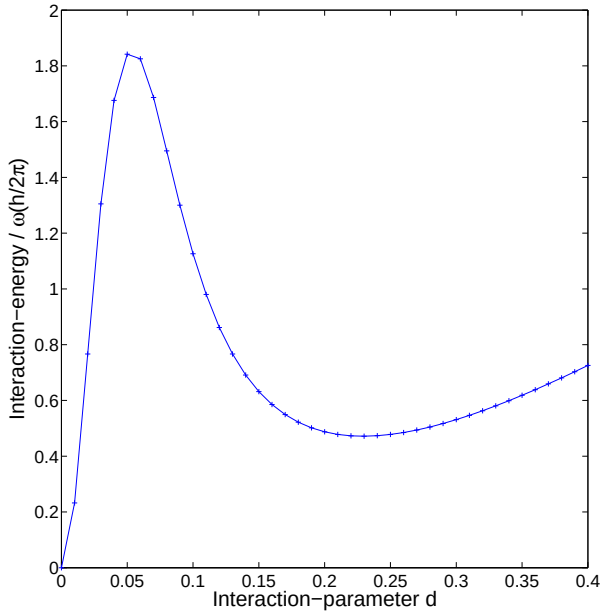

Figure 48: Interaction energy for the ground state of four bosons in a quasi one-dimensional harmonic trap with $l_p = 0.04$. (Dipole angle $\theta = \frac{\pi}{2} \rightarrow Ang(\theta) = 2$ and the lines are interpolations between data points indicated by the markings.)

The different interaction regions of systems are interesting since the validity of the dipole approximation in particular depends the distance between the dipoles. One should expect the dipole-dipole approximation to fail for real dipoles in the "very short range" region, since the particles come within very small distances compared to the other regions of repulsive interaction. Since the high-harmonic mixing reduces the very-short range interaction, it is however still possible that the short range interaction region actually can be simulated for real dipoles.

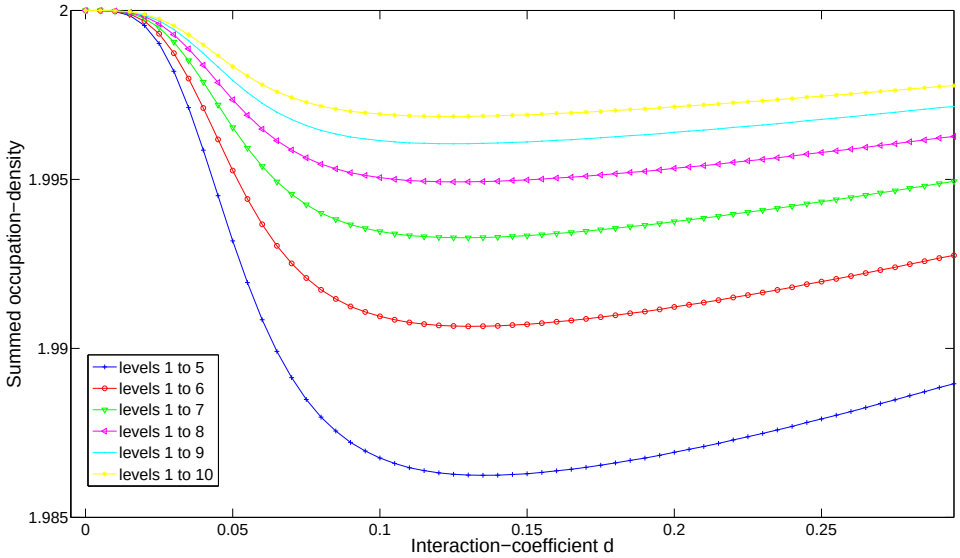

Figure 49: Summed occupation numbers for the ground state of two bosons in a quasi one-dimensional harmonic trap with $l_p = 0.04$. (Dipole angle $\theta = \frac{\pi}{2} \rightarrow Ang(\theta) = 2$ and the lines are interpolations between data points indicated by the markings.) An indication of the rate of convergence for the results are shown in figure (64)

Results for $N < 4$ bosons

In the same way as for the four-boson case the short range dipole-dipole interaction causes a mixing with higher harmonic levels for the ground state of systems with lower numbers of bosons, which can be seen in figure (49). (This has also been seen for systems with three bosons, but the results are not shown here.)

Interaction regimes of the four-fermion ground state

The occupation densities of the four-fermion ground state, which are seen in figure (50), show that the mixing with high harmonic levels for the fermion ground state is at its largest at around $d \approx 0.8$. Since the fermions have anti-symmetric wavefunctions, they are naturally further apart than the bosons. Therefore the "very short range" interaction will not have have as much effect on the fermions at $d \approx 0.1$, since they cannot overlap like bosons. At higher interaction strengths, $d \approx 0.5$, the fermions will however also feel a strong and quickly decaying dipole-dipole force which causes high-harmonic mixing. For stronger interaction strengths, $d \approx 1$, the short range interaction then leads to separation of the ground state.

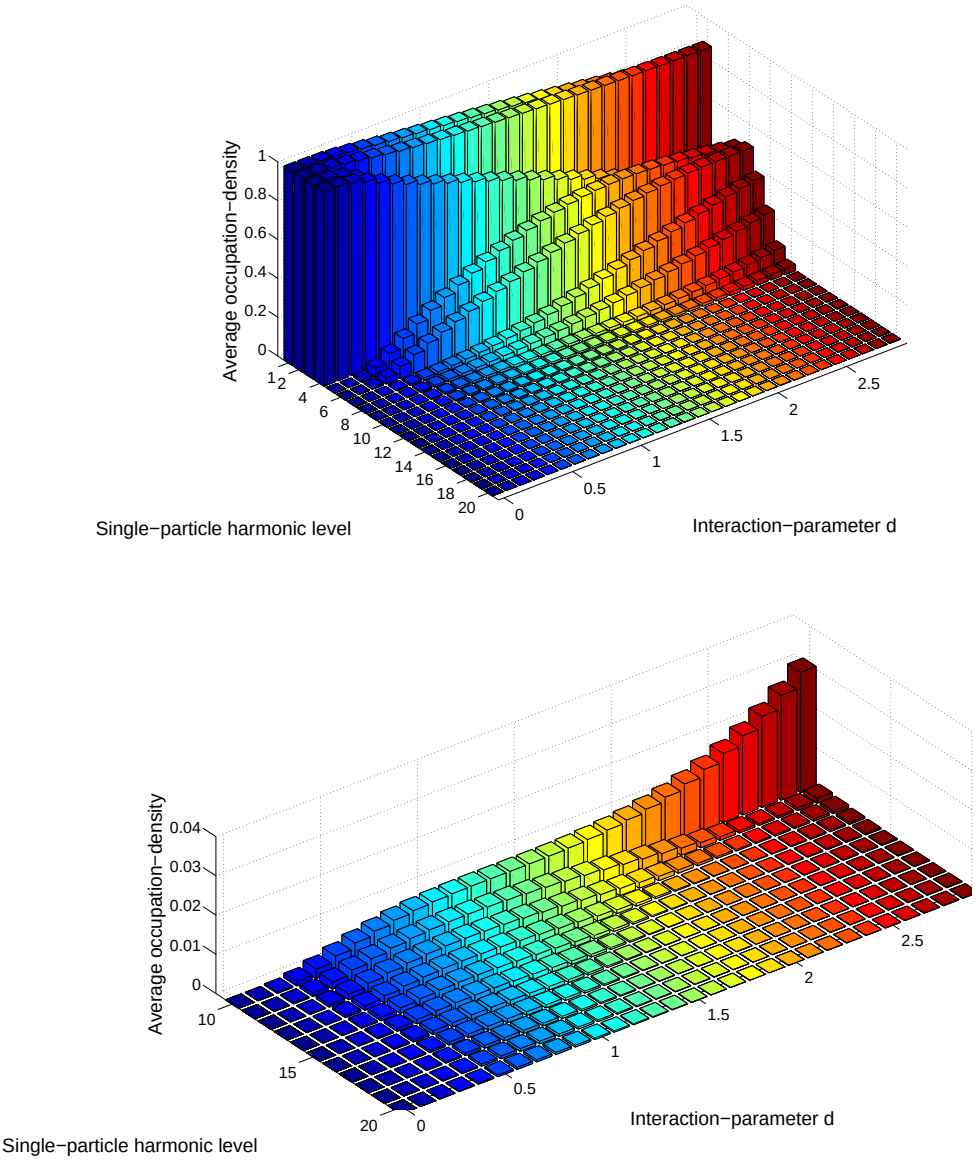

Figure 50: Occupation numbers of single-particle states for the ground state of four dipolar fermions in a quasi one-dimensional harmonic trap with $l_p = 0.04$ (Dipole angle $\theta = \frac{\pi}{2} \rightarrow Ang(\theta) = 2$)

12.3 Excited states in the spectra of bosons - The "very weak" repulsive interaction regime $d \lesssim 0.12$

The difference between bosons and fermions at very weak, $d \lesssim 0.12$, repulsive dipole-dipole interaction can be analyzed in terms of the low-lying energy spectra. For $d \lesssim 0.12$ the interaction between particles is mainly governed by the "very short range" dipole-dipole interaction and in this section I will discuss a clear difference between bosons and fermions in this interaction regime. I have only seen this effect for excited states in the boson spectra, and in particular when comparing states which are degenerate for $d = 0$. From the results in this section it will again be shown that a system of interacting particles can be analyzed in terms of the energy spectra, and that the features of the density distributions of energy-eigenstates are correlated with the features seen in the spectra.

In figure (51) the density distribution of the four bosons in the third excited state is plotted. Like for the ground state the density distribution of the third excited state begins to change into a "separated" distribution for $d \gtrsim 0.12$. For $d \lesssim 0.3$ the distribution shows dependence on the ambiguous dipole delta-term, which can be seen in the lowest part of the same figure, but the important results are similar for both simulations.

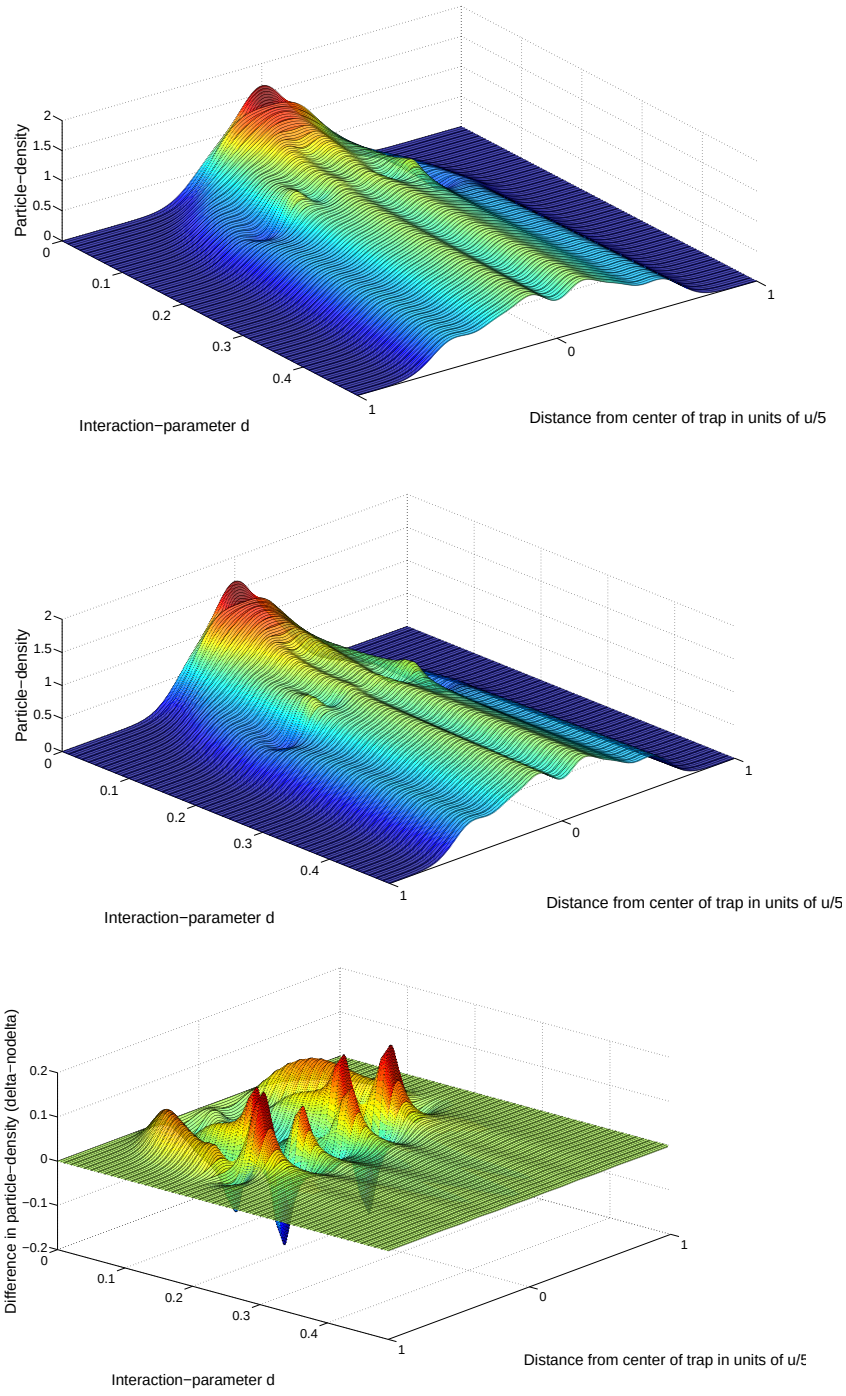

Figure 51: Density distribution of the third excited state for four bosons in a quasi one-dimensional harmonic trap with $l_p = 0.04$ (Dipole angle $\theta = \frac{\pi}{2}$ $Ang(\theta) = 2$ and electric dipole delta-term) Upper: Simulation with dipole delta. Middle: Simulation without dipole delta. Lower: Difference between simulations with and without dipole delta.

For interaction parameters $d \approx 0.15$ the density distribution of the third excited level clearly differs from the density distribution at $d \gtrsim 0.3$. The distribution seems to change its basic shape in the region $d \approx 0.15$, from a structure of six points of higher density to a structure with four points of higher density. I have not seen this behavior for interaction $d \lesssim 1$ in any of the density distributions in the fermionic system, so one might ask if this behavior is specific for bosons.

There is an explanation for the changing density distribution in the energy spectrum of the four-boson system. In figure (52) the four-boson energy levels 3 and 4 are plotted for against the interaction parameter d. The results unfortunately depend on the dipole delta but it is plausible that there is an avoided crossing of two states at $d \approx 0.15$. (Both simulations with and without dipole delta show the same behavior.)

This avoided crossing would explain the change in density which can be seen for the density distribution of level 4.

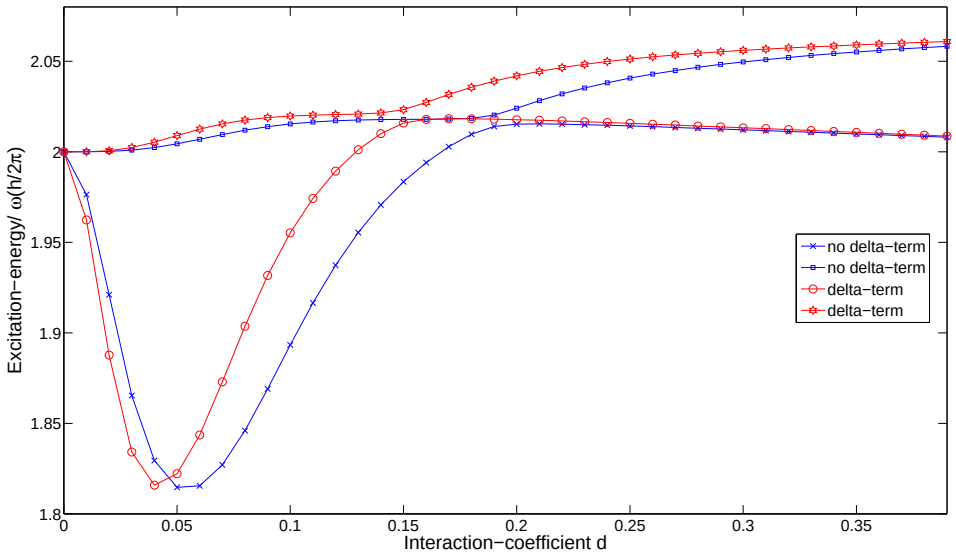

Figure 52: Excitation energies relative the ground state for energy levels 3 and 4 in a system of four bosons in a quasi one-dimensional harmonic trap with $l_p = 0.04$. (Dipole angle $\theta = \frac{\pi}{2} \rightarrow Ang(\theta) = 2$ and electric dipole delta-term and the lines are interpolations between data points indicated by the markings.)An indication of the rate of convergence for the results is shown in figure (63).

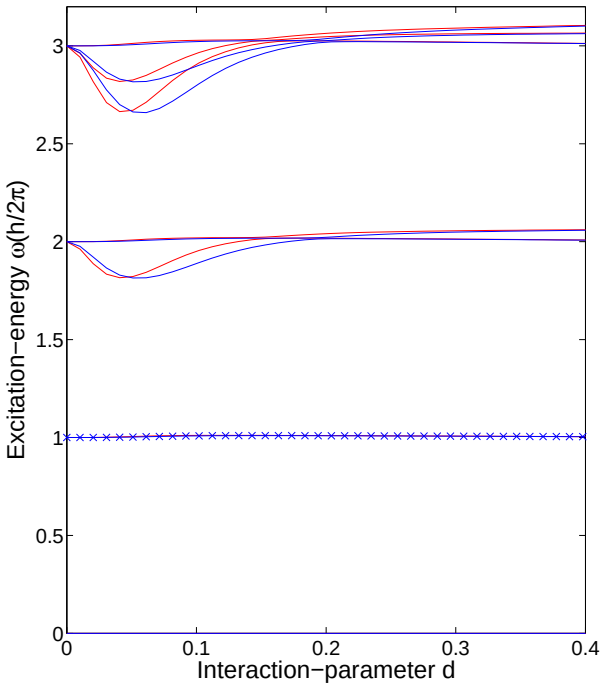

Figure 53: Excitation energies relative the ground state for energy levels 1 to 7 in a system of four bosons in a quasi one-dimensional harmonic trap with $l_p = 0.04$. (Dipole angle $\theta = \frac{\pi}{2} \rightarrow Ang(\theta) = 2$) Results are shown for simulations with dipole delta (red) and without dipole delta (blue). (The lines are interpolations between data points indicated by the markings on the second line.)

In figure (54) one can see that the transition in density around $d \approx 0.15$ is present also for the second excited level, which lies in the same bundle as the third excited level. In this small region of values for d, the density distribution of the second excited level shows a clear structure of four regions of high density. For larger values of d the density distribution changes and has five regions of higher density. Comparing the density distributions of the second and third excited state one can see that there is a mixing of the two distributions at $d \approx 0.15$. The density distribution of the second excited level has four regions of high density for $d \lesssim 0.15$, and for $d \gtrsim 0.15$ the third excited energy-level has a density distribution with four regions of higher density. This again suggests that for $d \approx 0.15$ there is an avoided crossing of two states with different basic density distributions.

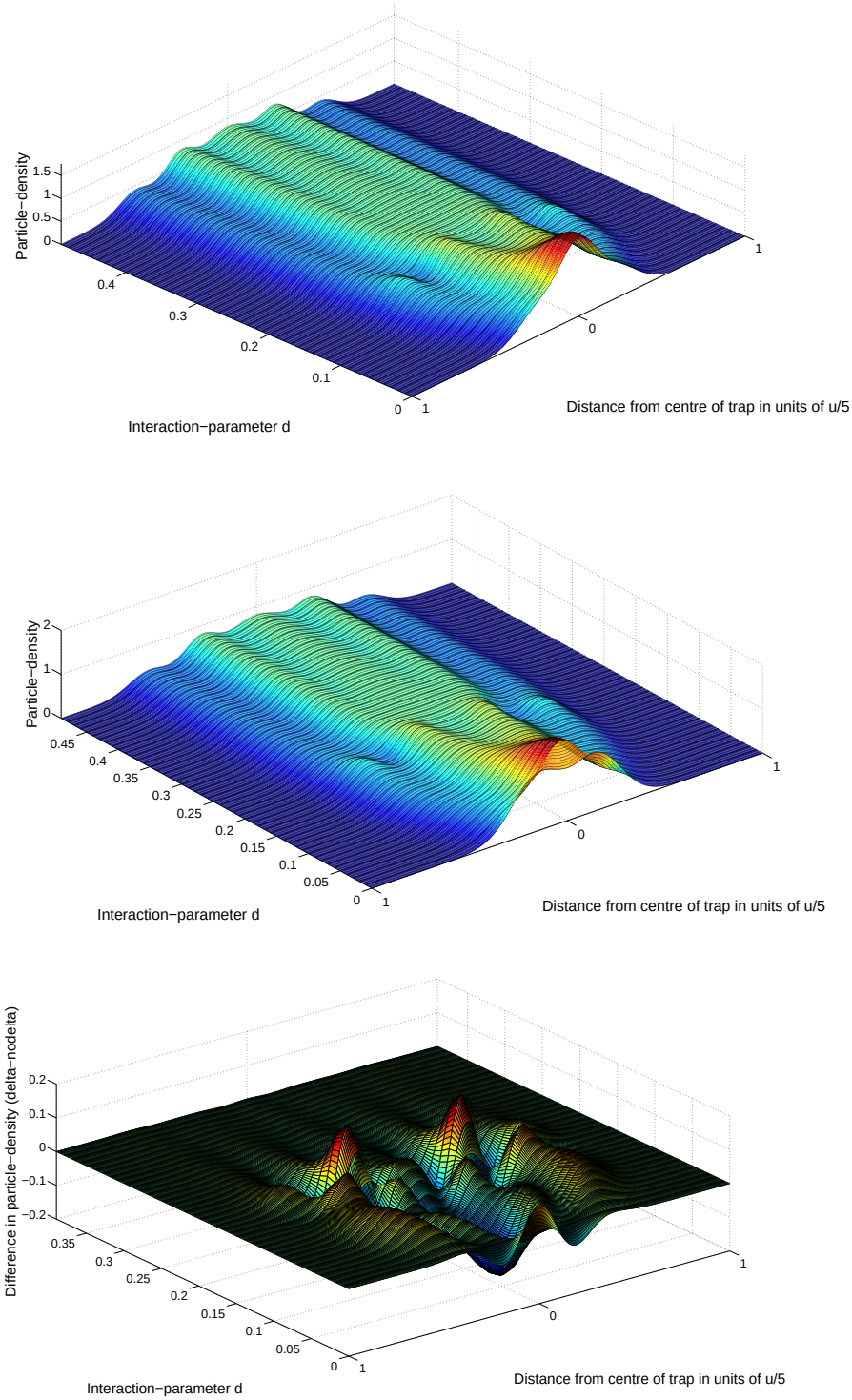

Figure 54: Density distribution of the second excited state for four bosons in a quasi one-dimensional harmonic trap with $l_p = 0.04$ (Dipole angle $\theta = \frac{\pi}{2} \rightarrow Ang(\theta) = 2$) Upper: Simulation with dipole delta. Middle: Simulation without dipole delta-term. Lower: Difference between simulations with and without dipole delta-term.

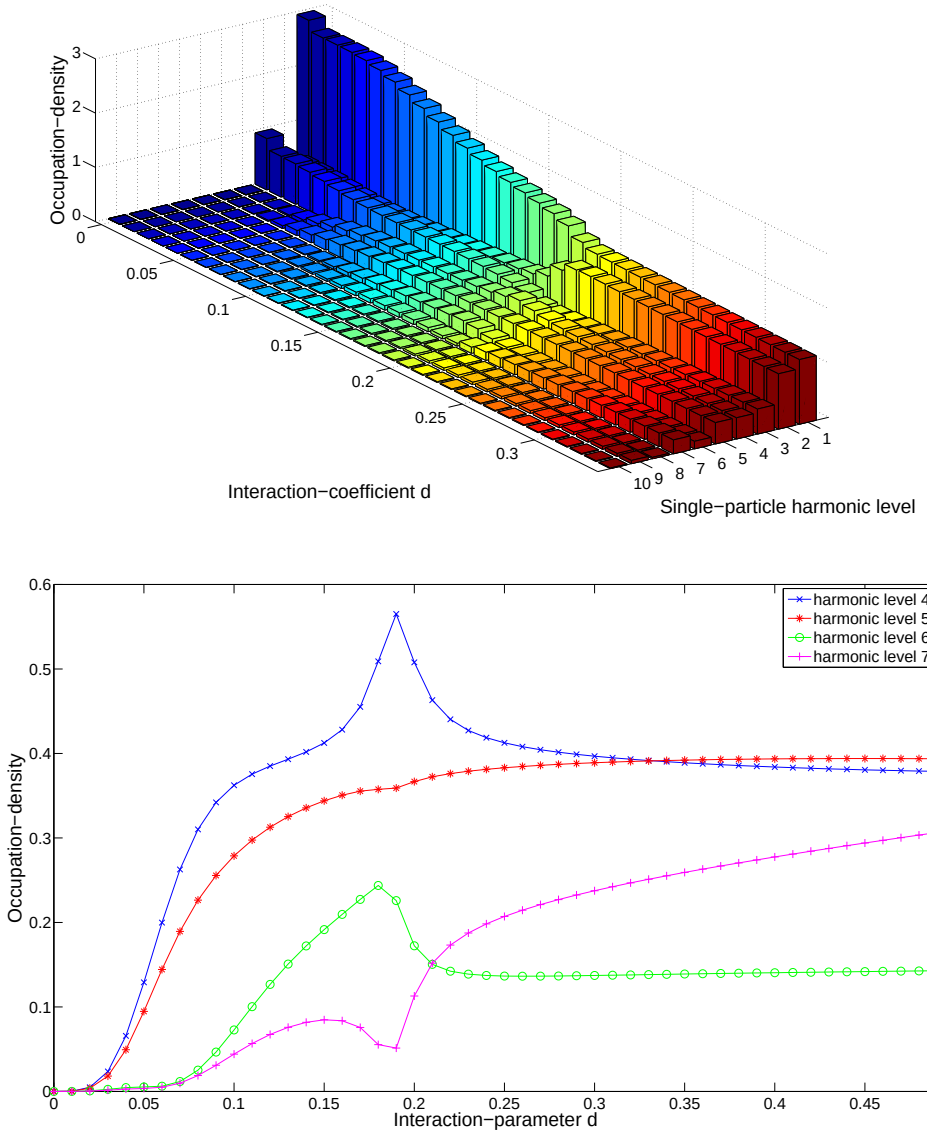

Figure 55: Occupation numbers of single-particle states for the second excited state of four dipole bosons in a quasi one-dimensional harmonic trap with $l_p = 0.04$. (Dipole angle $\theta = \frac{\pi}{2} \rightarrow Ang(\theta) = 2$ and no electric dipole delta-term) For the lower figure an indication of the rate of convergence for the results are shown in figure (62). (The lines are interpolations between data points indicated by the markings.)

In the energy spectrum of four bosons with $d \lesssim 0.3$, it is clear that all plotted levels show these avoided crossings within the bundles. In figure (55) the avoided crossing is also seen from the occupations of the second excited level. Note that the single-particle levels h_1,h_2,h_3,h_4, h_6 and h_7 all make "jumps" in occupation at $d \approx 0.15$, which is further evidence for the mixing of two many-particle states due to the avoided crossing. Looking at the spectrum of two bosons in figure (59) one can see that avoided crossings also appear here, so that this might be a feature of bosons in general. The density distribution of the second excited level for two bosons is also shown in figure (60). In the lower part of figure (59) one can see that the "sharp" change in the density distribution again seems to be an effect of the avoided crossing.

The fermion spectrum in figure (29) shows that no crossings appear for a system with four fermions and $d \lesssim 0.3$. This is also evident in the density plot in figure (58) where there is no "sharp" change like what was seen for the bosons.

The reason for the behavior of the boson-levels at low interaction strengths is associated with the "very short range" dipole-dipole interaction. All the states are dependent on this force in the "very weak" interaction region $d \lesssim 0.12$, where it causes a splitting of the degenerate levels. The avoided crossing of states at $d \approx 0.15$ is interesting since it indicates that there is a difference between the "very short range" interaction region $d \lesssim 0.12$ and the short range interaction region $0.12 \lesssim d \lesssim 1.2$ for bosons. Some states are more dependent on the "very short range" interaction compared to the short range interaction. An avoided crossing could therefore occur between a state which is more dependent on the very short range interaction than the short range interaction, and a state which is less dependent on the very short range interaction compared to the short range interaction.

The effect of the "very short range" interaction in the ground state was reduced by mixing with high harmonic levels at $d \approx 0.12$, which was discussed in the previous section. In figure (56) one can see that this is the case also for the second excited state, and that this state has the largest mixing with high-harmonic levels at around $d \approx 0.15$. The mixing causes the interaction energy in the excited states to become reduced, and the splitting of the degenerate states will therefore also be reduced.

In figure (56) one can also see that the high-harmonic mixing in the second excited state becomes reduced for successively higher interaction and reaches a minimum at $d \approx 1$. As was noted before, this is an effect of the separation in the state.

One might also wonder why the splitting causes levels to decrease in energy relative the ground state, since this is opposite to the case for the short range interaction region $d \gtrsim 0.15$.

It seems as the ground state of the bosonic system in general is more affected by the repulsive "very short range" dipole-dipole interaction than any of the other states in the lower spectra. This is interesting since it is a clear distinction

between the effects at $d \lesssim 1.2$ and $d \gtrsim 1.5$, but also between bosons and fermions.

The reason for this behavior is the fact that the one-particle harmonic-oscillator ground state is a Gaussian peaked in the center of the trap[12], so the "very weak" interacting many-boson state will have a large overlap between all particles. The excited states in the harmonic spectra have less overlap between particles than the ground state, so for the "very short range" interaction the excited many-boson states will be less dependent on the inter-particle interaction.

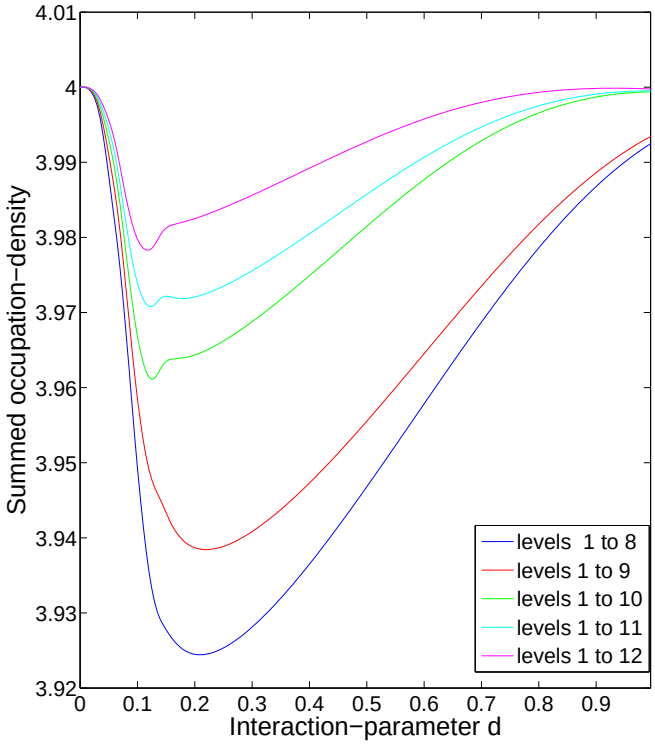

Figure 56: Summed occupation numbers for the second excited state of four bosons in a quasi one-dimensional harmonic trap with $l_p = 0.04$. (Dipole angle $\theta = \frac{\pi}{2} \rightarrow Ang(\theta) = 2$)

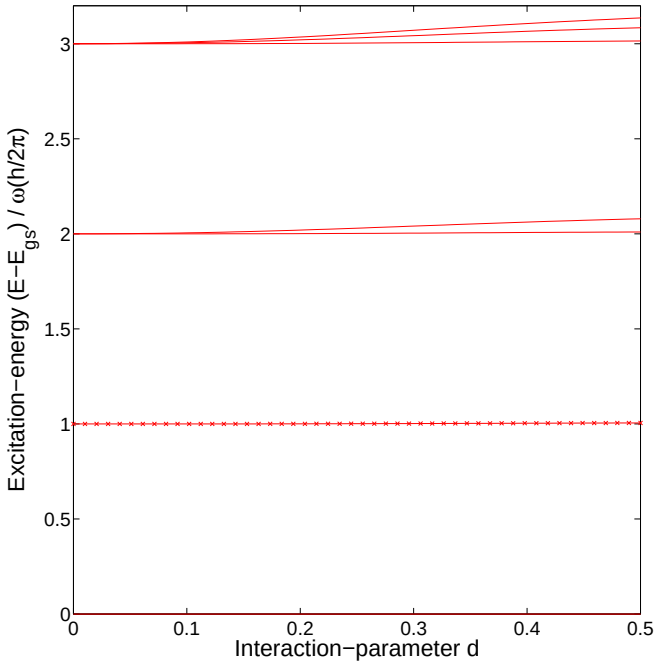

Figure 57: Excitation energies relative the ground state for energy levels 1 to 7 in a system of four fermions in a quasi one-dimensional harmonic trap with $l_p = 0.04$. (Dipole angle $\theta = \frac{\pi}{2} \rightarrow Ang(\theta) = 2$) (The lines are interpolations between data points indicated by the markings on the second line.)

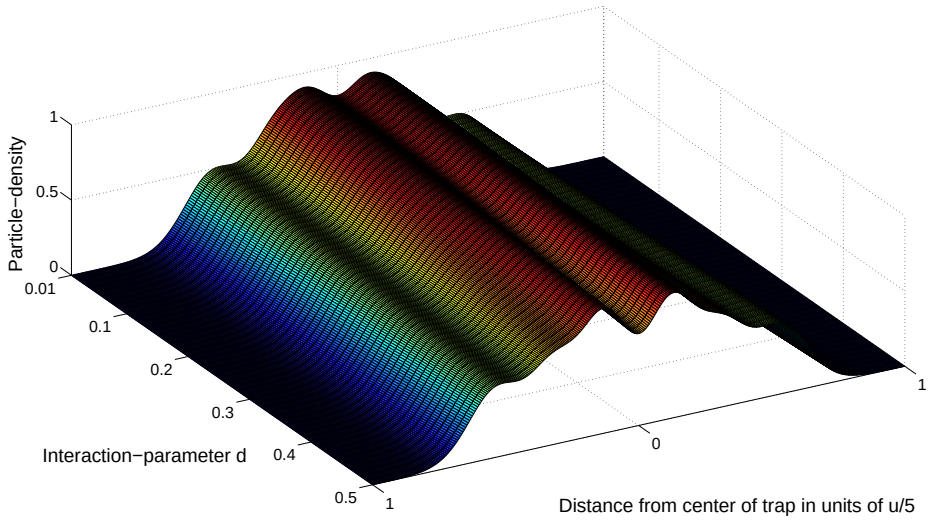

Figure 58: Density distribution of the third excited state for four fermions in a quasi one-dimensional harmonic trap with $l_p = 0.04$ (Dipole angle $\theta = \frac{\pi}{2} \rightarrow Ang(\theta) = 2$)

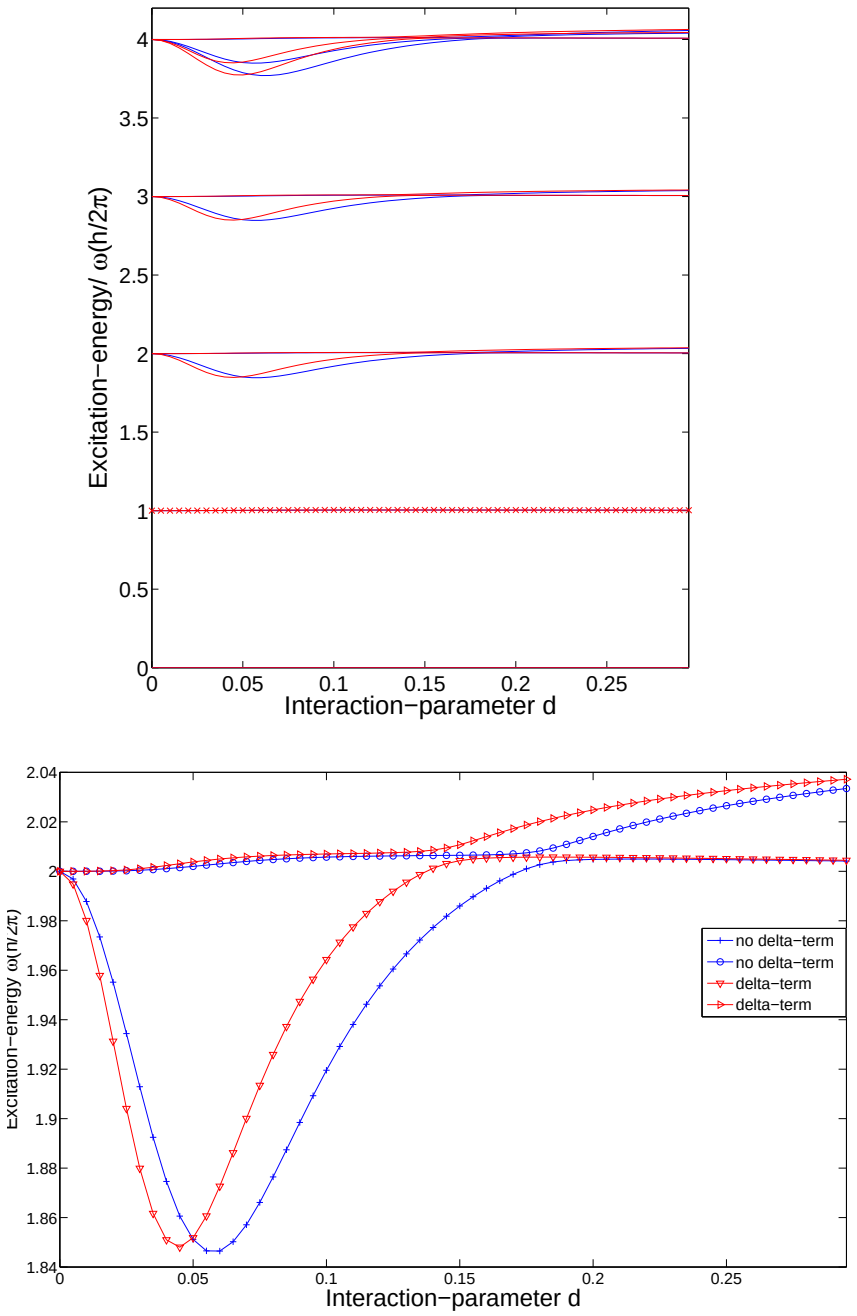

Figure 59: Excitetion energies relative the ground state for energy levels in a system of two bosons with (red) and without (blue) dipole delta in a quasi one-dimensional harmonic trap with $l_p = 0.04$. (Dipole angle $\theta = \frac{\pi}{2} \rightarrow Ang(\theta) = 2$ and the lines are interpolations between data points indicated by the markings.) Upper: energy levels 1 to 9 Lower: energy levels 3 to 4

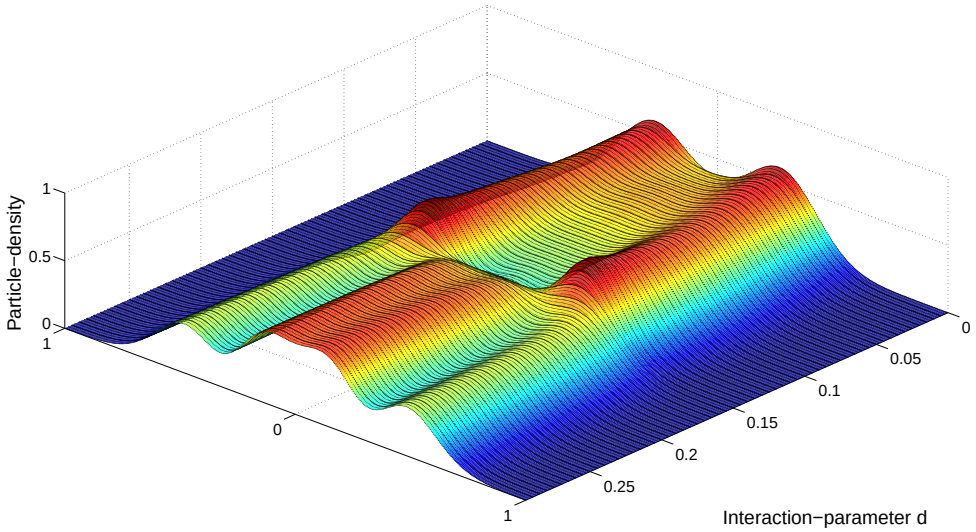

Figure 60: Density distribution of the second excited state for two bosons in a quasi one-dimensional harmonic trap with $l_p = 0.04$ (Dipole angle $\theta = \frac{\pi}{2} \rightarrow Ang(\theta) = 2$)

It should finally be noted once again that the results in this section are seen on the cusp of region where the dipole interaction becomes a bad approximation. It is however still interesting to note that the four-boson systems show such a specific feature as the avoided crossings. This behavior is clearly an effect of the "very short range" part of the dipole-dipole interaction, and the question remains if this can be seen for more realistic models.

Part IV
Conclusions and Appendix

13 Conclusions and Outlook

Systems of ultracold molecules and atoms with permanent dipole moments have been discussed in many publications.

In this project I have studied quasi one-dimensional systems of a few ideal dipoles in harmonic traps. The aim of the project has been to investigate the effects and prospects of the dipole-dipole interaction in such systems, both from analytical and numerical calculations.

The possibilities of dipoles in low-dimensional systems are especially interesting since the mutual interaction between dipoles can be modified externally via the alignment of the dipole moments. The interaction can be tuned to become either attractive or repulsive using an external electric field with a specified inclination-angle θ, given relative to the linear alignment of the dipoles in the one-dimensional trap. Depending on the strength and nature of the interaction, particles in such traps can become pushed apart or drawn together by the dipole-dipole force. The effective one-dimensional dipole-dipole force is therefore often discussed in terms of the long-range or short range interaction, so that systems are affected by different parts of the dipole-dipole force depending on the expected distances between particles.

In particular the long-range interaction regime of the dipole-force has attracted much interest, but in recent years the effects of the short range regime of the dipole-dipole force have also been investigated, particularly in connection with the experimental possibilities of Feshbach resonances. In this regime the details of the short range dipole-dipole interaction have been seen to play an important role for the properties of quasi one-dimensional systems, and such details have therefore been investigated with special care in this project.

Investigations showed that for two ideal dipoles there are strong indications of an inherent delta term in the energy-expression for the three-dimensional dipole-dipole interaction. The existence of this delta term was however a difficult analytical question which left inconclusive answers, even after applying more advanced mathematical methods such as generalized functions.

For certain parameters of the quasi one-dimensional harmonic system of dipoles the delta term has been seen to significantly alter the results of density distributions, occupation numbers and energy eigenvalues.

The delta term indeed plays a large role even though the other terms of the three-dimensional dipole-dipole interaction approach infinity for successively smaller distances between the dipoles.

It has therefore suggested that all calculations involving ideal dipoles should include a comparison between results obtained with and without the ambiguous delta term, and that interaction regimes which showed dependence on this term

should be avoided.

In the quasi one-dimensional system the dipoles are situated in an anisotropic harmonic trap which enables the effective dipole-dipole interaction between particles to be tuned repulsive or attractive via an external electric field. It was seen that the repulsive interaction in general caused systems of both dipolar bosons and fermions to separate, meaning that particles became pushed apart by the repulsive dipole-dipole interaction.

The concept of separation should be important when simulating systems of real dipoles, since the dipole approximation in general fails for "small" distances between the particles. It was seen that the energy spectra of the quasi one-dimensional systems in general showed many distinctive features which allowed categorization of states as "separated". The detection of the separated regime, where particles are pushed apart, should be important since this regime represents a system where real dipoles are well-approximated by ideal dipoles.

By investigating quasi one-dimensional systems of bosons I have also seen some interesting effects of the "very short range" dipole-dipole interaction. In this project I have chosen to divide the interaction into different parts, depending on the distance between the dipoles. The interaction between two dipoles at the same place, or very close to each other, is called the "very short range" interaction. For larger distances between the dipoles the interaction is discussed in terms of the "short range" and the "long-range" interaction, where the long-range interaction governs the interaction between dipoles separated by a large distance and can be approximated according to $V_{1D}(z) \approx \frac{4}{z^3}$. The short range interaction denotes the region between the "very short range" and long-range interaction.

The "very short range" interaction is large compared to the short range and long-range interaction and decays quickly and almost linearly for increasing distance between the dipoles, which can be seen from the potential plots in figure (6).

The Pauli principle prevents spin-polarized fermions with the same quantum numbers from overlapping, so the "very-short range" regime of the dipole-dipole interaction has been investigated by simulating a system of bosons.
It was seen that the transition from the "very short range" interaction regime to the short range interaction regime was clearly manifested in the energy spectra in terms of avoided crossings between excited states when changing the interaction strength.

The transition was also indicated by the fact that the many-particle states mixed with high harmonic one-particle states, $n \gtrsim 12$, in the "very short range" regime. This mixing was lost when states started to become separated on larger length scales, so the occupation-numbers again manifested a transition from a system governed by the "very short range" interaction into a system governed by the short range interaction.

These characteristics could become important since this transition indicates a change from a system where particles come close, into a system where particles become pushed apart on relatively large length scales.

It is possible that this transition denotes a change into a system where dipolar bosons separate sufficiently for the ideal dipole approximation to be valid for real dipoles, and the avoided crossings could then be viewed as indications of an interaction regime which lies on the limit of the dipole approximation. A possible continuation of this project is therefore to search for avoided crossings in boson spectra calculated from models of real dipoles.

In relation to the general features of the fermion-spectra it was also discussed how the crossings of energy levels for different particle numbers could lead to interesting prospects for tunneling transport through quasi one-dimensional systems of dipoles. Tuning the parameters of the interaction and the total system it turned out that it was possible to intersect the ground state-energies of two (or possibly more) different numbers of particles. These intersections could possibly be used to modify the tunneling transport through such systems at these given energies, and this prospect should therefore be an interesting continuation of this project.

14 Appendix

14.1 Generalized functions

In order to describe physics involving point-sources it is often useful to understand the concept of generalized functions. It is tempting to describe a point charge in three-dimensional space mathematically as a classical function $\delta(\bar{r})$ of position.

This interpretation may however land you in trouble since the concept of a delta-function as a classical function is incorrect.

The "delta-function" $\delta(\bar{r})$ is actually not a function in the classical sense, since it cannot be defined by its value at every $\bar{r}$. [6]

In order to be correct we must define δ as a *generalized function,* i.e a distribution, by using a set of test functions $\tau(\bar{r})$, which themselves are real-valued and *smooth* classical functions of position.

All test functions are also defined to be zero outside any *finite region* so that products of them can be integrated over the entire space.

A proper definition of the generalized Dirac function δ is given by [6-1] ;

> *The Dirac δ function $\delta(x)$ is a function of test functions $\tau(x)$, i.e., a functional.*
>
> *It is defined by a set of numbers, one for each τ in the space of the test functions; the number associated with $\tau(x)$*
>
> *is denoted by $< \delta \mid \tau >$, and it is defined to be $\tau \mid_{x=0}$.*

It should also be noted that the number $< \delta \mid \tau >$ is linear in the test functions.

Integrals involving products of the function δ could now be *defined* as[6];

$$\int_{-\infty}^{\infty} \delta(x)\tau(x)\,dx \equiv < \delta \mid \tau > \tag{66}$$

These definitions can be used for any generalized function ${}^{g}F$, so that there is one assigned number $<{}^{g}\ F \mid \tau >$ for each test function τ.

For an arbitrary function ${}^{g}F$ the rule for assigning a value to $<{}^{g}\ F \mid \tau >$ must not be as for the Dirac delta function δ, as we will see for the generalized electrical field from an ideal dipole.

The defining property of a generalized derivative D is given according to [9]:

$$< D\,[{}^{g}F] \mid \tau > \equiv - <{}^{g}\ F \mid D\,[\tau] > \tag{67}$$

The relation (67) must hold for any test-function and is the fundamental requirement in order to define a meaningful derivative.

The main point of generalized functions is that they can allow a mathematically consistent definition of physical concepts such as point-charges, and could therefore possibly be used in derivations of their physical properties. The remaining question is now if the formulations of the physical laws describing the

"implications" of charge can be applied to these definitions and, more importantly, if the new definitions can allow mathematically consistent derivations of physical effects originating from point-like objects.

Generalized functions in physics

In order to apply generalized functions to electrostatics one needs a new form of the Maxwell's equations. The form itself must of course make all the physical predictions that Maxwell's classical equations does, so that form is a new representation of the equations. A generalized form of Maxwell's equations can be found using limits of smooth sources.[6]

Generalizations of this type was performed by G. Temple in 1955, and using this method will give Maxwell's equations as relations between numbers like $<^g F \mid \tau >$ and $< \nabla^g F \mid \tau >$, where ∇ is a generalized derivative.

For example one could look at the generalized form of the Poisson equation $\nabla^{\mathbf{2}}\Phi = -\rho/\epsilon_0$, which can be generalized to [6];

$$< \nabla^{\mathbf{2}}[^g\Phi] \mid \tau >= - <^g \rho/\epsilon_0 \mid \tau >$$

which by (67) is equivalent to;

$$<^g \Phi \mid \nabla^{\mathbf{2}}[\tau] >= - <^g \rho/\epsilon_0 \mid \tau > \tag{68}$$

This is the Poisson equation for generalized functions ${}^g\Phi$ and ${}^g\rho$, and it makes the same predictions as its classical counterpart.

All of Maxwell's equations can be put into generalized form[6], so that generalized fields can be derived from point-sources.

14.2 Derivation of $V_{1D}^{T1}(z)$

Separating $V_{DDI}^{3D}(\varrho cos\varphi, \varrho sin\varphi, z)$ into two terms we first perform the integration for the first term, remembering that we must invoke the rules of integration which apply to the total function.

For the first term we use the improper integral;

$$V_{1D}^{T1}(z) = \frac{d^2}{2\pi l_\perp^2} \int_0^{2\pi} d\varphi \int_0^{\infty} d\varrho\varrho \, \frac{\left(1 - 3cos^2\beta_{rd}\right)}{\left(z^2 + \varrho^2\right)^{3/2}} \, e^{-\varrho^2/(2l_\perp^2)} \tag{69}$$

where $cos\beta_{rd}$ can be expressed in cylindrical coordinates according to, (see figure (5)):

$$cos\beta_{rd} = \frac{\overline{r} \cdot \overline{p}}{|\overline{r}| \, |\overline{p}|} = \frac{\varrho cos\varphi sin\theta + zcos\theta}{\sqrt{\varrho^2 + z^2}}$$

One could now rewrite $V_{DDI}^{3D}(\varrho cos\varphi, \varrho sin\varphi, z)$ according to;

$$V_{DDI}^{3D} = \frac{d^2}{\left(z^2 + \varrho^2\right)^{3/2}} \left(1 - 3\frac{\left(\varrho cos\varphi sin\theta + zcos\theta\right)^2}{\varrho^2 + z^2}\right) \tag{70}$$

The integral (69) can now be computed:

$$V_{1D}^{T1}(z) = \frac{d^2}{2\pi l_\perp^2}\int_0^{2\pi} d\varphi \int_0^{\infty} d\varrho\varrho\, \frac{\left(z^2+\varrho^2-3(\varrho cos\varphi sin\theta + z cos\theta)^2\right)}{(z^2+\varrho^2)^{5/2}}\, e^{-\varrho^2/(2l_\perp^2)}$$
$$= \frac{d^2}{2\pi l_\perp^2}\int_0^{\infty} d\varrho\, \frac{\varrho e^{-\varrho^2/(2l_\perp^2)}}{(z^2+\varrho^2)^{5/2}} \int_0^{2\pi} d\varphi \left(z^2 + \right.$$
$$\left.\varrho^2 - 3\left(\varrho^2 cos^2\varphi sin^2\theta + 2\varrho z cos\varphi cos\theta sin\theta + z^2 cos^2\theta\right)\right)$$
$$= \frac{d^2}{2\pi l_\perp^2}\int_0^{\infty} d\varrho\, \frac{\varrho e^{-\varrho^2/(2l_\perp^2)}}{(z^2+\varrho^2)^{5/2}} \left(2\pi\left[z^2 + \varrho^2 - 3z^2 cos^2\theta - \tfrac{3}{2}\varrho^2 sin^2\theta\right]\right)$$

Using the trigonometrical identities $sin^2\theta = \frac{1}{2} - \frac{1}{2}cos2\theta$ and $sin^2\theta + cos^2\theta = 1$ one could rewrite the expression within the square-brackets:

$$\left[z^2 + \varrho^2 - 3z^2 cos^2\theta - \tfrac{3}{2}\varrho^2 sin^2\theta\right]$$
$$\Longleftrightarrow \left[(z^2 + \varrho^2 - 3z^2(1 - (\tfrac{1}{2} - \tfrac{1}{2}cos2\theta)) - \tfrac{3}{2}\varrho^2\left(\tfrac{1}{2} - \tfrac{1}{2}cos2\theta\right)\right]$$
$$\Longleftrightarrow \left[(z^2 + \varrho^2 - \tfrac{1}{2}z^2(3 + 3cos2\theta) - \tfrac{1}{4}\varrho^2\left(3 - 3cos2\theta\right)\right]$$
$$\Longleftrightarrow \left[(-\tfrac{1}{2}z^2(1 + 3cos2\theta) + \tfrac{1}{4}\varrho^2\left(1 + 3cos2\theta\right))\right]$$
$$\Longleftrightarrow (1 + 3cos2\theta)\left[(-\tfrac{1}{2}z^2 + \tfrac{1}{4}\varrho^2)\right] = \tfrac{1}{4}\left(1 + 3cos2\theta\right)\left[(\varrho^2 - 2z^2)\right]$$

The one-dimensional potential $V_{1D}^{T1}(z)$ is now given by the improper integral;

$$V_{1D}^{T1}(z) = \frac{d^2(1 + 3cos2\theta)}{4l_\perp^2}\int_0^{\infty} d\varrho\varrho \frac{\varrho^2 - 2z^2}{\left(\varrho^2 + z^2\right)^{5/2}} e^{-\varrho^2/(2l_\perp^2)}$$

Transforming coordinates $w = \varrho/l_\perp$ and $z = z$ puts the integral on a more convenient form:

$$V_{1D}^{T1}(z) = \frac{d^2(1 + 3cos2\theta)}{4l_\perp^3}\int_0^{\infty} dw w \frac{w^2 - 2z^2}{\left(w^2 + z^2\right)^{5/2}} e^{-w^2/2} \tag{71}$$

14.3 Derivation of $V_{1D}^{T2}(z)$

The integral defining $V_{1D}^{T2}(z)$ can be written according to:

$$V_{1D}^{T2}(z) = \left(\frac{d^2}{\pi^2 l_\perp^4}\int \frac{4\pi\delta^{(3)}(\bar{r}_1 - \bar{r}_2)}{3} * \right.$$
$$\left. e^{-(x_1^2+x_2^2)/(2l_\perp^2)} e^{-(y_1^2+y_2^2)/(2l_\perp^2)} e^{-(x_1^2-x_2^2)/(2l_\perp^2)} e^{-(y_1^2-y_2^2)/(2l_\perp^2)} dx_1 dx_2 dy_1 dy_2\right) \tag{72}$$

Switching to relative coordinates $X = x_1 + x_2$,$Y = y_1 + y_2$, $x = x_1 - x_2$ and $y = y_1 - y_2$ this becomes:

$$\frac{4d^2}{3\pi l_\perp^4}\int \frac{1}{4}\delta^{(3)}(x, y, z_1 - z_2) e^{-(X^2+Y^2)/(2l_\perp^2)} e^{-(y^2+x^2)/(2l_\perp^2)} dX dY dy dx$$
$$= \frac{d^2}{3\pi l_\perp^4}\int \delta(x)\delta\left(y\right)\delta\left(z_1 - z_2\right) e^{-(X^2+Y^2)/(2l_\perp^2)} e^{-(y^2+x^2)/(2l_\perp^2)} dX dY dy dx$$
$$= \frac{d^2}{3\pi l_\perp^4}\int e^{-(X^2+Y^2)/(2l_\perp^2)}\delta\left(z_1 - z_2\right) dX dY$$

Using cylindrical coordinates the last line can be rewritten as;

$\frac{d^2}{3\pi l_\perp^4}\int \varrho e^{-\varrho^2/(2l_\perp^2)}\delta\left(z_1-z_2\right)d\varrho d\varphi = \frac{d^2}{3\pi l_\perp^4}\delta\left(z_1-z_2\right)2\pi\left[-l_\perp^2 e^{-\varrho^2/(2l_\perp^2)}\right]_0^\infty$
$= \frac{2d^2}{3l_\perp^2}\delta\left(z_1-z_2\right)$

The total effective one-dimensional electric dipole-dipole interaction can now be written

$$V_{1D}(z) = D(\theta)\left(\sqrt{2\pi}\left(z^2+1\right)e^{\frac{1}{2}z^2}erfc\left(\frac{z}{\sqrt{2}}\right)-2z\right)+\frac{2d^2}{3l_\perp^2}\delta\left(z\right) \tag{73}$$

with $z = z_1 - z_2$.

14.4 Asymptotic expansion of effective dipole-dipole interaction in one dimension

An asymptotic expansion of the complementary error-function $erfc$ is [15]

$$erfc\left(x/\sqrt{2}\right) = \frac{e^{-\frac{x^2}{2}}}{x\sqrt{\frac{\pi}{2}}}\sum_{n=0}^{\infty}\left(-1\right)^n\frac{\left(2n-1\right)!!}{\left(x^2\right)^n}$$

so that:

$V_{DDI}^{1D\,T1}\left(z\right) = -2z + \frac{\sqrt{2\pi}\left(1+z^2\right)}{\sqrt{\frac{\pi}{2}}z}e^{-\frac{z^2}{2}}e^{\frac{z^2}{2}}\sum_{n=0}^{\infty}\left(-1\right)^n\frac{\left(2n-1\right)!!}{\left(z^2\right)^n}$
$= -2z + 2\frac{\left(1+z^2\right)}{z}\sum_{n=0}^{\infty}\left(-1\right)^n\frac{\left(2n-1\right)!!}{\left(z^2\right)^n}$

Taking the first five terms in the expansion

$$\begin{aligned}
T1 &= \frac{(-1)!!}{(z^2)^0} = 1\\
T2 &= -1\cdot\frac{(-1)!!}{(z^2)^1} = -\frac{1}{z^2}\\
T3 &= \frac{3}{z^4}\\
T4 &= -\frac{15}{z^6}\\
T5 &= \frac{3\cdot 35}{z^8}
\end{aligned}$$

gives:

$$\begin{aligned}
&V_{DDI}^{1D\,T1}\left(z\right)/D(\theta)\\
&\approx -2 + \frac{2\left(1+z^2\right)}{z} - \frac{2\left(1+z^2\right)}{z^3} + \frac{2\cdot 3\left(1+z^2\right)}{z^5} - \frac{2\cdot 15\left(1+z^2\right)}{z^7} + \frac{2\cdot 105\left(1+z^2\right)}{z^9}\\
&= \frac{4}{z^3} - \frac{24}{z^5} + \frac{180}{z^7} - \frac{210}{z^9}
\end{aligned} \tag{74}$$

14.5 Convergence-plots

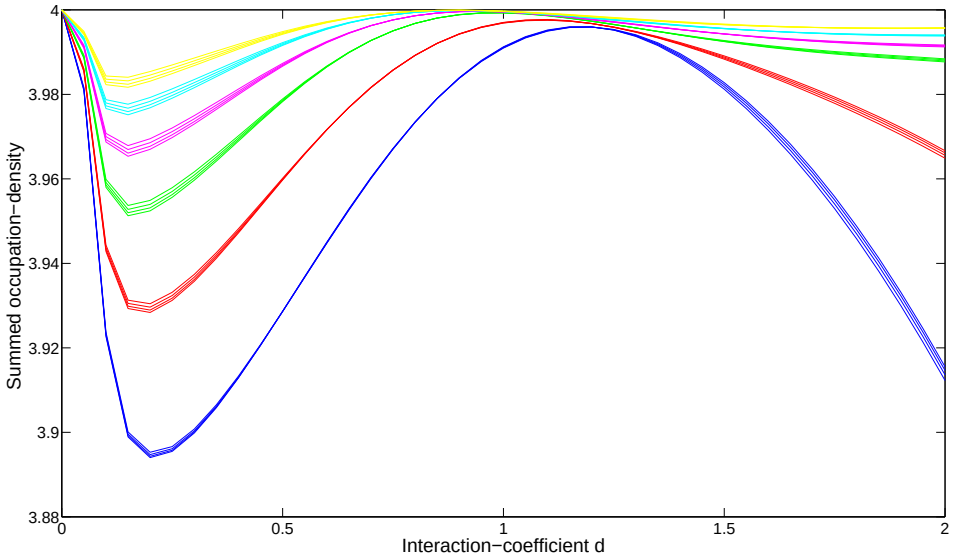

Figure 61: Rate of convergence pictured for figure (46)(The different lines of the same color show results obtained with 21,22,23 and 24 harmonic basis-functions respectively.)

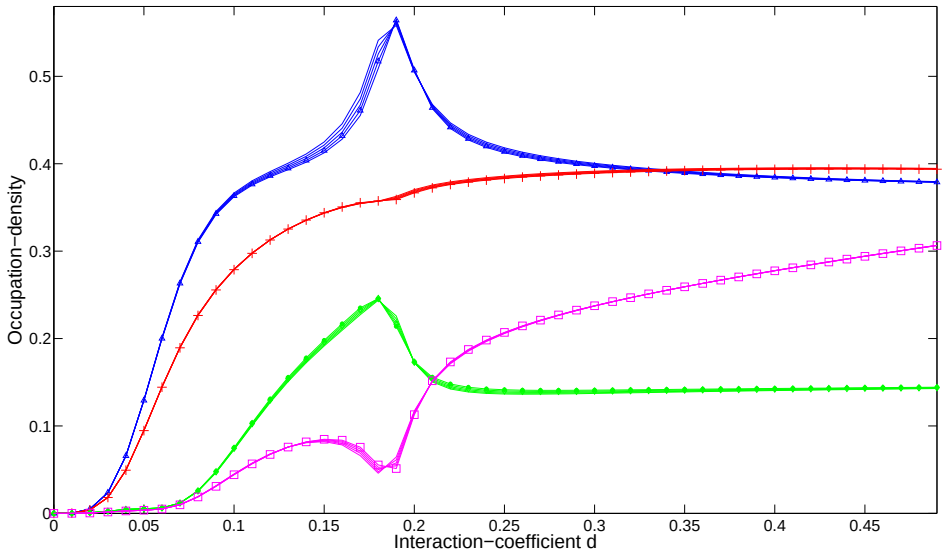

Figure 62: Rate of convergence pictured for figure (55)(The different lines of the same color show results obtained with 31,32,33, 34 and 35 harmonic basis-functions respectively.)

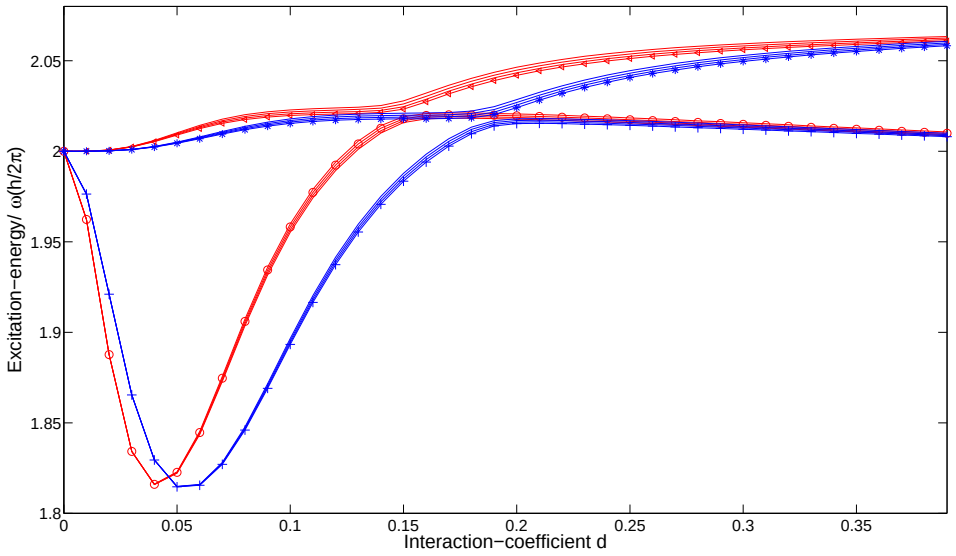

Figure 63: Rate of convergence pictured for figure (52)(The different lines of the same color show results obtained with 31,32,33 and 34 harmonic basis-functions respectively.)

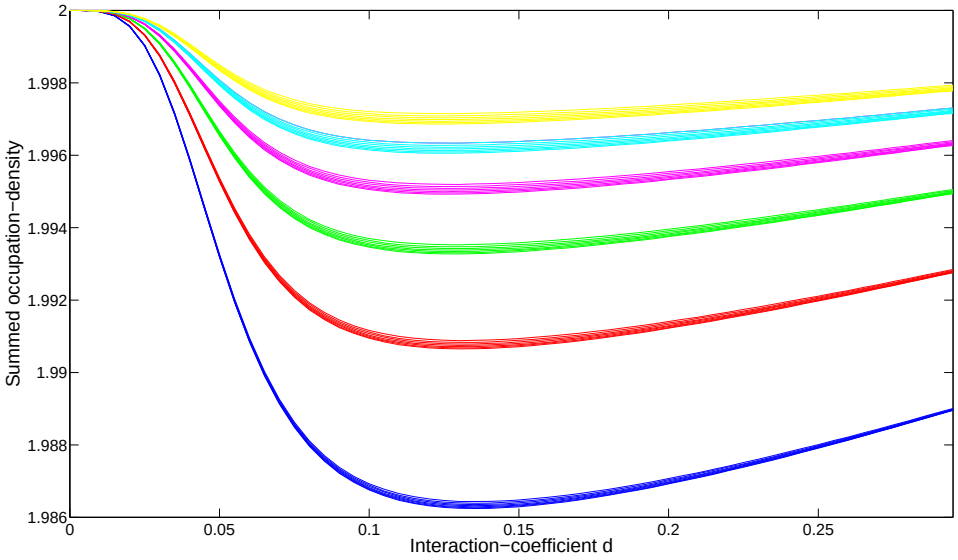

Figure 64: Rate of convergence pictured for figure (49)(The different lines of the same color show results obtained with 24,25,26,27,28,29 and 30 harmonic basis-functions respectively.)

15 Acknowledgments

I would like to thank my supervisor Stephanie Reimann for her patience, guidance and encouragement. I would also like to thank Liney Halla Kristinsdottir and Jonas Cremon for valuable discussion and support during the work. A special thank also to Jonas Cremon for his CI method program-package, and also to the whole CI-team at the department of Mathematical Physics in Lund. Finally I would like to thank Francesc Malet for organizing and inviting me to many of the social activities which made me feel apart of the department.

References

[1] Jackson, J. D. *Classical Electrodynamics,* 3rd ed.; Wiley 1999

[2] Atkin, R. H. *Theoretical Electromagnetism*; Heineman 1962

[3] Dugdale, D. *Essentials of Electromagnetism*; Springer 1993

[4] Blinder S. M. *Am. J. Phys.* **2003**, *71*, 816

[5] Boykin, T. B *Am. J. Phys.* **2003**, *72*, 462-468

[6] Skinner, R.; Weil, J. A. *Am. J. Phys.* **1989**, *57*, 777-791

[6-1] Ref [5] pp. 778

[7] Gsponer, A. *J. Math. Phys.* **2008**, *49,* 102901 (22 pages)

[8] Gsponer, A. *Eur. J. Phys.* **2006**, *30*, 19

[9] Temple, G. *Proc. R. Soc. Lond.* **1955,** 19341990 *228*, 175-190

[10] Gross, E. K. U.; Runge, E.; Heinonen, O. *Many-Particle Theory*, A. Hilger 1991

[11] Peskin, M.E.; Schroeder, D.V. *An Introduction to Quantum Field Theory*, Addison–Wesley 1995

[12] Sakurai, J. J. *Modern Quantum Mechanics*, revised ed., Addison-Wesley 1993

[13] Cremon, J. C. *Quantum few-body physics with the configuration interaction approach- Method Development and application to physical systems.* Ph. D Thesis, Lund University, 2010

[14] Hibbert, A. *Computational Atomic Structure* (Compendium), the Queens University of Belfast, 2009

[15] http://en.wikipedia.org/wiki/Error_function, February 9 2012

[16] Atkin, R. H. *Theoretical Electromagnetism*, Heinemann 1962

[17] http://en.wikipedia.org/wiki/Fock_space, February 9 2012

[18] Cowan, R. D. *The Theory of Atomic Structure and Spectra*, University of California Press 1981

[21] Deuretzbacher, F; Cremon J. C; Reimann S. M *Phys. Rev.* A 81, 063616 (**2010**)

[22] [21], Figure 3

[23] Davies, J. H. *The Physics of Low-dimensional Semiconductors: An Introduction*, Cambridge University Press 1998

[24] Inouye, S; Andrews, M. R.; Stenger, J.; Miesner, H. J; Stamper-Kurn, D. M.; Ketterle, W. *Nature Lond.* **1998,** *392*, 151-154

[25] Bohn, J. L.; Wilson, R. M.; Ronen, S. *Laser Physics* **2009**, *19, No. 4*, 547-549

[26] Harju, A. *Journal of Low Temperature Physics* 140, Nos. 3/4 (2005)

[27] Minguzzi, A.;Vignolo, P.; Tosi, M. P. *Phys. Rev. Lett.* A 294, 222 (2002)

[28] Kristinsdóttir, L. H.; Cremon, J. C.; Nilsson, H. A.; Honqi Xu; Samuelson, L.; Linke, H.; Wacker, A.; Reimann, S. M *Phys. Rev.* B 83, 041101 (2011)

[29] Arkhipov, A.S.; Astrakharchik, G.E.; Belikov, A.V.; Lozovic, Yu. E. *Pis'ma v ZhETF*, vol 82, iss. 1, pp 41-45 (2005)

[31] Giovanazzi, S.; Görliz, A.; Pfau, T. *Phys. Rev. Lett.* 89, 130401 (2002)

[33] Sussman, B. J.; Underwood, J. G.; Lausten, R.; Ivanov, M. Y.; Stolow, A. *Physical Review* A 73, 1-14 (2006).

[34] Pethick, C.; Smith, H. *Bose-Einstein Condensation in Dilute Gases*, Cambridge University Press 2002

[35] Girardeau, M. *J. Math. Phys.* 1, 516 (1960).

[36] Trefethen, L. N.; Bau, D. *Numerical Linear Algebra*, SIAM 1997

[37] Pedersen, J. N.; Wacker, A. *Phys. Rev.* B 72, 195330 (2005)

[38] Deuretzbacher, F., *Institute for Theoretical Physics, Hannover*, private communication

[39] Kristinsdottir, L. H., *Division of Mathematical Physics,University of Lund,* private communication

[40] Lahaye1, T.; Koch1, T.; Fröhlich1, B.; Fattori1, M.; Metz1, J.; Griesmaierl, A.; Giovanazzi1, S.; Pfau1, T. *Nature* 448, 672-675 (2007)

[41] Malet, F.; Kristensen, T.; Reimann, S. M.; Kavoulakis G. M. *Phys. Rev.* A 83, 033628 (2011)